Università degli Studi del Piemonte Orientale "Amedeo Avogadro"

Dipartimento di Scienze del Farmaco

PhD program in Chemistry & Biology

Curriculum: Drug discovery and development

XXIX ciclo a.a. 2013-2016

SSD MED/04

Inflammation and cancer: relevance of myeloid cells recruitment and plasticity in tumor biology

Francesca Maria Consonni

Supervised by Prof. Antonio Sica

PhD program coordinator: Prof. Domenico Osella

Università degli Studi del Piemonte Orientale "Amedeo Avogadro"

Dipartimento di Scienze del Farmaco

PhD program in Chemistry & Biology

Curriculum: Drug discovery and development

XXIX ciclo a.a. 2013-2016

SSD MED/04

Inflammation and cancer: relevance of myeloid cells recruitment and plasticity in tumor biology

Francesca Maria Consonni

Supervised by Prof. Antonio Sica

PhD program coordinator: Prof. Domenico Osella

Contents

Chapter 1

1.1 Inflammation and cancer

The relationship between inflammation and cancer was described for the first time in 1863, when Rudolf Virchow observed leukocyte infiltration in neoplastic tissues ("lymphoreticular infiltration") and hypothesized that the origin of cancer was at site of chronic inflammation. In the last decade several lines of evidences – based on a range of findings from epidemiological studies of patients to molecular studies of genetically modified mice – demonstrated the critical role of infection and chronic inflammatory diseases in tumorigenesis, and some of the underlying molecular mechanisms have been elucidated [1-3].
Inflammation is a well-coordinated process fundamental either in physiological conditions or in protecting body against different exogenous and/or endogenous treats. Any disorder in tissue homeostasis activates innate immune cells that are a first line of defense designed to "heal" the afflicted tissue. In response to chemotactic cytokines, the innate immune cells (macrophages, mast cells, dendritic cells and natural killer cells) migrate from the venous system to sites of damage, where initiate the inflammatory response by releasing cytokines, chemokines, matrix-remodeling proteases, and reactive oxygen and nitrogen species, leading to the elimination of pathogens and repair of tissue damage [4].
The key concept is that physiological inflammation, for example inflammation associated with wound healing, is a strictly controlled and self-limiting process; however, any deregulation in the specific control of immune components can lead to chronic inflammation that may favor the initiation and progression of cancer. In this scenario, a sustained inflammatory microenvironment provides a constant supply of a variety of factors (i.e. cytokines, chemokines and growth factors) which can counteract cell death and/or repair programs, resulting in genomic instability and predisposes tissues for cancer development [5, 6].
Hence, the mediators and cellular effectors of inflammation are important components of the local environment of tumors. It is estimated that 20% of all

cancers is associated with chronic infection and inflammation [7], indicating inflammation as the "Seventh hallmark of cancer" (Fig. 1) [8, 9].

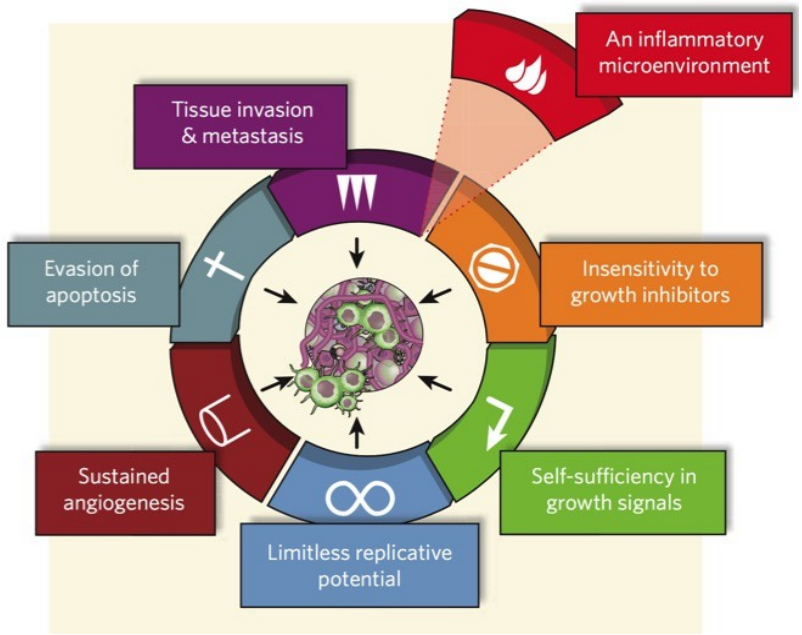

Figure 1: Inflammation as the seventh hallmark of cancer.
In 2000, Hanahan and Weinberg proposed a model to define the six hallmarks that a tumor acquires: unlimited replicative potential, ability to develop blood vessels, evasion of programmed cell death, self-sufficiency in growth signals, insensitivity to growth inhibitors and tissue remodeling and metastasis. Next studies suggest that this model should be revised to include cancer-related inflammation as an additional hallmark [10].

The connection between inflammation and cancer can be viewed as consisting of two pathways; in some types of cancer, inflammatory conditions are present before a malignant change occurs (extrinsic pathway) [7, 11]. Conversely, in other types of cancer, an oncogenic change induces an inflammatory microenvironment that promotes the development of tumors (intrinsic pathway) [12, 13]. These two pathways converge, resulting in the activation of transcription factors, among which nuclear factor-κB (NF-κB), signal transducer and activator of transcription 3 (STAT3) and hypoxia-inducible factor 1α (HIF1α) play a central role in tumor cell biology. These factors recruit and

activate various leukocytes, most notably cells of the myelo-monocytic lineage, and activate the same key transcription factors in inflammatory cells, stromal cells and tumor cells, resulting in more inflammatory mediators being produced and a cancer-related inflammatory microenvironment being generated. This uncontrolled and non self-limiting cancer-related inflammation has many tumor-promoting effects; in fact, it aids in the proliferation and survival of malignant cells, promotes angiogenesis and metastasis, subverts adaptive immune responses and alters responses to chemotherapeutic agents [3, 7].

However, despite these evidences, genetic studies of mouse models have demonstrated that innate immune cells activate an adaptive immune response capable of eliminating rising tumors [14]. It is generally accepted that immune cells continuously recognize and destroy nascent tumor cells but, due to the genetic, epigenetic and metabolic instability that characterizes neoplastic cells, the arising of new variants able to evade the immune surveillance results in tumor establishment and progression (immunoediting process) [15]. Several studies have emphasized that the "smouldering" inflammation associated with tumors is mainly oriented to tune the adaptive immune response. Thus, tumor-infiltrating lymphocytes have functional roles in promoting tumor immune escape by producing immunosuppressive cytokines and generating immunosuppressive networks. Indeed, myelo-monocytic cells recruited in tumors express an alternative M2 functional phenotype mainly oriented towards the suppression of the adaptive immune response [16, 17]. In agreement, clinical studies suggest that an established type-2 "suppressive" immunological profile correlates with poor prognosis, as shown in colorectal, hepatocellular and pancreatic carcinomas and in Hodgkin's lymphoma [18].

Hence, the immune system plays a dual role in cancer: not only it can suppress tumor progression by destroying cancer cells or inhibiting their outgrowth, but it can also promote tumor development by establishing favorable conditions within the tumor microenvironment that facilitate tumor growth and metastasis [19].

1.2 Myeloid cells in cancer

Myeloid cells are the most abundant hematopoietic cells in the human body and are a collection of distinct cell populations with different function. All myeloid cells arise from multipotent hematopoietic stem cells (HSCs) that develop into mature myeloid cells through sequential steps of differentiation. The three groups of terminally differentiated myeloid cells (macrophages, dendritic cells (DCs) and granulocytes) are essential for the normal functions of the innate and adaptive immune systems [20].

Steady-state myelopoiesis is a continuous homeostatic process, occurring in the bone marrow, for replacing hematopoietic cells that are lost to normal programmed cell death. In contrast, emergency (or stress) hematopoiesis is an episodic modification of the magnitude and composition of the hematopoietic output that occurs during immunological stress, including tumor progression, to ensure proper supply of immune cells to increased demand [21].

In this scenario, compelling evidences in literature indicate that dynamic changes in myeloid cell functions occur in parallel to tumor development and that cancer fuels myeloid cells heterogeneity by promoting sustained myelopoiesis. It is well recognized that tumor-derived factors (TDFs), such as cytokines, chemokines, metabolites and inflammatory messengers like prostaglandins, act in paracrine or systemic manner to induce tumor-reprogrammed myeloid cells not only to create a widespread tolerogenic environment by blocking T cell functions and proliferation, but also to drive tumor growth by promoting cancer stemness, angiogenesis, stroma deposition and metastasis formation. Consequently, chronic exposure of the bone marrow microenvironment to non-physiologic levels of ordinarily tightly regulated myelopoietic-like growth factors corrupts the normal process of myeloid cell development and differentiation [8, 20]. This phenomenon drives the increase of circulating myeloid cells in tumour-bearing hosts and it is associated with a partial blockade of myeloid cell differentiation and a consequent accumulation

of highly immunosuppressive, immature myeloid cells (iMCs). Indeed, many TDFs are myelopoietic factors making the myeloid compartment a major target of this 'tumor reconditioning' [22]. For example, granulocyte colony-stimulating factor (G-CSF) and granulocyte/macrophage colony-stimulating factor (GM-CSF) were reported to drive "emergency" myelopoiesis by securing supply of neutrophils and macrophages from bone marrow and extra-medullary hematopoietic stem cell niches (HSCs) [23, 24].

In addition, the macrophage colony-stimulating factor (M-CSF) promotes macrophage differentiation from marrow precursors cells and is required for differentiation and expansion of tissue macrophages involved in tissue homeostasis and tumor progression [25]. Investigation of signaling pathways controlling hematopoiesis revealed that G-CSF-induced granulopoiesis is mediated through the transcription factors c-EBPβ [26, 27], SOCS3 [28], Bcl3 [29] and STAT3 [30], whereas M-CSF supports monocyte differentiation through activation of the transcription factors PU.1 and IRF8 [31]. Of relevance, interleukin-17A (IL-17A) promotes G-CSF- and stem-cell-factor-mediated neutrophilia [32] and supports G-CSF-driven ''emergency'' myelopoiesis [33]. Importantly, reciprocal regulation of macrophage versus neutrophil/granulocyte differentiation might control tissue homeostasis; indeed, depletion of tissue macro- phages leads to exacerbated G-CSF-mediated granulopoiesis [34]. Thus, investigation of the molecular networks that dictate this reciprocal regulation appears to be crucial, as it may affect tissue homeostasis during cancerogenesis.

Myeloid deficiencies can occur at developmental and/or functional levels in essentially all myeloid lineages. To distinguish "normal" myeloid cells from their dysfunctional counterparts, the latter populations have been variously renamed myeloid-derived suppressor cells (MDSCs), tumor-associated macrophages (TAMs), tumor-associated neutrophils (TANs), immature DCs or tolerogenic DCs [35]. Among these, TAMs and MDSCs represent the major orchestrators of the immunosuppressive circuits arising in tumor bearers (Fig. 2) [36, 37].

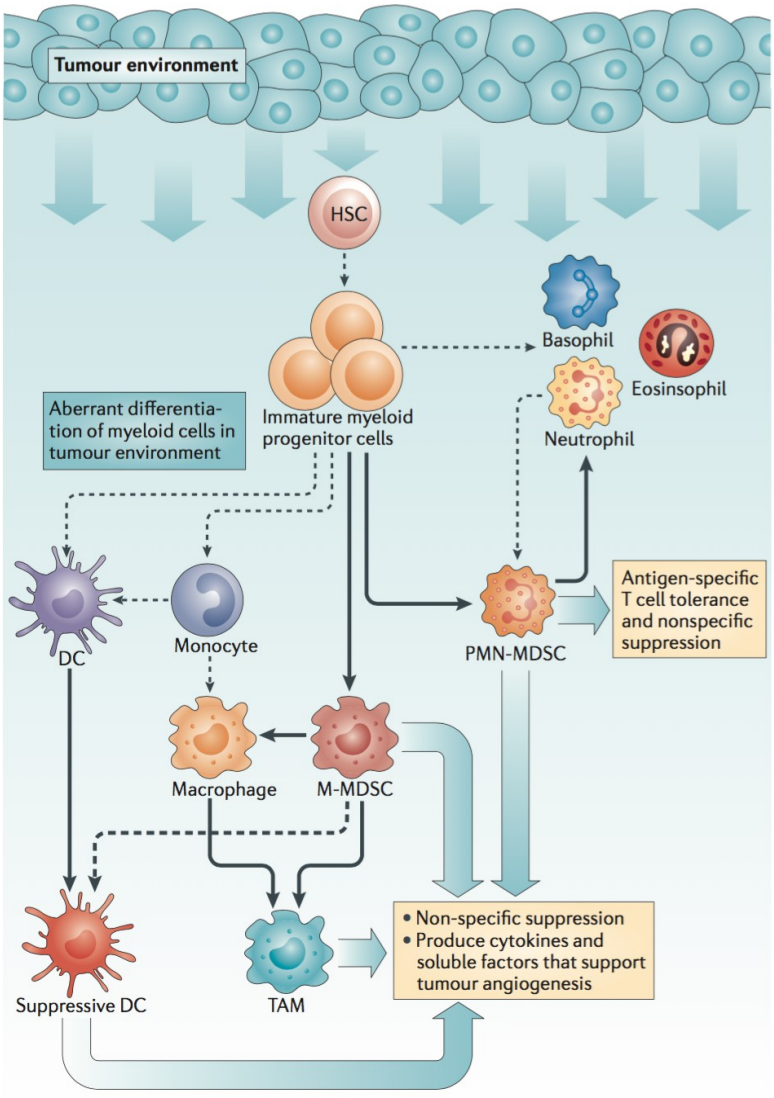

Figure 2: Myeloid cells in cancer.

Factors produced in the tumor microenvironment by tumor cells and stromal cells promote the aberrant differentiation of myeloid lineage cells. The dotted lines show the normal pathways of myeloid cell differentiation from immature myeloid precursor cells to dendritic cells, macrophages and granulocytes. The solid bold lines indicate the aberrant pathways of myeloid cell differentiation that occur in cancer, in which the tumor environment can promote the development of various immunosuppressive populations, including monocytic MDSCs, polymorphonuclear MDSCs, suppressive DCs and TAMs and TANs [20].

1.3 Myeloid-derived suppressor cells

MDSCs are a heterogeneous population of cells of myeloid origin that comprises myeloid progenitor cells and immature macrophages, immature granulocytes and immature dendritic cells [38]. They expand during cancer, inflammation and infection and have a remarkable ability to suppress T-cell responses. In particular, MDSCs are generated in the bone marrow and, in tumor-bearing hosts, migrate to peripheral lymphoid organs and tumor tissues contributing to the formation of the pro-tumor microenvironment [39, 40]. Although initial observations and most of the current information on the role of MDSCs in immune responses has come from studies in the field of cancer research, accumulating evidence has shown that MDSCs also regulate immune responses during bacterial and parasitic infections, acute and chronic inflammation and sepsis [38].

1.3.1 MDSCs phenotype

MDSCs are characterized by a morphological mixture of granulocytic and monocytic cells lacking the expression of cell-surface markers associated with fully differentiated monocytes, macrophages or dendritic cells [41]. In particular, MDSCs include a group of immature mononuclear cells, which are morphologically and phenotypically similar to monocytes (M-MDSCs), and immature polymorphonuclear (PMN) cells, which are morphologically and phenotypically similar to neutrophils (PMN-MDSCs). In mice, MDSCs are identified by co-expression of myeloid lineage differentiation antigens Gr-1 and CD11b [42]. The two major subsets of MDSCs can be distinguished by different expression of the Gr-1 marker ($Gr1^{high}$ cells are mostly PMN-MDSCs and $Gr1^{low}$ cells are mostly M-MDSC). However, the Gr-1 marker is a combination of the Ly6C and Ly6G markers, so these subsets can be more accurately identified based on Ly6C and Ly6G expression (M-MDSCs as

$CD11b^{+}Ly6C^{high}Ly6G^{low}$ and PMN-MDSCs as $CD11b^{+}Ly6G^{+}Ly6C^{low}$). In humans, MDSCs are identified in the mononuclear fraction as cells that express the CD33 marker but lack the expression of markers of mature myeloid and lymphoid cells and the HLA-DR. The identification of human MDSCs subsets is, actually, really difficult because of their heterogeneity. However, human PMN-MDSCs are defined as $CD14^{-}CD33^{+}CD15^{+}$ HLA-$DR^{-/low}$ cells and M-MDSCs as $CD14^{+}$HLA-$DR^{-/low}CD33^{+}CD15^{-}$ cells [43-46]. These cells represent ≈0.5% of peripheral blood mononuclear cells in healthy individuals with a 10-fold increase in cancer patients, such as those with renal cell carcinoma and colorectal carcinoma [47].

Several biochemical and genomic features distinguish MDSCs from neutrophils and monocytes. In particular, MDSCs are characterized by increased expression of of NADPH oxidase (*Nox2*), resulting in increased production of ROS [48]; increased expression of arginase 1 (*arg1*) and nitric oxide synthase 2 (*nos2*) genes, resulting in increased production of Arg1 and NO [49]; increased expression of the transcriptional factors c/EBPβ [27] and STAT3 [50] and decreased expression of IRF8 [51]. As a result, MDSCs display decreased ability to differentiate into mature myeloid cells and their immune suppressive effects are due to the hyper production of ROS, NO and Arg1 [20].

1.3.2 Mechanisms of MDSCs suppressive activity

MDSCs exert their immunosuppression through several mechanisms. In particular, they can mediate suppression of T-lymphocytes in an antigen-specific and -nonspecific manner, deploying strategies that can be either direct or indirect, leading to the generation or expansion of regulatory cell populations, such as $CD4^{+}CD25^{+}$ Tregs. Main mechanisms of action include:

- *ARG1, iNOS and peroxynitrite:* the suppressive activity of MDSCs has been associated with the metabolism of L-arginine, which serves as a substrate for two enzymes: iNOS, which generates NO, and arginase, which converts L-

arginine into urea and L-ornithine. MDSCs express high levels of both arginase and iNOS, and the direct role for both of these enzymes in the inhibition of T-cell function is now well established [52]. In fact, high levels of Arg1 expression by MDSCs can accelerate the depletion of L-arginine in the tumor microenvironment, which subsequently promotes T cell proliferation arrest and functional inhibition by down regulation of the CD3ζ chain in the T cell receptor (TCR) complex. [53]. NO suppresses T-cell function through a variety of different mechanisms that involve the inhibition of JAK3 and STAT5 in T cells [54], the inhibition of MHC class II expression [55] and the induction of T-cell apoptosis [56]. NO is mainly produced by M-MDSCs while both subsets express Arg1. More recently, it has emerged that reactive nitrogen species, such as peroxynitrite ($ONOO^-$), are byproducts of the combined activity of iNOS, ARG1 and NOX2 that can alter the formation of a correct peptide-MHC complex in MHCI molecules and interfere with T cell migration and viability.
In fact, they induce the nitration and nitrosylation of the amino acids cystine, methionine, tryptophan and tyrosine in many types of T cells, driving their un-responsiveness to tumor antigens [57], and modify trafficking of leukocytes through aromatic amino acid nitration and nitrosylation of chemokines (CCL2, CCL5, CCL21, CXCL12) or chemokine receptors (CXCR4) [58].

- *Reactive oxygen species (ROS):* ROS production is the major regulator of the suppressive activity of the PMN-MDSCs in both murine models and human cancers; it affect T-cell fitness by down regulating CD3ζ chain expression and reducing cytokine secretion [59].
- *TGFβ:* TGFβ is an immunosuppressive cytokine that has been associated with MDSCs functions and with the regulation of tumor induction and expansion [60].
- *Induction of regulatory T cells (Tregs):* emerging evidence indicates that MDSCs are involved in Tregs recruitment and differentiation through the production of several chemokines (acting on CCR5 and CCR6) and cytokines (i.e. IFN-γ, IL-10) and/or through direct cell-cell contacts (including CD40-

CD40L interactions) [61]. Moreover, to sustain the immune-suppressive environment, MDSCs also skew TAMs activation towards an M2 polarized phenotype, characterized by impaired production of functional IL-12 supporting immune escape and tumor growth, through a cell contact–dependent mechanism [40]. MDSCs also promote immune dysfunction by expressing membrane surface ligands of T cell–inhibitory receptors, such as programmed cell death ligand 1/2 (PD-L1/2), which bind programmed death 1 (PD-1), and B7-1/2, which bind to cytotoxic T lymphocyte antigen 4 (CTLA4) and CD28 as well as FASL [62, 63].

Hence, in tumor-bearing hosts MDSCs inhibit the immune response through four processes: 1) driving the differentiation of immune cells toward regulatory cells; 2) interfering with T cell migration; 3) altering T cell functionality by production of NO, ROS and RNS; and 4) depleting essential metabolites for T lymphocyte fitness. Several studies indicate that M-MDSCs are highly immunosuppressive and exert their effects largely in an antigen-nonspecific manner, whereas PMN-MDSCs are moderately immunosuppressive and promote T cell tolerance via antigen-specific mechanisms (Fig. 3) [41].

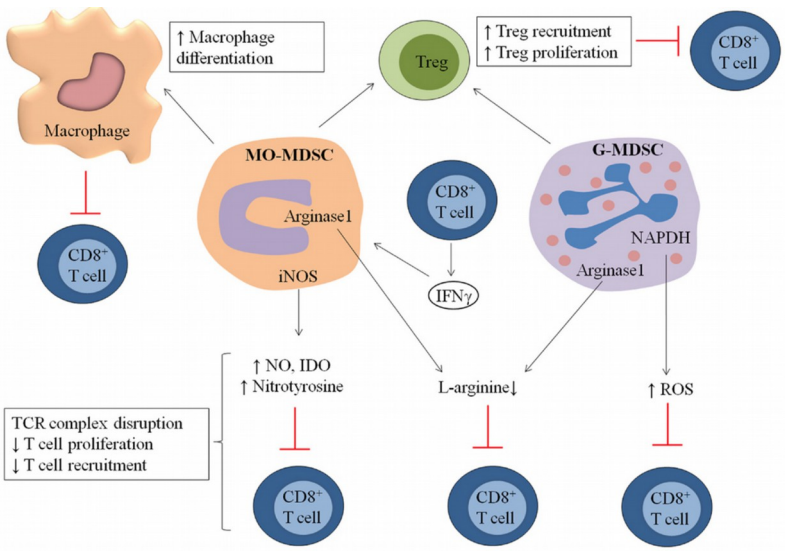

Figure 3: Mechanisms of MDSC's suppression

MDSCs suppress the immune system by distinct mechanisms including increased Tregs proliferation, direct actions of MDSC on T cells by increased NO, nitrotyrosine and ROS secretion, and decreased l-arginine production [64].

1.3.3 Expansion and activation of MDSCs in cancer

Accumulating evidence from tumor-bearing mice and human cancers indicates that the expansion and activation of MDSCs in the tumor microenvironment requires the integration of at least two types of signals: signals promoting accumulation of immature myeloid cells, followed by signals providing for the pathological activation of these cells [43].

MDSCs are generated in the bone marrow from common myeloid progenitor cells (CMP). The expansion of immature myeloid cells is mediated largely by granulocyte-macrophage CSF (GM- CSF), macrophage CSF (M-CSF), granulocyte CSF (G-CSF) and other factors, such as pro-inflammatory cytokines and damage-associated molecular pattern molecules (DAMPs), produced by tumor cells and stroma (e.g. cyclooxygenase 2, prostaglandins, IL-6, IL-17, C5a, VEGF) [65-70]. MDSCs expansion is facilitated by triggering a cascade through the signaling molecules that regulate cell survival, proliferation, differentiation and apoptosis, which are known as family members of Janus tyrosine kinase and STAT3 [71]. In recent years, more evidence has emerged regarding the mechanism of MDSCs regulation by STAT3. Indeed, it was reported that MDSCs from tumor-bearing mice have markedly increased levels of phosphorylated STAT3 compared with Immature Myeloid Cells (IMCs) from naive mice. Several evidence *in vitro* indicate also that the exposure of hematopoietic progenitor cells to the supernatant from tumor-cell cultures activate JAK2 and STAT3 in parallel with an expansion of MDSCs, and that this expansion is abrogated when STAT3 expression in hematopoietic progenitor cells is inhibited [72]. Moreover, ablation of STAT3 expression through the use of conditional knockout mice or selective STAT3 inhibitors

markedly reduced the expansion of MDSCs and increased T-cell responses in tumor-bearing mice [73].

The effect of STAT3 on MDSCs accumulation is mediated by C/EBPβ and IRF8 and is associated with increased survival and proliferation of myeloid progenitor cells, probably through the up-regulation of the expression of B-cell lymphoma XL, cyclin D1, MYC and survivin. So, abnormal and persistent activation of STAT3 in myeloid progenitor cells prevents their differentiation into mature myeloid cells and thereby promotes MDSCs expansion [27, 51].

However, the activity of MDSCs does not only require factors that promote their expansion but also activating factors that exert their effect through multiple signaling pathways including STAT6, STAT1 and NF-κB. These factors are mainly produced by activated T cells and tumor stromal cells and include IFN-γ, ligands for TLRs, IL-13, IL-4 and TGF-β [20]. STAT1 is the major transcription factor that is activated by IFN-γ and drives the up-regulation of Arg1 and iNOS expression in MDSCs within the tumor microenvironment. MDSCs from STAT1-knockout mice could not up-regulate Arg1 and iNOS expression and subsequently had no inhibitory effect on T cells [74, 75]. Moreover, also the signaling pathway that involves IL-4 receptor α-chain (IL-4Rα) and STAT6 (which is activated by the binding of either IL-4 or IL-13 to IL-4Rα) is important for MDSCs activation, but probably only in some tumor models [76].

Hence, the impact of MDSCs in cancer is characterized both by an abnormal myelopoiesis and recruitment of MDSCs into the tumor site, resulting from the persistent stimulation of the myeloid compartment with signals coming from tumors, and by an active MDSCs cytokine production and cell–cell interactions within the environment that promote tumor immune evasion by limiting T-cell responses and infiltration into the tumor microenvironment [39, 77].

MDSCs are also capable of supporting tumor growth through nonimmune-related mechanisms designed to remodeling tumor microenvironment. They have been shown to produce several mediators implicated in the neoangiogenesis and tissue invasion [78]. In the tumor microenvironment in

fact, MDSCs promote the angiogenic switch, by producing proteases (cathepsin and matrix metallo-proteinases 9 (MMP9)) and enhancing VEGF bioavailability [79]. In addition, MDSCs also play an active role in promoting the spread of distal tumor cells. In a murine model of melanoma, it was reported that MDSCs promote cancer cell dissemination by inducing epithelial–to-mesenchymal transition (EMT) through the production of TGF-β in primary tumor [80]. Moreover, mouse models have shown that MDSCs appear in the lungs as early as two weeks prior to the appearance of metastases in parallel with decreased immune function in the lungs. Importantly, myeloid-specific deletion of MMP9 essentially eliminated metastasis, suggesting indispensable role of MDSCs in the establishment of the premetastatic niche [81-83].

1.3.4 Therapeutic strategies targeting MDSCs

The fact that MDSCs strongly contribute to the establishment of an immunosuppressive tumor-microenvironment has stimulated the search for a way to therapeutically target these cells in order to allow for increased antitumor immunity. Several therapeutic strategies are currently being tested in clinic with the aim to elimination, deactivation, or skewing of myelopoiesis away from the accumulation of MDSCs [43, 84].

MDSCs can be eliminated with some first-generation chemotherapeutic agents, probably because these cells are more sensitive than tumor cells to low-dose chemotherapy [85]. In this scenario, gemcitabine has been shown to specifically deplete splenic MDSCs in tumor-bearing mice, resulting in enhanced antitumor response and prolonged survival [86, 87].

Similar success in selectively MDSCs targeting has been achieved with a single administration of 5-fluorouracil, which resulted in increased $CD8^+$ T-cell responses [88]. Moreover, it was shown that selective up regulation of TRAIL receptor DR5 on mouse MDSCs induce their depletion selectively, resulting in tumor growth inhibition [89].

MDSCs can be functionally inactivated by targeting their suppressive machinery. In particular, the up regulation by a synthetic triterpenoid of Nf-E2–related factor 2 (NRF2), that plays an important role in protecting cells against free radical damage, has been shown to reduce the production of ROS by MDSCs *ex vivo* [90]. Moreover, phosphodiesterase-5 (PDE-5) inhibitor is able to inhibit MDSCs functions by decreasing their production of both Arg1 and iNOS restoring the *in vitro* T-cell proliferation in multiple myeloma and head and neck cancer patients [91, 92].

Finally, also nitroaspirin has been shown to down regulate NO and ROS production and thus eliminates the suppressive functions of MDSCs [93].

Other compounds have been reported to affect MDSCs accumulation in cancer; for example all-trans-retinoic acid (ATRA) at therapeutic levels has been shown to induce MDSCs differentiation into DCs and macrophages, leading to a subsequent reduction in the number of MDSCs in renal and lung carcinoma patients and mice [94, 95]. Additionally, sunitinib, which inhibits STAT3, VEGF, c-kit, and M-CSF signaling, has been shown to reduce MDSCs accumulation in renal cell carcinoma patients and may provide a strategy for improving antitumor immunity in these patients [96].

Therefore, different approaches have been explored to harness the potency of the immune system to target cancer. However, till now, efforts to actively stimulate the immune system against tumors in patients have been largely disappointing despite substantial evidence that peripheral immune responses against tumor antigens can be generated. Moreover, immune-modulating activities of chemotherapeutic agents are often very complex to understand, in fact, the same molecules may play opposite roles depending on tumor type, immune contexture, and/or precise therapeutic strategy. For example, gemcitabine and 5-fluorouracil, have been reported to deplete immunosuppressive MDSCs but also to induce the release of cathepsin B from lysosomes and the activation of the NLRP3 inflammasome and caspase-1,

which causes IL-1β secretion from MDSCs, resulting in IL-17 production by T-cells and promotion of tumor growth [97].

These complexities underscore the need for an ever more profound comprehension of the dynamic changes in the tumor microenvironment and in systemic immune responses as tumors evolve, progress, and respond to therapy, in order to facilitate the rational design of highly efficient, synergistic regimens that combine anticancer agents and immunotherapies.

1.4 Tumor-associated macrophages

Macrophages are a group of terminally differentiated tissue-resident myeloid cells found in all tissues, derived from monocytes circulating in peripheral blood [98]. They are key players in tissue homeostasis maintenance, tissue repair and immune surveillance, with important functions in both innate and acquired immunity. Resident macrophages provide immediate defense against foreign pathogens contributing to the balance between antigen availability and clearance through phagocytosis and subsequent degradation of senescent or apoptotic cells, microbes and possibly neoplastic cells. Macrophages also coordinate leukocyte infiltration and their role is essential for triggering, instructing and terminating the adaptive immune response [99].

Macrophages are the most plastic cells of the hematopoietic system able to finely modulate their programs in response to different microenvironmental conditions [100]. In the last decade, there have been numerous reports about the relationship between macrophages and tumors. In fact, tumor-associated macrophages (TAMs) represent the major population of leucocytes infiltrating tumors and, despite their potential anti-tumor activities, there is an extensive literature demonstrating that in both mouse and man, TAMs are co-opted during malignancy to facilitate tumor development and invasion [101].

1.4.1 Macrophage polarization

Macrophages are highly plastic cells that can adopt different phenotypes or activation states in response to different microenvironmental signals (e.g. cytokines, pathogen-associated molecular patterns, danger stimuli) [102, 103]. This plasticity increases the heterogeneity of macrophage populations in a given tissue and in particular, the M1/M2 dichotomy is the widely used model for describing their different functional states (Fig. 4) [104, 105].

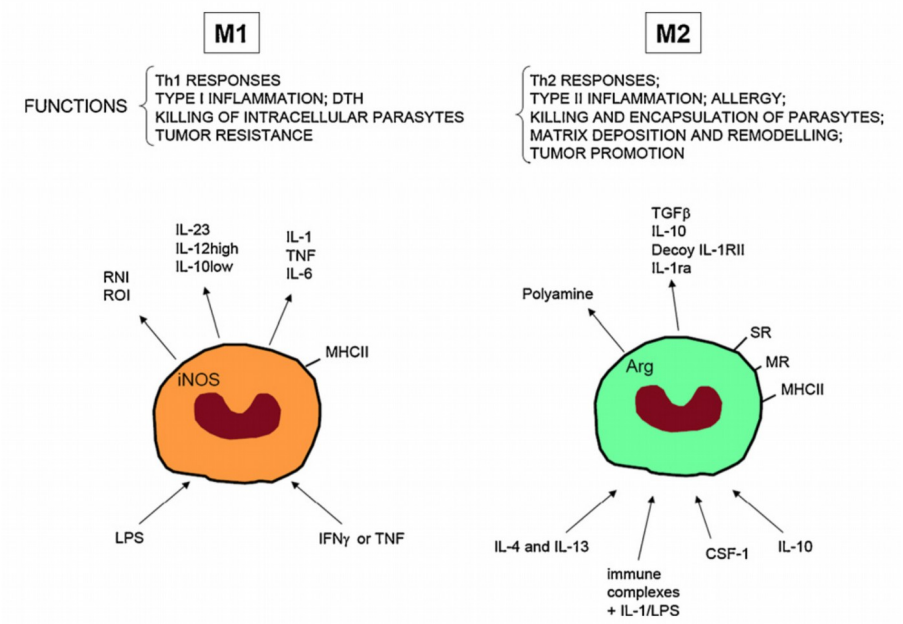

Figure 4: M1 and M2 macrophages.
In the presence of IFN–γ, LPS and other microbial products, monocytes differentiate into M1 macrophages. In the presence of macrophage colony-stimulating factor (CSF-1), IL-4, IL-13, IL-10 and immunocomplexes in association with either IL-1R or TLR-ligands, monocytes differentiate into M2 macrophages. M1 and M2 subsets differ in term of phenotype and functions. M1 cells have microbial activity, immuno-stimulatory functions and tumor cytotoxicity. M2 cells have high scavenging ability, promote tissue repair and angiogenesis and favour tumor progression [106].

"Classical activated" M1 macrophages are potent antigen presenter cells involved in T helper 1 (Th1)-cell-mediated immune resolution of infection and exert their cytotoxic activities by secreting nitric oxide and ROS. Typical drivers of M1 activation are Th1 cytokines such as IFN-γ and microbial

products (LPS). These signals trigger the activation of NF-κB- and STAT1-pathways with subsequent transcription of NF-κB- and STAT1- dependent proinflammatory cytokines (e.g. IL-12, IL- 23 and TNFα) [107, 108].

On the contrary the "alternative activated" M2 macrophages secrete anti-inflammatory cytokines and are involved in scavenge debris, tissue remodelling and repair, angiogenesis and humoral immunity and are able to tune inflammatory response [109]. They show strong activation of arginase pathway with generation of ornithine and polyamines. Important drivers of M2 activation are the Th2 cytokines, such as IL-4 and IL-13, the anti-inflammatory cytokines IL-10 and TGF-β, hormones (e.g. glucocorticoids), and immune complexes. These M2-polarizing signals generally inhibit the expression of M1 cytokines and chemokines. These inhibitory effects principally relay on STAT-3 dependent mechanisms and the direct inhibition of NF-κB [110].

In vivo, macrophages can be exposed to a large number of stimuli that may induce opposing signaling pathways and thus result in mixed functional states. Nevertheless, there is considerable plasticity between distinct types. For this reason macrophage activation should not be seen as existing of discrete states M1 and M2, but rather as a continuum that emphasize the extremes of macrophage plasticity (Fig. 5) [109]. M1 and M2 extremes exhibit specific characteristic expression of metabolic enzymes (iNOS vs. ARG1), cytokines ($IL\text{-}12^{high}IL\text{-}10^{low}$ vs. $IL\text{-}12^{low}IL\text{-}10^{high}$), chemokines (CXCL9 and CXCL10 vs. CCL17 and CCL22), as well as transcription factors (NF-κB, STAT1 and IRF5 vs. STAT6, MYC, IRF4 and PPARγ) [104].

A large body of literature indicates that monocytes and macrophages associated with established tumors show an immunosuppressive, M2 phenotype which supports immune escape, tumor growth and malignancy exerting crucial tumor-promoting functions [109, 111]. However, when applied to TAMs the M1/M2 dichotomy is too simplistic since their phenotype varies significantly between tumors or even among different areas of the same tumor [112, 113]. Monocytes

from patients with renal cell carcinoma indeed coexpress proinflammatory genes, such as TNFα, together with tumor-promoting genes VEGFA, MMP9 and CXCR4 [44]. Moreover, similar mixed phenotypes have been observed in various other tumor models [114]. Thus, defining TAMs polarization status require integration of a multiparameter analysis of cell surface markers, and comparison of the TAMs transcriptome with the gene profile of resident macrophages isolated from the same tissues [17, 104].

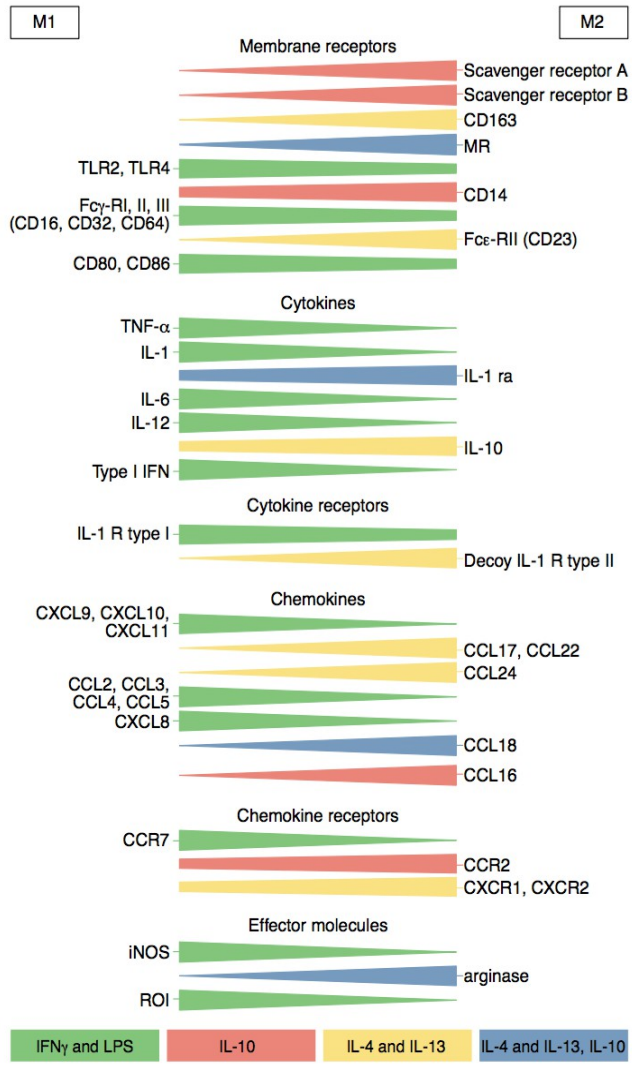

Figure 5: M1 and M2 macrophages are the extremes of a continuum [109].

1.4.2 Origin, recruitment and activation of TAMs

As mentioned above, TAMs are the main orchestrators of inflammation associated with cancer and constitute the dominant myeloid cell population, both in terms of number and functions, in most solid tumors. However, the details regarding TAMs origins and the stimuli that drive their differentiation and functional states are still being defined [25, 105, 115].

It has long been held that macrophages originate from the blood compartment and that chemotactic signals originating from tumor cells or from normal cells present in the cancer microenvironment recruit monocytic precursors at the primary and metastatic tumor sites [116]. Recent studies, however, have shown that most tissue macrophages, although with some exceptions such as intestine, arise during early embryonic development from yolk sac and do not require input from the bone marrow (BM) but rather maintain their populations via local proliferation. In contrast, macrophages involved in pathogen responses appear to come from circulating BM monocytes (Fig. 6) [98, 117-120].

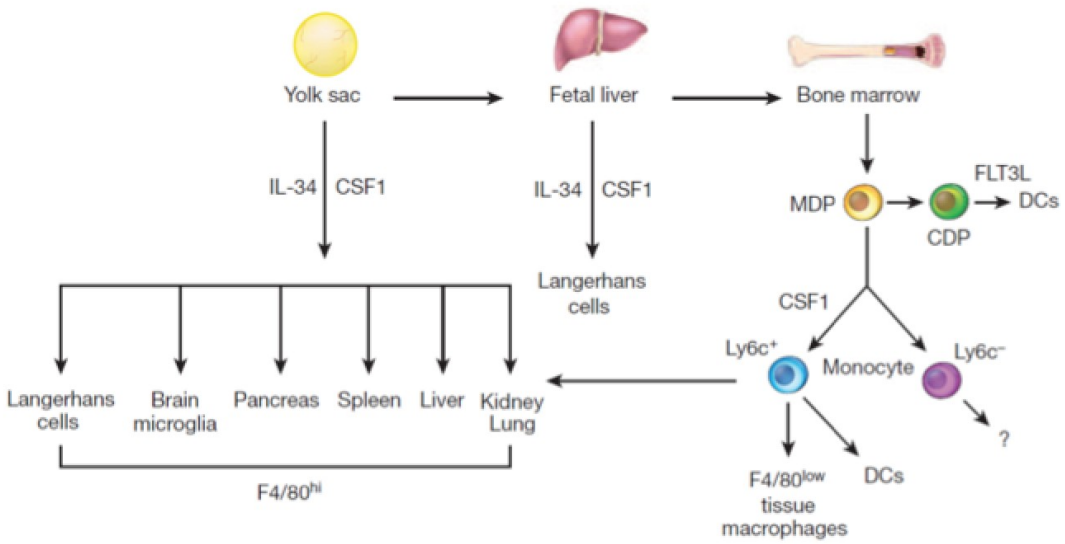

Figure 6: Macrophage ontogeny in mice.
The mononuclear phagocytic system in adults derives from at least three sources. The first is the yolk sac (YS) that results in progenitors that populate all tissues and their progeny persist throughout life as F4/80 bright resident macrophages. These lineages are largely regulated by CSF1R. The second from the fetal liver is less well defined but seems to contribute to adult LCs

perhaps through a progenitor derived from the YS. The third lineage derives from the bone marrow (BM) to give circulating monocytes and their progeny F4/80 ^{low} macrophages and DCs. In this case the Ly6C $^{+}$ monocytes give rise to classical DCs under the regulation of FLT3 and these are continuously replenished. Other macrophages that are F4/80^{low} also emanate from Ly6C^{+} monocytes and in some cases such as kidney and lung, co-exist with those derived from YS to give chimeric organs. The exact role of the patrolling Ly6C $^{+}$ macrophages remains unclear, as is the contribution of fetal liver to adult tissue macrophages [98].

Hence, in light of these recent findings, macrophage ontogeny in carcinogenesis has been revisited. A relevant question is whether TAMs are derived from the local tissue macrophage pool or whether they are newly recruited BM-derived cells. To date, developmental origins of TAMs have been best studied in mouse tumor models of the breast and lung and experimental indicationssuggest a monocyte origin for TAMs [112, 121-124]. In this regard, a recent study by Franklin *et al.*, conducted in the polyoma middle T (PyMT) oncogene-driven mouse model of breast cancer (MMTV-PyMT), showed that these monocyte-derived TAMs are continuously replaced via peripheral recruitment. In fact, they pointed out that the major TAMs population (MHCII ^{high}CD11b^{low}), as well as the mammary tissue-resident macrophage population ((MTMs) MHCII^{high}CD11b^{high}) originates from Ly6C ^{high}CCR2^{+} monocytes. However, the role of local renewal cannot be excluded, since they observed that TAMs also expand their population through *in situ* proliferation [122]. In line with these results, in another spontaneous breast cancer model MMTV-Neu, two TAMs populations were identified (CD11b^{high}F4/80^{low}MHCII^{high} and CD11b^{low}F4/80^{high}MHCII^{int}) and both were also found to be derived from monocytes, with the CD11b^{low} population heavily dependent on *in situ* proliferation [123].

Recent experimental evidences conducted in mouse models of lung carcinoma, suggest that TAMs also in the lung tumor are monocyte-derived, similar to their counterparts in breast cancers [121, 124]. A study by Cortez-Retamozo *et al.* showed that in the genetic Kras$^{LSL–G12D/+}$p53$^{fl/fl}$ lung carcinoma model, fluorescently tagged monocyte precursors were found to differentiate into macrophages in developing tumors. Furthermore, this study suggested that

instead of coming directly from the BM, a substantial fraction of TAMs arise from extra-medullary hematopoiesis within the spleen, which may function as a reservoir that continuously supplies the tumor with fresh progenitors [121], although the relative contribution of BM and spleen to the monocyte reservoire and tumor trafficking is not clear and might be tumor dependent [125].

Together, these findings suggest that TAMs can arise from tissue-resident macrophages, originating either from embryonic precursors which seed peripheral locations and self-sustain or from circulating monocytes, that may undergo a change in phenotype and/or activation state during carcinogenesis, or from inflammatory $Ly6C^{+}$ circulating monocytes that undergo a distinct differentiation step to become macrophages in response to tumor microenvironment, and that these two populations may both be present simultaneously in the tumor microenvironment potentially having differential roles.

TAMs differentiation and localization is not a defined and preserved track but depends on both anatomical location and the tumor stage: cancers with different histology are infiltrated by TAMs with phenotypic and functionally distinct properties [112]. Interestingly, TAMs heterogeneity may be due to the nature of the monocytic precursor that is recruited to the tumor. Clear indications emerging from several tumor models suggest that $Ly6C^{high}$ monocytes, which rely on the CCL2-CCR2 axis, are the major precursor of TAMs [112, 121, 122, 126].

In addition, a smaller subset of TAMs, encompasses monocytes that express the angiopoietin-2 receptor TIE2, may arise from $Ly6C^{low}CCR2^{-}$ monocytes. These pro-angiogenic TAMs, known as Tie2-expressing monocytes (TEMs), are recruited to the tumor by angiopoietin-2, localize preferentially in areas of angiogenesis, aligned along the abluminal surface of blood vessels, and play important non-redundant roles in tumor neovascularization [114, 127].

The development of macrophages from monocytes is regulated by several cytokines, such as IL-6, and myelopoietic growth factors, such as M-CSF and

GM-CSF [128]. Among these, M-CSF, also known as colony stimulating factor 1 (CSF1), is the major lineage regulator of macrophages regardless their arising from the yolk sac or BM, and in addition it is a chemotactic factor for macrophages [129]. In this regard, in several models of cancer, genetic deletion of CSF1 or CSF-1R signaling inhibition with anti-CSFR1 antibodies, results in reduced number of TAMs recruited in the tumor microenvironment associated with slowed tumor initiation or decreased disease progression and distal metastatic spread [130-132]. Indeed, elevated CSF1 levels correlated with marked macrophage infiltration in human metastatic breast cancer [25]. In addition, the transcription factor PU.1, which among other functions controls the expression of CSF1R, regulates differentiation of progenitors to the macrophage lineage [133].

Moreover, in a xenograft model of skin cancer, it was reported that also VEGFA recruits macrophage progenitors that then differentiate to TAMs under IL-4 influence and that loss of these VEGF-recruited TAMs inhibited tumor growth, angiogenesis and invasion [134]. These observations indicate that CSF1 and VEGFA can be independent recruiters of macrophages to tumors in mouse models and that this effect could be explicated via recruitment of monocytes and/or through proliferation of recruited or resident cells.

Compelling evidence indicate that these growth factors act collaboratively in the tumor microenvironment with locally synthesized TDFs, such as cytokines (e.g. IL-10, IL-4, IL-13, IFN-γ, IL-1β), chemokines (e.g. CCL2, CXCL12, CCL5) as well as growth factors and noncanonical chemotactic peptides (e.g. TGF-β, PGE2), to drive the monocyte-to-macrophage differentiation and the macrophage activation state inside tumors [122, 126, 135-137].

Several factors controlling TAMs phenotype coincide with signals driving "alternative" macrophage activation such as IL-10, IL-4 and IL-13. These latter, bind different receptors sharing the IL-4Rα chain that is responsible for recruiting and phosphorylating STAT6, which induces the transcription of genes

involved in the immune-suppressive program [138]. Recently, genetic evidence in the mouse suggested that complement components, C5a in particular, play an important role in recruitment and functional polarization of TAMs [139].

Interestingly, macrophages may also be affected by the metabolic environmental signals that are associated with malignant neoplasms. The tumor microenvironment is typically hypoxic and characterized by a high concentration of lactate due to the 'Warburg effect' namely the metabolic shift occurring in highly proliferating cells which predominantly convert glucose into lactate even in the presence of oxygen (aerobic glycolysis) [140]. This results in substantial production of lactic acid, which was recently shown to polarize TAMs activation toward an M2 state and to influence their spatial dissemination within specific areas of tumors [141]. In particolar, TAMs accumulate preferentially in poorly vascularized regions of tumors, suggesting that oxygen availability has a role in guiding their localization and function. Hypoxia promotes the metabolic adaptation of TAMs through the activation of hypoxia-inducible factors HIF-1α and HIF-2α. HIF-1α influences the positioning and function of tumor cells, stromal cells and TAMs by up-regulating their expression of CXCR4. Moreover, HIF-1α activation can have a role in the induction of the CXCR4 ligand CXCL12, a chemokine involved in cancer metastasis [142-144].

Despite these several indications, the detailed mechanisms for the recruitment and tumor-promoting function of TAMs are not fully understood; thus, further investigation is required to identify new targets for cancer immunotherapy.

1.4.3 Pro-tumoral mechanism of TAMs

For decades, solid tumors have been known to be strongly infiltrated by inflammatory leukocytes and accumulating evidences have clearly demonstrated in various mouse and human malignancies, that despite high levels of infiltration, macrophages are unable to stimulate an effective antitumor response and are instead generally associated with poor patient prognosis [4, 145, 146].
One of the most important characteristic of TAMs include their ability to directly affect tumor growth through promotion of tumor angiogenesis as well as the survival and metastasis of tumor cells [147, 148].
As already discussed, in terms of cytotoxicity and expression of inflammatory cytokines, we can say that TAMs resemble the M2 macrophages: both are poor producers of NO and of ROIs [149]; both are poor antigen presenting cells and not only they are unable to trigger Th1 polarized immune responses, but also they induce Treg cells and suppress T cell activation and proliferation [111].
Moreover, TAMs express high levels of both scavenger receptor-A (SR-A) and the mannose receptor (MR) together with other M2 markers like Arginase I, YM1, FIZZ1 [150].
In agreement with the M2 signature, TAMs were reported to express low levels of inflammatory cytokines (e.g. IL-12, IL-1β, TNFα, IL-6) [109].
Activation of the transcriptional factor NF- κB is a necessary event promoting transcription of several proinflammatory genes. TAMs display a defective NF-κB activation in response to M1 polarizing signals LPS and TNFα [151]. The defect in NF-κB was shown to be due to the over expression of nuclear p50 NF-κB homodimers which inhibit the transcription of proinflammatory genes [152].
The defective NF-κB activity was seen in TAMs isolated from tumors characterized by advanced stages and is in apparent contrast with TAMs NF- κB dependent pro-tumorigenic functions observed in murine models of inflammation-associated liver and colorectal cancer [153, 154]. This discrepancy might reflect a dynamic change in the tumor microenvironment

during the transition from early-neoplastic events to advanced tumor stages, which would result in progressive modulation of the NF- κB activity expressed by infiltrating inflammatory cells and progressive conversion of the TAMs from an M1 to an M2 macrophage phenotype (Fig. 7) [15].

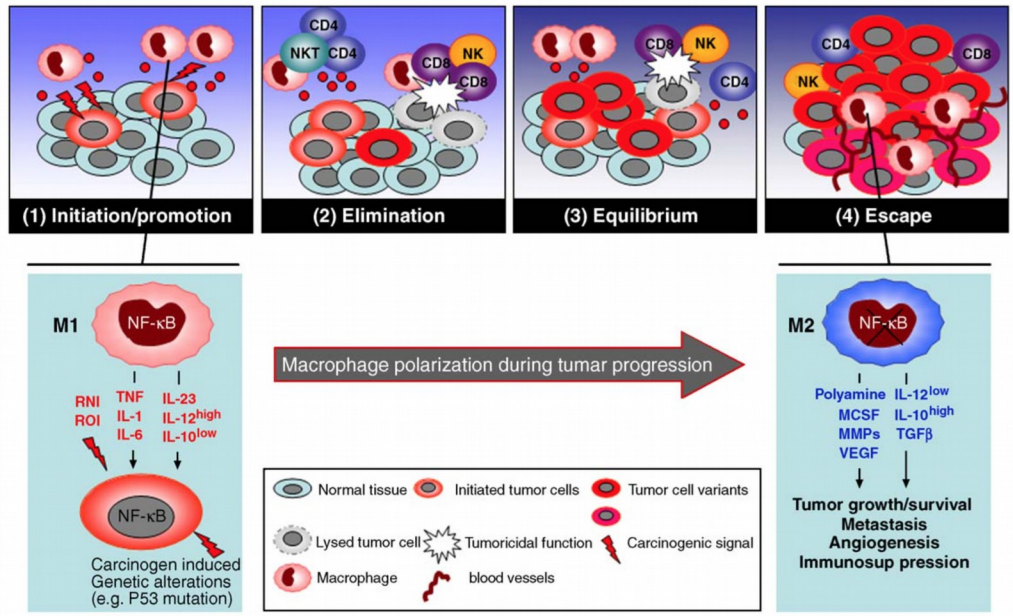

Figure 7: Macrophage polarization in tumor immunoediting and progression.
During tumor progression a gradual switching of macrophage polarization, M1 versus M2, is paralleled by the gradual inhibition of NF-κB activity. These events concur to establish permissive conditions for tumor growth and spread [100].

Interestingly, over-expression of p50 NF-κB has also been reported in endotoxin tolerant human monocytes which show defective TNFα production but overexpress IL-10, similar to the TAMs [155]. However, while in sepsis the over-expression of the p50 NF-κB represents a protective response against deregulation of the inflammatory process, in cancer it may be part of the immunosuppressive mechanisms associated with tumor growth [37].

TAMs favor tumor growth through non-immune and immune processes. Angiogenesis is an M2-associated function, which represents a key event in

tumor progression. Indeed, in several human cancers, TAMs accumulation has been associated with angiogenesis and with the production of angiogenic factors such as VEGF and platelet-derived endothelial cell growth factor [1, 156]. Additionally, TAMs participate to the proangiogenic process by producing the angiogenic factor thymidine phosphorylase, which promotes endothelial cell migration *in vitro* and whose level of expression is associated with tumor neovascularization [157].

TAMs also play an active role in promoting the spread of distal tumor cells. They express enzymes that regulate the digestion of the extracellular matrix, such as MMPs, plasmin, urokinase-type plasminogen activator [158] and the uPA receptor. In mammary tumors, TAMs promote metastatic diffusion via a paracrine loop involving CSF1 and EGF, which induces macrophages and tumor cells to cluster around blood vessels, where macrophages create a gate for tumor cell intravasation into the circulation, thus producing a tumor microenvironment for metastasis [35, 148, 159, 160].

As mentioned above, the most important pathogenic activity of TAMs is the suppression of anticancer immune responses. This ability is due at least partially on their reduced immunostimulatory properties. For instance, TAMs produce low levels of IL-12, which triggers tumoricidal actions of natural killer cells and the generation of cytotoxic $CD4^+$ T-cells, and high levels of immunosuppressive factors such as IL-10, TGFβ and PGE2, which recruit Treg-cells [150]. In particular, TAMs-derived IL-10 negatively regulates the production of IL-12 by tumor-associated myeloid cells and thus indirectly stimulates the differentiation of Th2 cells that release high levels of IL-4 and IL-13 reinforcing TAMs protumor phenotype [161].

TAMs can also direct suppress the cytotoxic functions of T-cells and this immunosuppression is mediated, at least in part, by nitrosylation of T-cell receptors via ARG1, iNOS and peroxynitrite, inducing T cell apoptosis [20, 162, 163]. Moreover, TAMs may also promote apoptosis of T-cells by

expressing on their cell surface the inhibitory B7 family molecules PD-L1 and B7-H1, which trigger checkpoint blockade in T cells [164].

Finally, TAMs maintain the cancer cell reservoir by providing a niche for cancer stem cells (CSC). Indeed, TAMs can sustain CSC proliferation by releasing proinflammatory cytokines such as TNF-α and IL-6, which reinforce tumor cell proliferation through NF-κB and STAT3 signaling pathways, and by producing milk fat globule EGF factor 8 (MFGE8), which favored CSC reservoir survival during chemotherapeutic treatment [165-167].

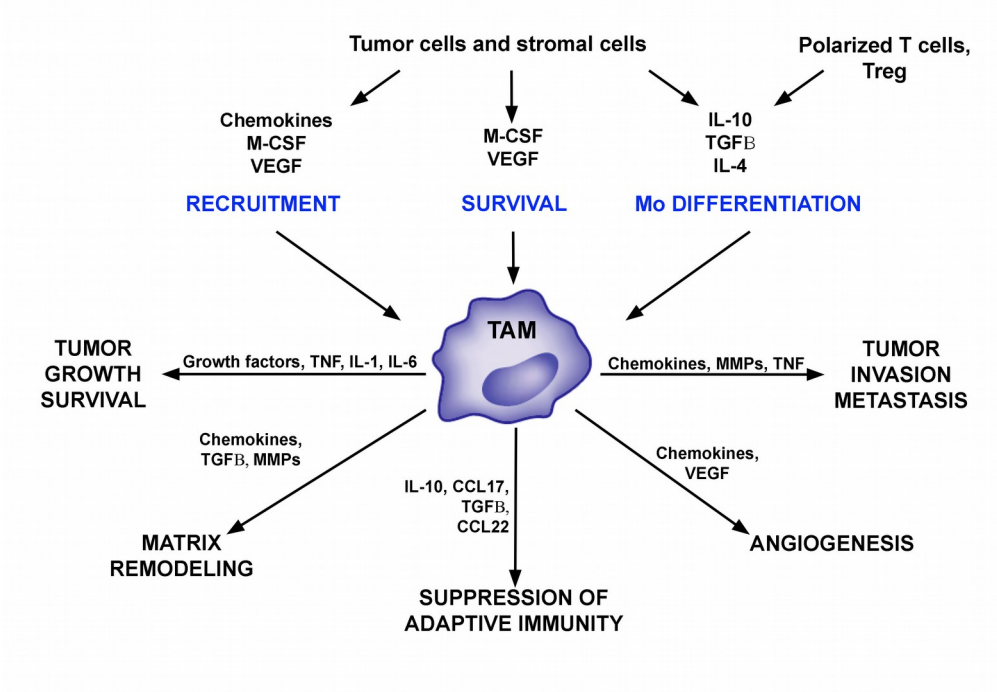

Figure 8: Pro-tumoral mechanisms of TAMs [101].

1.4.4 TAMs as therapeutic targets

It is now clear that cells of the monocyte-macrophage lineage are an essential element of the inflammatory component in the tumor contest that play a key role in supporting cancer development [168, 169]. In addition to these pro-tumoral activities, TAMs can also modulate the efficacy of various form of anticancer therapy [162, 170]. Based on this, both the recruitment and activation of TAMs are considered putative targets for therapeutic intervention. In particular, current therapeutic approaches affecting TAMs compartment are aimed either at reeducating their functional activation to an antitumor, M1-like phenotype or inhibiting their recruitment and/or survival in tumors [171].

As mentioned above, mediators involved in macrophage recruitment in tumors include for instance CCL2, CCL5, complement components, CSF-1 and VEGF and the inhibition of these molecules with specific monoclonal antibodies or antagonist prevent TAMs recruitment, reducing tumor growth and dissemination [122, 126]. Indeed, compelling evidences indicate that inhibition of CCL2 with specific antibodies reduced tumor growth in several experimental models such as prostate, melanoma, breast and lung cancer; moreover, when administered in combination with chemotherapy, anti-CCL2 antibodies improved the therapeutic efficacy [172-174]. However, it has been also shown in a breast cancer mouse model, that recession of anti-CCL2 treatment increased the mobilization and recruitment of circulating monocyte, thus accelerating lung metastasis [175].

Analysis of leukocyte migration in colon cancer (CRC) metastasis revealed overproduction of CCL5, a TAMs attractant also responsible for their functional skewing. Recent clinical studies reveal that treatment with a CCR5 antagonist result in biological and clinical responses in a small cohort of advanced CRC patients, indicating the CCL5-CCR5 axis another possible therapeutic target [176].

The CSF-1 receptor (CSF-1R) is exclusively expressed by the monocytic lineage, thus representing an obvious target to hit TAMs; accordingly, anti-CSF-1R neutralizing antibodies or small molecule inhibitors interfering with this pathway have been developed and tested in preclinical models [177, 178]. *Ries et al.* reported that treatment with anti-CSF-1R antibody (RG7155) strongly reduced TAMs infiltration in tumors accompanied by an increase of the $CD8^+/CD4^+$ T cell ratio, in animal models; in addition, administration of RG7155 to diffuse-type giant cell tumor (Dt-GCT) patients led to reductions of macrophages in tumor biopsies [131].

Moreover, TAMs depletion by anti-CSF1 antibodies enhanced the efficacy of combination chemotherapy (cyclophosphamide, methotrexate, and 5-fluoro-uracil) in chemoresistant, human breast cancer xenografts grown in immunodeficient mice [162]. Similarly, TAMs depletion improved the efficacy of paclitaxel in a transgenic mouse model of mammary adenocarcinoma [179]. Small molecule inhibitors to CSF1R have also been shown to deplete some populations of TAMs and to dramatically enhance responses to chemotherapy. This effect is at least in part consequent to the removal of macrophage-mediated immunosuppression leading to the increased of $CD8^+$ T cell infiltration during the tumor recovery period [162, 170].

Trabectedin is an anticancer drug licensed in Europe and several other countries for the treatment of soft tissue sarcoma patients and ovarian carcinoma patients; it was initially identified for its potent cytotoxic and antiproliferative activity against malignant cells [180]. Further clinical and experimental evidences indicate that trabectedin not only hits neoplastic cells but also importantly modulate tumor microenvironment; in particular, it activates a caspase-dependent pathway of apoptosis selectively in cells of the monocyte lineage, causing a partial depletion of circulating monocytes and TAMs. In murine tumors and in human sarcomas Trabectedin-induced TAMs reduction was associated with decreased angiogenesis and increased T-cell infiltration [62, 181, 182].

The contribution of TAMs to the modulation of tumor responses to chemotherapy can vary markedly among different cytotoxic agents and tumor models and intriguingly, increasing data suggest that the efficacy of some forms of immunotherapy may also depend on effective reprogramming of TAMs toward an M1-like phenotype. For example, the antitumor activity of the taxane docetaxel involves the depletion of immunosuppressive (M2-like) TAMs and the concomitant activation or expansion of antitumoral (M1-like) monocytes in 4T1-Neu mammary tumor implants. Indeed, *in vivo* T cell assays showed that docetaxel-treated monocytes/MDSCs are able to enhance tumor-specific cytotoxic T cell responses [183].

More specific macrophage targeting came from the administration of an anti-CD40 antibody in a preclinical model of pancreatic cancer, where alternatively activated, M2-like macrophages were re-educated in the tumor microenvironment to acquire antigen-presenting capabilities, leading to re-establishment of tumor immune surveillance and reduction of tumor progression [184].

Finally, recent clinical studies suggest that usage of nonsteroidal anti-inflammatory drugs, aspirin in particular, is associated with protection against occurrence of many tumors and metastasis and that this protective function relies on the inhibition of prostaglandin production [185, 186]. Ineed, PGE2 is well-known to have immune-suppressive effects and to favour M2-like polarization of TAMs [187, 188].

Overall these reports strongly indicate that macrophage-targeting strategies have the potential to complement and synergize with cytoreductive therapies, anti-angiogenic agents and immunotherapy [171].

1.5 The transcription factor NF-κB

NF-κB family has been considered the central mediator of the inflammatory process and a key participant in innate and adaptive immune responses; moreover during the last years it has been demonstrated that NF-κB could play a crucial role in cancer development [189].

NF-κB is evolutionarily conserved and plays a critical role in many biological systems, above all the immune system, where it acts as the major orchestrator of the transcriptional responses to many different stimuli. The engagement of several immune receptors such as B and T cell receptor (BCR, TCR), TLRs, Tumor Necrosis Factor Receptor (TNFR) or CD40 [190] triggers NF-κB activation which in turn results in the expression of cytokines, growth factors and effector enzymes. At present, more than 150 genes under control of NF-κB have been identified, as a demonstration of its vast spectrum of biological functions [191, 192].

Because NF-κB activation drives expression of key genes in inflammation, immunity, cell survival and proliferation its mis-regulation, such as constitutive activation, could be associated with pathological conditions such as rheumatoid arthritis, asthma, intestinal bowel diseases (IBDs), multiple sclerosis and cancer [193-196]. Given this great variety of biological roles, a better understanding of NF-κB pathways could provide the basis for the development of therapeutic strategies with a relevant impact on human diseases.

1.5.1 NF-κB family and activation

NF-κB family includes five members: RELA (p65), RELB, cREL, NF-κB1 (p105-p50) and NF-κB2 (p100-p52). All these proteins possess a conserved 300-amino acid REL homology domain (RHD) that is located toward the N-terminus of the proteins and is responsible for dimerization, binding to inhibitors of nuclear factor κB (IκBs) and binding to DNA. Instead, the carboxy-

terminal non-homologous transactivation domain (TAD), which strongly activates the transcription of targeted genes, is present only in cREL, RELB and RELA [197, 198]. p50 and p52 are generated by proteolytic degradation of p105 and p100 precursors and they lack the transactivation domain, therefore if they form homodimers they still bind the DNA consensus sites, but they do not activate transcription [199, 200]. Each member of NF-κB family, except for RELB, can form homodimers as well as heterodimers with one another and the main activated form of NF-κB is the heterodimer containing p65 together with p50 or p52 (Fig.9) [110].

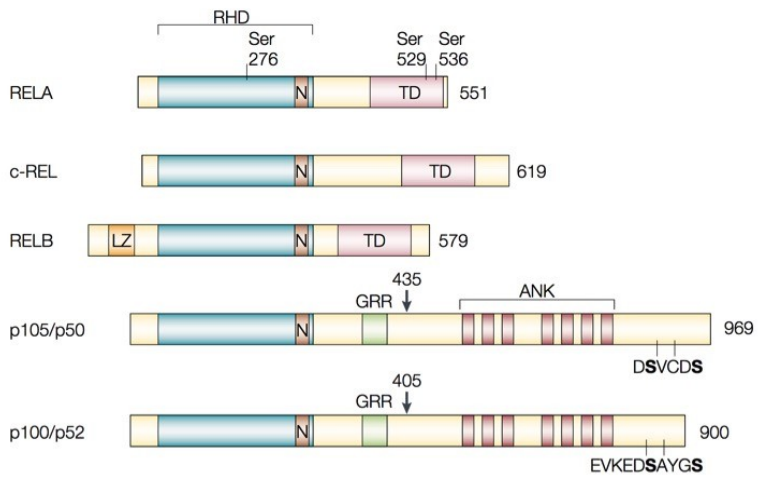

Figure 9: Mammalian NF-κB-family members.
NF-**k**B family comprises five members: RELA (p65), cREL, RELB, p105/p50 and p100/p52. Proteolytic processing of p105 and p100 at residues 435 and 405 (as indicated by arrows), respectively, generates the p50 and p52 NF-κB proteins. The glycine-rich region (GRR) and the carboxy-terminal sites of inducible phosphorylation (in the DSVCDS and EVKEDSAYGS sequences for p105 and p100, respectively) are required for processing. Phosphorylation of RELA at Ser276, Ser529 and Ser536 is important for its transactivation activity. The size of each human protein is shown on the right (number of amino acids) [110].

In resting conditions, IκBs exhert their regulatory function binding NF-κB proteins masking their Nuclear Localization Sequence (NLS). So, the complexes IκBs-NF-κB cannot translocate into the nucleus and are retained in

the cytoplasm in inactive forms. Triggering of many different receptors can induce NF-κB activation that is initiated upon phosphorylation of IκBs by IκB Kinases (IKK). IKK is a complex made by kinase subunits IKKα and IKKβ and the regulatory subunit IKKγ or NEMO (NF-κB Essencial Modifier). Hence, upon activation of IKKβ, IκB is phosphorylated and degraded by the proteasome, so the released NF-κB dimers can go to the nucleus and activate gene transcription [201-204].

NF-κB could be activated through two different pathways: classical and alternative[190]. The classical pathway is particularly involved in innate immunity, is activated predominantly by the subunit IKKβ in a NEMO dependent manner and is mainly mediated by Toll like receptors (TLRs), scavenger receptors and complement system. Signalling through TLRs leads to activation of canonical IKKs complexes, degradation of IκBs and activation of RELA and cREL containing NF-κB dimers. The released NF-κB dimers, that in this pathway are predominantly p65-p50 heterodimers, go to the nucleus and activate gene transcription. The beginning of an inflammatory response is strictly dependent on NF-κB classical pathway. Signals coming from the environment lead to the recruitment and activation of effector cells, initially neutrophils and later macrophages and other leukocytes, resulting in the tissue changes characteristic of inflammation – *rubor, calor, dolor and tumor* (redness, heat, pain and swelling, respectively) [199, 203, 205, 206].

The alternative pathway is particularly active in cells of the adaptive immunity, such as B and T lymphocytes, is independent of IKKβ and NEMO but it is dependent of IKKα homodimers, which selectively phosphorylate p100 associated with RELB. Therefore, the consequence is the release of active RELB-p52 heterodimers [207, 208]. Activation of NF-κB downstream B cell receptor (BCR) and T cell receptor (TCR) is a critical step for mounting adaptive immune responses allowing antigen specific maturation and proliferation of lymphocytes into effector cells [209].

1.5.2 NF-κB and cancer

Several evidence suggest that NF-κB is a molecular bridge between inflammation and cancer. Indeed, among all the different signaling pathways activated by inflammation and infection, NF-κB is the major activator of genes encoding for proteins important for cell proliferation (e.g. cyclin D1, c-Myc) survival (BCL-2, c-FLIP) adhesion, and angiogenesis (e.g. CXCL8, VEGF) [210].

In fact, as a master regulator of inflammation, NF-κB triggers the transcription of several proinflammatory mediators such as IL-1β, TNFα, IL-6 and IL-8. These factors are themself able to induce higher NF-κB activation, thus providing a positive feedback loop at the site of inflammation. This inflammatory environment favours DNA damage, cell proliferation, transformation and survival and consequently cancer initiation, growth and progression [154, 192].

The pro-inflammatory stimuli, such as bacterial products via Toll-like receptors or inflammatory cytokines (e.g. TNFα and IL1β), activate NF-κB that translocates into the nucleus inducing the expression of cytokines (such as TNFα and IL6) and chemokines, which contribute to the inflammation-related tissue damage. This elevated IKK/ NF-κB activity may also lead to aberrant up-regulation of certain tumorigenic, adhesion proteins, chemokines, and inhibitors of apoptosis that promote cell survival [211].

Hence, NF-κB is involved not only in tumor development at early stages, but also in the migration, invasion and metastasis of malignant cells [154]. For instance, the invasive capacity of cancer cells can increase in the presence of inflammatory cytokines such as TNFα, IL-1β and IL6 [3]. In particular, TNFα is a potent stimulator of epithelial-mesenchimal transition by breast cancer cells for its ability on activate NF-κB activation [212]. NF-κB was also found to promote metastatization in a genetic mouse model of prostate cancer, in which inactivation of IKKα was found to reduce metastatic spread [213].

Moreover, compelling indications demonstrate that in many cancers, NF-κB is constitutively active, even if the exact mechanism that sustain this activation is not fully understood and several mechanisms have been proposed, such as IL-1β and TNFα production, shorter IκBα half life or IκBα mutations [214, 215].
For these reasons, NF-κB represents an ideal therapeutic target for the development of new anti-tumor strategies.

p50/NF-κB1

The NF-κB1 gene encodes two functional proteins: p50 and p105. In particular, p105 is the precursor of p50, which is the active form of the protein and could form dimers with itself or with other NF-κB subunits. The role of p50 and its precursor in cell physiology and function is very complex. Indeed, although originally considered a repressor of transcription, p50 could also be a transcriptional activator and the balance between pro- and anti- inflammatory activity of p50 depends on cell type and environmental conditions [216, 217].
The nuclear translocation of p50 homodimers deeply controls functions of myeloid cells in cancer. In fact, it has been demonstrated that in LPS-tolerant macrophages increased expression of the p50 subunit of NF-κB directly results in the downregulation of LPS-induced TNFα production, whereas in p50 $^{-/-}$ macrophages long-term pre-treatment with LPS was unable to induce tolerance [100, 218]. Accordingly, as mentioned above, our group has demonstrated that TAMs display a defective NF-κB activation in response to the M1 polarizing signals (LPS and TNFα) and that this phenotype is due to the over expression of nuclear p50 NF-κB homodimers which inhibits the transcription of pro-inflammatory genes. On the contrary, we have shown that LPS stimulated p50 $^{-/-}$ TAMs recover an M1 (IL-12 ^{high}TNFα^{high}IL-10^{low}) phenotype that correlates, *in vivo*, with tumor growth inhibition [219]. Further, a detailed analysis of the role of p50 NF-κB homodimer in macrophage functions revealed that its nuclear accumulation, both in TAMs and LPS-tolerant macrophages, not only mediates

a status of unresponsiveness (tolerance) toward pro-inflammatory signals, but actually plays a role as key regulator of M2-driven inflammatory responses [152]. Hence p50 NF-κB regulates the orientation of macrophage polarization, playing a crucial role in the control of M1- vs. M2-driven inflammation [100]. Moreover, recently our group demonstrated that nuclear accumulation of p50 NF-κB promotes a tolerogenic phenotype in DCs, affecting both their survival and capacity to drive effective activation of effector T cells. In fact, lack of p50 in murine DCs promoted increased lifespan, enhanced level of maturation associated with increased expression of the pro-inflammatory cytokines IL-1, IL-18 and IFN-β, enhanced capacity of activating and expanding $CD4^+$ and $CD8^+$ T cells *in vivo* and decreased ability to induce differentiation of $FoxP3^+$ regulatory T cells [220].

So targeting p50 could represent a novel fascinating strategy to revert the immunosuppressive phenotype of tumor infiltrating myeloid cells and boost anti-tumor immunity.

1.6 Retinoid-related orphan receptors RORs

As mentioned above, it is well known that cancer is associated with a profound perturbation in myelopoiesis and that circulating hematopoietic stem and progenitor cells from patients with solid tumors have "myeloid-biased differentiation" [23]. Moreover, while "emergency" myelopoiesis to infection or trauma increases rapidly the inflammatory neutrophil and monocyte/macrophage pools, chronic cancer inflammation-driven myelopoiesis converges in splenic accumulation of immature MDSCs and TAMs recruitment at the tumor site [22, 37, 221]. While the pro-tumor functions of MDSCs and TAMs are well characterized [20], a large gap remains in our understanding of the mechanisms that translate persistent inflammation into reactive "emergency" myelopoiesis.

IL-17 is becoming of great interest, since in response to inflammation or infection it promotes G-CSF- and stem-cell-factor-mediated neutrophilia and supports G-CSF-driven “emergency” granulopoiesis [32]. Interestingly, it was also shown that IL-17 is required for the development of MDSCs in tumor-bearing mice; indeed, a defect in IL-17R reduces the number of MDSCs in the blood, spleen, and tumors whereas administration of exogenous IL-17 increases the number of MDSCs in wild-type tumor-bearing mice [222]. Therefore, despite IL-17 expression in tumor has been so far greatly restricted to the adaptive arm of immunity, TAMs and MDSCs produce the T-helper 17 (Th17)-driving cytokines TGFβ and IL-6 [223], suggesting that adaptive and innate immunity share IL-17-related molecular signaling pathways. Indeed, IL-17-expressing cells with macrophage morphology have been described in cancer patients [224].

Although in literature it is well described that retinoic-acid-related orphan receptor gamma (RORγ) full-length protein (RORC1) and the RORγt splice variant (RORC2) are master regulators of IL-17A gene transcription and of Th17 response [225-227], the signaling pathways that drive IL-17-producing innate immune cells have been poorly investigated. In subjects with arthritis mast cells express a dual IL-17A/RORC finger print in response to TLR4 ligands [228] and a population of RORγt-expressing neutrophils that express IL-17 in response to IL-6 and IL-23 was recently identified in a model of fungal infection [229]. These findings suggest a major role for IL-17 and related signaling cytokines and transcription factors in myeloid lineage commitment and function in inflammatory diseases, including cancer.

1.6.1 RORs structure and activity

RORs, together with receptors for steroid hormones, retinoids, thyroid hormone, eicosanoid metabolites, are member of the nuclear receptors (NRs) superfamily of transcription factors [230]. The ROR family comprises three members: RORα (NR1F1), ROR β (NR1F2) and ROR γ (NR1F3); these are considered to be 'orphan' receptors because their endogenous physiological ligands are either unknown or may not exist. Hence, they represent an active area of research due to the potential for identification of ligands that may be used to modulate these receptors with the goal of developing targeted therapeutics for various diseases [231, 232].

RORs exhibit a domain structure typical of NRs and contain an N-terminal domain, the function of which has not yet been clearly defined, a highly conserved DNA-binding domain (DBD) consisting of two zinc finger motifs, a carboxy-terminal ligand binding domain (LBD) and a hinge domain spacing the DBD and LBD [232]. RORs regulate transcription by binding as monomers to ROR response elements (RORE), which consist of the core sequence "AGGTCA" preceded by an A/T-rich sequence, in the regulatory region of target genes. When bound to this element within the promoters of their target genes, RORs constitutively recruit coactivators, leading to continual activation of transcription of their target genes. By using different promoters and/or alternative splicing each ROR gene produces several isoforms that vary only in their N-terminal region (Fig. 10) [233].

RORs display distinct patterns of tissue expression and because of their important regulatory roles in many key physiological processes (e.g. inflammation, lipid/glucose homeostasis and insuline resistance [234, 235]) dysregulation of signaling controlled by these receptors is associated with many diseases, including cancer [236].

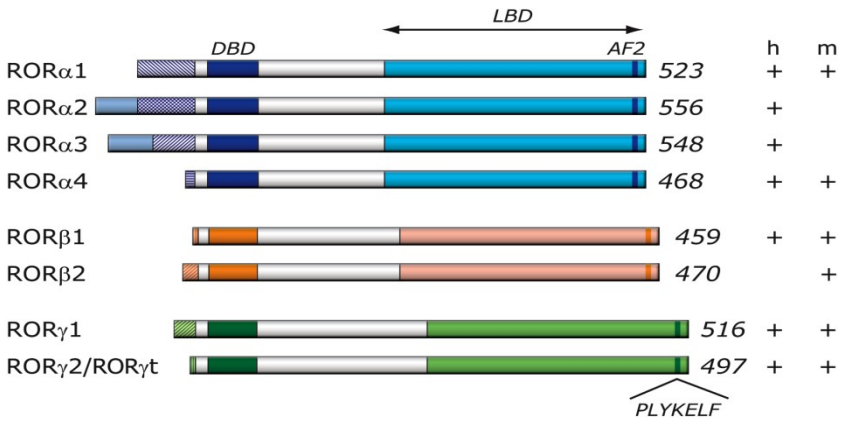

Figure 10: Schematic representation of RORs family members.
The different RORs isoforms identified in human and mouse are shown on the right (+/-) [233].

RORγ- RORγt

The RORγ (*RORC*) gene has been found to express two different isoforms, RORγ1 and RORγt (γ2)/RORC2 (mouse/human) that are expressed in a highly tissue-specific manner. In particular, RORγ1 is expressed in many tissues, including liver, adipose, skeletal muscle, and kidney, while the expression of RORγt is exclusively expressed in few distinct cell types of the immune system (i.e. immature $CD4^{+}/CD8^{+}$ thymocys and lymphoid tissue inducer (LTi) cells) [233, 237].

Mice deficient in RORγ expression lack lymph nodes and Peyer's patches (PPs) suggesting that RORγ is essential for lymph node organogenesis and development of PPs. RORγt also plays an important regulatory role in thymopoiesis, by reducing apoptosis of thymocytes and promoting thymocyte differentiation into pro-inflammatory Th17 cells [238-240].

Recent studies indicate also that RORγ provide an important link between the circadian clock machinery and its regulation of metabolic genes and metabolic syndrome [241, 242]. Accordingly, accumulating evidence indicates that RORγ play an important role in the regulation of several metabolic pathways,

particularly lipid and steroid metabolism. Moreover, deficiency in RORγ also protects against diet-induced insulin resistance [234, 243].

1.6.2 RORγ and cancer

The role of RORγt/RORC2 (mice/humans) in modulating mouse/human Th17 cell differentiation under conditions such as autoimmune and inflammatory diseases has been widely investigated; accordingly, a number of studies have provided evidence for a role of RORγ in cancer [233, 236, 244, 245]. For instance, mice deficient in the expression of RORγ exhibit a high incidence of thymic lymphomas that metastasize frequently to liver and spleen; as a consequence, the lifespan of $ROR\gamma^{-/-}$ mice is greatly reduced. The enhanced lymphoma formation may be related to the dysregulation of differentiation and proliferation in $ROR\gamma^{-/-}$ thymocytes [246].

Another potential link between RORγ and cancer is emerging from studies showing increased expression of Th17-associated genes, (e.g. RORγ, IL-17 and IL-23) in gastric tumors, an increase in the population of circulating Th17 cells in gastric cancer patients, and a high incidence of Th17 cells at sites of ovarian cancer [247, 248].

Several clinical studies have demonstrated that both IL-17 and RORC2 is expressed in tumor-infiltrating immune cells in human lung tissues from chronic obstructive pulmonary disease (COPD) patients [249] and that cutaneous T cell lymphoma, cervical carcinoma, prostate cancer and ovarian carcinoma spontaneously secrete IL-17 [250, 251]. Moreover, RORC2 was found to be expressed in melanoma [252] and in non-small cell lung cancer (NSCLC) patients where greatly contributes to tumor cell proliferation [253].

These findings highlight that RORγ plays critical roles in tumor generation and may represent therapeutic targets for many malignancies.

Bibliography

1. Balkwill, F. and A. Mantovani, *Inflammation and cancer: back to Virchow?* Lancet, 2001. **357**(9255): p. 539-45.
2. Grivennikov, S.I., F.R. Greten, and M. Karin, *Immunity, inflammation, and cancer.* Cell, 2010. **140**(6): p. 883-99.
3. Balkwill, F., K.A. Charles, and A. Mantovani, *Smoldering and polarized inflammation in the initiation and promotion of malignant disease.* Cancer Cell, 2005. **7**(3): p. 211-7.
4. Coussens, L.M. and Z. Werb, *Inflammation and cancer.* Nature, 2002. **420**(6917): p. 860-7.
5. Mantovani, A. and M.A. Pierotti, *Cancer and inflammation: a complex relationship.* Cancer Lett, 2008. **267**(2): p. 180-1.
6. Hussain, S.P. and C.C. Harris, *Inflammation and cancer: an ancient link with novel potentials.* Int J Cancer, 2007. **121**(11): p. 2373-80.
7. Mantovani, A., et al., *Cancer-related inflammation.* Nature, 2008. **454**(7203): p. 436-44.
8. Hanahan, D. and R.A. Weinberg, *The hallmarks of cancer.* Cell, 2000. **100**(1): p. 57-70.
9. Hanahan, D. and R.A. Weinberg, *Hallmarks of cancer: the next generation.* Cell, 2011. **144**(5): p. 646-74.
10. Mantovani, A., *Cancer: Inflaming metastasis.* Nature, 2009. **457**(7225): p. 36-7.
11. Balkwill, F. and L.M. Coussens, *Cancer: an inflammatory link.* Nature, 2004. **431**(7007): p. 405-6.
12. Borrello, M.G., et al., *Induction of a proinflammatory program in normal human thyrocytes by the RET/PTC1 oncogene.* Proc Natl Acad Sci U S A, 2005. **102**(41): p. 14825-30.
13. Ancrile, B., K.H. Lim, and C.M. Counter, *Oncogenic Ras-induced secretion of IL6 is required for tumorigenesis.* Genes Dev, 2007. **21**(14): p. 1714-9.
14. Negus, R.P., et al., *Quantitative assessment of the leukocyte infiltrate in ovarian cancer and its relationship to the expression of C-C chemokines.* Am J Pathol, 1997. **150**(5): p. 1723-34.
15. Dunn, G.P., et al., *Cancer immunoediting: from immunosurveillance to tumor escape.* Nat Immunol, 2002. **3**(11): p. 991-8.
16. Sica, A., et al., *Tumour-associated macrophages are a distinct M2 polarised population promoting tumour progression: potential targets of anti-cancer therapy.* Eur J Cancer, 2006. **42**(6): p. 717-27.
17. Mantovani, A., et al., *Tumor-associated macrophages and the related myeloid-derived suppressor cells as a paradigm of the diversity of macrophage activation.* Hum Immunol, 2009. **70**(5): p. 325-30.

18. Tosolini, M., et al., *Clinical impact of different classes of infiltrating T cytotoxic and helper cells (Th1, th2, treg, th17) in patients with colorectal cancer.* Cancer Res, 2011. **71**(4): p. 1263-71.
19. Liu, Y. and X. Cao, *Immunosuppressive cells in tumor immune escape and metastasis.* J Mol Med (Berl), 2016. **94**(5): p. 509-22.
20. Gabrilovich, D.I., S. Ostrand-Rosenberg, and V. Bronte, *Coordinated regulation of myeloid cells by tumours.* Nat Rev Immunol, 2012. **12**(4): p. 253-68.
21. Hu, L., et al., *The Interferon Consensus Sequence Binding Protein (Icsbp/Irf8) Is Required for Termination of Emergency Granulopoiesis.* J Biol Chem, 2016. **291**(8): p. 4107-20.
22. Messmer, M.N., et al., *Tumor-induced myeloid dysfunction and its implications for cancer immunotherapy.* Cancer Immunol Immunother, 2015. **64**(1): p. 1-13.
23. Ueha, S., F.H. Shand, and K. Matsushima, *Myeloid cell population dynamics in healthy and tumor-bearing mice.* Int Immunopharmacol, 2011. **11**(7): p. 783-8.
24. Metcalf, D., *Hematopoietic cytokines.* Blood, 2008. **111**(2): p. 485-91.
25. Qian, B.Z. and J.W. Pollard, *Macrophage diversity enhances tumor progression and metastasis.* Cell, 2010. **141**(1): p. 39-51.
26. Hirai, H., et al., *Non-steady-state hematopoiesis regulated by the C/EBPbeta transcription factor.* Cancer Sci, 2015. **106**(7): p. 797-802.
27. Marigo, I., et al., *Tumor-induced tolerance and immune suppression depend on the C/EBPbeta transcription factor.* Immunity, 2010. **32**(6): p. 790-802.
28. Croker, B.A., et al., *SOCS3 is a critical physiological negative regulator of G-CSF signaling and emergency granulopoiesis.* Immunity, 2004. **20**(2): p. 153-65.
29. Kreisel, D., et al., *Bcl3 prevents acute inflammatory lung injury in mice by restraining emergency granulopoiesis.* J Clin Invest, 2011. **121**(1): p. 265-76.
30. Zhang, H., et al., *STAT3 controls myeloid progenitor growth during emergency granulopoiesis.* Blood, 2010. **116**(14): p. 2462-71.
31. Friedman, A.D., *Transcriptional control of granulocyte and monocyte development.* Oncogene, 2007. **26**(47): p. 6816-28.
32. Liu, B., et al., *IL-17 is a potent synergistic factor with GM-CSF in mice in stimulating myelopoiesis, dendritic cell expansion, proliferation, and functional enhancement.* Exp Hematol, 2010. **38**(10): p. 877-884 e1.
33. Schwarzenberger, P., et al., *Requirement of endogenous stem cell factor and granulocyte-colony-stimulating factor for IL-17-mediated granulopoiesis.* J Immunol, 2000. **164**(9): p. 4783-9.
34. Gordy, C., et al., *Regulation of steady-state neutrophil homeostasis by macrophages.* Blood, 2011. **117**(2): p. 618-29.

35. Ugel, S., et al., *Tumor-induced myeloid deviation: when myeloid-derived suppressor cells meet tumor-associated macrophages.* J Clin Invest, 2015. **125**(9): p. 3365-76.
36. Bronte, V. and P.J. Murray, *Understanding local macrophage phenotypes in disease: modulating macrophage function to treat cancer.* Nat Med, 2015. **21**(2): p. 117-9.
37. Sica, A. and V. Bronte, *Altered macrophage differentiation and immune dysfunction in tumor development.* J Clin Invest, 2007. **117**(5): p. 1155-66.
38. Gabrilovich, D.I. and S. Nagaraj, *Myeloid-derived suppressor cells as regulators of the immune system.* Nat Rev Immunol, 2009. **9**(3): p. 162-74.
39. Kumar, V., et al., *The Nature of Myeloid-Derived Suppressor Cells in the Tumor Microenvironment.* Trends Immunol, 2016. **37**(3): p. 208-20.
40. Sinha, P., et al., *Cross-talk between myeloid-derived suppressor cells and macrophages subverts tumor immunity toward a type 2 response.* J Immunol, 2007. **179**(2): p. 977-83.
41. Youn, J.I., et al., *Subsets of myeloid-derived suppressor cells in tumor-bearing mice.* J Immunol, 2008. **181**(8): p. 5791-802.
42. Kusmartsev, S. and D.I. Gabrilovich, *Immature myeloid cells and cancer-associated immune suppression.* Cancer Immunol Immunother, 2002. **51**(6): p. 293-8.
43. Marvel, D. and D.I. Gabrilovich, *Myeloid-derived suppressor cells in the tumor microenvironment: expect the unexpected.* J Clin Invest, 2015. **125**(9): p. 3356-64.
44. Bronte, V., et al., *Recommendations for myeloid-derived suppressor cell nomenclature and characterization standards.* Nat Commun, 2016. **7**: p. 12150.
45. Talmadge, J.E. and D.I. Gabrilovich, *History of myeloid-derived suppressor cells.* Nat Rev Cancer, 2013. **13**(10): p. 739-52.
46. Mandruzzato, S., et al., *Toward harmonized phenotyping of human myeloid-derived suppressor cells by flow cytometry: results from an interim study.* Cancer Immunol Immunother, 2016. **65**(2): p. 161-9.
47. Almand, B., et al., *Increased production of immature myeloid cells in cancer patients: a mechanism of immunosuppression in cancer.* J Immunol, 2001. **166**(1): p. 678-89.
48. Corzo, C.A., et al., *Mechanism regulating reactive oxygen species in tumor-induced myeloid-derived suppressor cells.* J Immunol, 2009. **182**(9): p. 5693-701.
49. Highfill, S.L., et al., *Bone marrow myeloid-derived suppressor cells (MDSCs) inhibit graft-versus-host disease (GVHD) via an arginase-1-dependent mechanism that is up-regulated by interleukin-13.* Blood, 2010. **116**(25): p. 5738-47.

50. Chalmin, F., et al., *Membrane-associated Hsp72 from tumor-derived exosomes mediates STAT3-dependent immunosuppressive function of mouse and human myeloid-derived suppressor cells.* J Clin Invest, 2010. **120**(2): p. 457-71.
51. Waight, J.D., et al., *Myeloid-derived suppressor cell development is regulated by a STAT/IRF-8 axis.* J Clin Invest, 2013. **123**(10): p. 4464-78.
52. Bronte, V. and P. Zanovello, *Regulation of immune responses by L-arginine metabolism.* Nat Rev Immunol, 2005. **5**(8): p. 641-54.
53. Rodriguez, P.C., A.H. Zea, and A.C. Ochoa, *Mechanisms of tumor evasion from the immune response.* Cancer Chemother Biol Response Modif, 2003. **21**: p. 351-64.
54. Bingisser, R.M., et al., *Macrophage-derived nitric oxide regulates T cell activation via reversible disruption of the Jak3/STAT5 signaling pathway.* J Immunol, 1998. **160**(12): p. 5729-34.
55. Harari, O. and J.K. Liao, *Inhibition of MHC II gene transcription by nitric oxide and antioxidants.* Curr Pharm Des, 2004. **10**(8): p. 893-8.
56. Rivoltini, L., et al., *Immunity to cancer: attack and escape in T lymphocyte-tumor cell interaction.* Immunol Rev, 2002. **188**: p. 97-113.
57. Nagaraj, S., et al., *Altered recognition of antigen is a mechanism of CD8+ T cell tolerance in cancer.* Nat Med, 2007. **13**(7): p. 828-35.
58. De Sanctis, F., et al., *The emerging immunological role of post-translational modifications by reactive nitrogen species in cancer microenvironment.* Front Immunol, 2014. **5**: p. 69.
59. Agostinelli, E. and N. Seiler, *Non-irradiation-derived reactive oxygen species (ROS) and cancer: therapeutic implications.* Amino Acids, 2006. **31**(3): p. 341-55.
60. Letterio, J.J. and A.B. Roberts, *Regulation of immune responses by TGF-beta.* Annu Rev Immunol, 1998. **16**: p. 137-61.
61. Huang, B., et al., *Gr-1+CD115+ immature myeloid suppressor cells mediate the development of tumor-induced T regulatory cells and T-cell anergy in tumor-bearing host.* Cancer Res, 2006. **66**(2): p. 1123-31.
62. Germano, G., et al., *Role of macrophage targeting in the antitumor activity of trabectedin.* Cancer Cell, 2013. **23**(2): p. 249-62.
63. Duraiswamy, J., G.J. Freeman, and G. Coukos, *Therapeutic PD-1 pathway blockade augments with other modalities of immunotherapy T-cell function to prevent immune decline in ovarian cancer.* Cancer Res, 2013. **73**(23): p. 6900-12.
64. De Veirman, K., et al., *Myeloid-derived suppressor cells as therapeutic target in hematological malignancies.* Front Oncol, 2014. **4**: p. 349.
65. Bayne, L.J., et al., *Tumor-derived granulocyte-macrophage colony-stimulating factor regulates myeloid inflammation and T cell immunity in pancreatic cancer.* Cancer Cell, 2012. **21**(6): p. 822-35.

66. Sinha, P., et al., *Prostaglandin E2 promotes tumor progression by inducing myeloid-derived suppressor cells.* Cancer Res, 2007. **67**(9): p. 4507-13.
67. Bunt, S.K., et al., *Reduced inflammation in the tumor microenvironment delays the accumulation of myeloid-derived suppressor cells and limits tumor progression.* Cancer Res, 2007. **67**(20): p. 10019-26.
68. Mao, Y., et al., *Inhibition of tumor-derived prostaglandin-e2 blocks the induction of myeloid-derived suppressor cells and recovers natural killer cell activity.* Clin Cancer Res, 2014. **20**(15): p. 4096-106.
69. Wang, L., et al., *IL-17 can promote tumor growth through an IL-6-Stat3 signaling pathway.* J Exp Med, 2009. **206**(7): p. 1457-64.
70. Parker, K.H., D.W. Beury, and S. Ostrand-Rosenberg, *Myeloid-Derived Suppressor Cells: Critical Cells Driving Immune Suppression in the Tumor Microenvironment.* Adv Cancer Res, 2015. **128**: p. 95-139.
71. Gautier, E.L., et al., *Gene-expression profiles and transcriptional regulatory pathways that underlie the identity and diversity of mouse tissue macrophages.* Nat Immunol, 2012. **13**(11): p. 1118-28.
72. Nefedova, Y., et al., *Hyperactivation of STAT3 is involved in abnormal differentiation of dendritic cells in cancer.* J Immunol, 2004. **172**(1): p. 464-74.
73. Farren, M.R., et al., *Tumor-induced STAT3 signaling in myeloid cells impairs dendritic cell generation by decreasing PKCbetaII abundance.* Sci Signal, 2014. **7**(313): p. ra16.
74. Kusmartsev, S., S. Nagaraj, and D.I. Gabrilovich, *Tumor-associated CD8+ T cell tolerance induced by bone marrow-derived immature myeloid cells.* J Immunol, 2005. **175**(7): p. 4583-92.
75. Kusmartsev, S. and D.I. Gabrilovich, *STAT1 signaling regulates tumor-associated macrophage-mediated T cell deletion.* J Immunol, 2005. **174**(8): p. 4880-91.
76. Bronte, V., et al., *IL-4-induced arginase 1 suppresses alloreactive T cells in tumor-bearing mice.* J Immunol, 2003. **170**(1): p. 270-8.
77. Youn, J.I., et al., *Characterization of the nature of granulocytic myeloid-derived suppressor cells in tumor-bearing mice.* J Leukoc Biol, 2012. **91**(1): p. 167-81.
78. Sevko, A. and V. Umansky, *Myeloid-derived suppressor cells interact with tumors in terms of myelopoiesis, tumorigenesis and immunosuppression: thick as thieves.* J Cancer, 2013. **4**(1): p. 3-11.
79. Yang, L., et al., *Expansion of myeloid immune suppressor Gr+CD11b+ cells in tumor-bearing host directly promotes tumor angiogenesis.* Cancer Cell, 2004. **6**(4): p. 409-21.
80. Toh, B., et al., *Mesenchymal transition and dissemination of cancer cells is driven by myeloid-derived suppressor cells infiltrating the primary tumor.* PLoS Biol, 2011. **9**(9): p. e1001162.

81. Yan, H.H., et al., *Gr-1+CD11b+ myeloid cells tip the balance of immune protection to tumor promotion in the premetastatic lung.* Cancer Res, 2010. **70**(15): p. 6139-49.
82. Erler, J.T., et al., *Hypoxia-induced lysyl oxidase is a critical mediator of bone marrow cell recruitment to form the premetastatic niche.* Cancer Cell, 2009. **15**(1): p. 35-44.
83. Deng, J., et al., *S1PR1-STAT3 signaling is crucial for myeloid cell colonization at future metastatic sites.* Cancer Cell, 2012. **21**(5): p. 642-54.
84. Wesolowski, R., J. Markowitz, and W.E. Carson, 3rd, *Myeloid derived suppressor cells - a new therapeutic target in the treatment of cancer.* J Immunother Cancer, 2013. **1**: p. 10.
85. Naiditch, H., M.R. Shurin, and G.V. Shurin, *Targeting myeloid regulatory cells in cancer by chemotherapeutic agents.* Immunol Res, 2011. **50**(2-3): p. 276-85.
86. Suzuki, E., et al., *Gemcitabine selectively eliminates splenic Gr-1+/CD11b+ myeloid suppressor cells in tumor-bearing animals and enhances antitumor immune activity.* Clin Cancer Res, 2005. **11**(18): p. 6713-21.
87. Gujar, S.A., et al., *Gemcitabine enhances the efficacy of reovirus-based oncotherapy through anti-tumour immunological mechanisms.* Br J Cancer, 2014. **110**(1): p. 83-93.
88. Vincent, J., et al., *5-Fluorouracil selectively kills tumor-associated myeloid-derived suppressor cells resulting in enhanced T cell-dependent antitumor immunity.* Cancer Res, 2010. **70**(8): p. 3052-61.
89. Condamine, T., et al., *ER stress regulates myeloid-derived suppressor cell fate through TRAIL-R-mediated apoptosis.* J Clin Invest, 2014. **124**(6): p. 2626-39.
90. Nagaraj, S., et al., *Anti-inflammatory triterpenoid blocks immune suppressive function of MDSCs and improves immune response in cancer.* Clin Cancer Res, 2010. **16**(6): p. 1812-23.
91. Serafini, P., et al., *Phosphodiesterase-5 inhibition augments endogenous antitumor immunity by reducing myeloid-derived suppressor cell function.* J Exp Med, 2006. **203**(12): p. 2691-702.
92. Califano, J.A., et al., *Tadalafil augments tumor specific immunity in patients with head and neck squamous cell carcinoma.* Clin Cancer Res, 2015. **21**(1): p. 30-8.
93. De Santo, C., et al., *Nitroaspirin corrects immune dysfunction in tumor-bearing hosts and promotes tumor eradication by cancer vaccination.* Proc Natl Acad Sci U S A, 2005. **102**(11): p. 4185-90.
94. Kusmartsev, S., et al., *All-trans-retinoic acid eliminates immature myeloid cells from tumor-bearing mice and improves the effect of vaccination.* Cancer Res, 2003. **63**(15): p. 4441-9.

95. Mirza, N., et al., *All-trans-retinoic acid improves differentiation of myeloid cells and immune response in cancer patients.* Cancer Res, 2006. **66**(18): p. 9299-307.
96. Ko, J.S., et al., *Sunitinib mediates reversal of myeloid-derived suppressor cell accumulation in renal cell carcinoma patients.* Clin Cancer Res, 2009. **15**(6): p. 2148-57.
97. Bruchard, M., et al., *Chemotherapy-triggered cathepsin B release in myeloid-derived suppressor cells activates the Nlrp3 inflammasome and promotes tumor growth.* Nat Med, 2013. **19**(1): p. 57-64.
98. Wynn, T.A., A. Chawla, and J.W. Pollard, *Macrophage biology in development, homeostasis and disease.* Nature, 2013. **496**(7446): p. 445-55.
99. Mosser, D.M. and J.P. Edwards, *Exploring the full spectrum of macrophage activation.* Nat Rev Immunol, 2008. **8**(12): p. 958-69.
100. Mantovani, A. and A. Sica, *Macrophages, innate immunity and cancer: balance, tolerance, and diversity.* Curr Opin Immunol, 2010. **22**(2): p. 231-7.
101. Mantovani, A., P. Allavena, and A. Sica, *Tumour-associated macrophages as a prototypic type II polarised phagocyte population: role in tumour progression.* Eur J Cancer, 2004. **40**(11): p. 1660-7.
102. Mantovani, A., et al., *Macrophage plasticity and polarization in tissue repair and remodelling.* J Pathol, 2013. **229**(2): p. 176-85.
103. Biswas, S.K. and A. Mantovani, *Macrophage plasticity and interaction with lymphocyte subsets: cancer as a paradigm.* Nat Immunol, 2010. **11**(10): p. 889-96.
104. Murray, P.J., et al., *Macrophage activation and polarization: nomenclature and experimental guidelines.* Immunity, 2014. **41**(1): p. 14-20.
105. Sica, A. and A. Mantovani, *Macrophage plasticity and polarization: in vivo veritas.* J Clin Invest, 2012. **122**(3): p. 787-95.
106. Sica, A., et al., *Macrophage polarization in tumour progression.* Semin Cancer Biol, 2008. **18**(5): p. 349-55.
107. Gordon, S., *Alternative activation of macrophages.* Nat Rev Immunol, 2003. **3**(1): p. 23-35.
108. Martinez, F.O., L. Helming, and S. Gordon, *Alternative activation of macrophages: an immunologic functional perspective.* Annu Rev Immunol, 2009. **27**: p. 451-83.
109. Mantovani, A., et al., *Macrophage polarization: tumor-associated macrophages as a paradigm for polarized M2 mononuclear phagocytes.* Trends Immunol, 2002. **23**(11): p. 549-55.
110. Li, Q. and I.M. Verma, *NF-kappaB regulation in the immune system.* Nat Rev Immunol, 2002. **2**(10): p. 725-34.
111. Sica, A., et al., *Origin and Functions of Tumor-Associated Myeloid Cells (TAMCs).* Cancer Microenviron, 2012. **5**(2): p. 133-49.

112. Movahedi, K., et al., *Different tumor microenvironments contain functionally distinct subsets of macrophages derived from Ly6C(high) monocytes.* Cancer Res, 2010. **70**(14): p. 5728-39.
113. Ruffell, B., et al., *Leukocyte composition of human breast cancer.* Proc Natl Acad Sci U S A, 2012. **109**(8): p. 2796-801.
114. Pucci, F., et al., *A distinguishing gene signature shared by tumor-infiltrating Tie2-expressing monocytes, blood "resident" monocytes, and embryonic macrophages suggests common functions and developmental relationships.* Blood, 2009. **114**(4): p. 901-14.
115. De Palma, M. and C.E. Lewis, *Macrophage regulation of tumor responses to anticancer therapies.* Cancer Cell, 2013. **23**(3): p. 277-86.
116. Mantovani, A., et al., *The origin and function of tumor-associated macrophages.* Immunol Today, 1992. **13**(7): p. 265-70.
117. Gentek, R., K. Molawi, and M.H. Sieweke, *Tissue macrophage identity and self-renewal.* Immunol Rev, 2014. **262**(1): p. 56-73.
118. Sieweke, M.H. and J.E. Allen, *Beyond stem cells: self-renewal of differentiated macrophages.* Science, 2013. **342**(6161): p. 1242974.
119. Hambardzumyan, D., D.H. Gutmann, and H. Kettenmann, *The role of microglia and macrophages in glioma maintenance and progression.* Nat Neurosci, 2016. **19**(1): p. 20-7.
120. van de Laar, L., et al., *Yolk Sac Macrophages, Fetal Liver, and Adult Monocytes Can Colonize an Empty Niche and Develop into Functional Tissue-Resident Macrophages.* Immunity, 2016. **44**(4): p. 755-68.
121. Cortez-Retamozo, V., et al., *Origins of tumor-associated macrophages and neutrophils.* Proc Natl Acad Sci U S A, 2012. **109**(7): p. 2491-6.
122. Franklin, R.A., et al., *The cellular and molecular origin of tumor-associated macrophages.* Science, 2014. **344**(6186): p. 921-5.
123. Tymoszuk, P., et al., *In situ proliferation contributes to accumulation of tumor-associated macrophages in spontaneous mammary tumors.* Eur J Immunol, 2014. **44**(8): p. 2247-62.
124. Laoui, D., et al., *Tumor hypoxia does not drive differentiation of tumor-associated macrophages but rather fine-tunes the M2-like macrophage population.* Cancer Res, 2014. **74**(1): p. 24-30.
125. Shand, F.H., et al., *Tracking of intertissue migration reveals the origins of tumor-infiltrating monocytes.* Proc Natl Acad Sci U S A, 2014. **111**(21): p. 7771-6.
126. Qian, B.Z., et al., *CCL2 recruits inflammatory monocytes to facilitate breast-tumour metastasis.* Nature, 2011. **475**(7355): p. 222-5.
127. De Palma, M., et al., *Tie2 identifies a hematopoietic lineage of proangiogenic monocytes required for tumor vessel formation and a mesenchymal population of pericyte progenitors.* Cancer Cell, 2005. **8**(3): p. 211-26.

128. Movahedi, K. and J.A. Van Ginderachter, *The Ontogeny and Microenvironmental Regulation of Tumor-Associated Macrophages.* Antioxid Redox Signal, 2016.
129. Chitu, V. and E.R. Stanley, *Colony-stimulating factor-1 in immunity and inflammation.* Curr Opin Immunol, 2006. **18**(1): p. 39-48.
130. Laoui, D., et al., *Functional Relationship between Tumor-Associated Macrophages and Macrophage Colony-Stimulating Factor as Contributors to Cancer Progression.* Front Immunol, 2014. **5**: p. 489.
131. Ries, C.H., et al., *Targeting tumor-associated macrophages with anti-CSF-1R antibody reveals a strategy for cancer therapy.* Cancer Cell, 2014. **25**(6): p. 846-59.
132. Nowicki, A., et al., *Impaired tumor growth in colony-stimulating factor 1 (CSF-1)-deficient, macrophage-deficient op/op mouse: evidence for a role of CSF-1-dependent macrophages in formation of tumor stroma.* Int J Cancer, 1996. **65**(1): p. 112-9.
133. Hamilton, J.A., et al., *The critical role of the colony-stimulating factor-1 receptor in the differentiation of myeloblastic leukemia cells.* Mol Cancer Res, 2008. **6**(3): p. 458-67.
134. Linde, N., et al., *Vascular endothelial growth factor-induced skin carcinogenesis depends on recruitment and alternative activation of macrophages.* J Pathol, 2012. **227**(1): p. 17-28.
135. Su, S., et al., *A positive feedback loop between mesenchymal-like cancer cells and macrophages is essential to breast cancer metastasis.* Cancer Cell, 2014. **25**(5): p. 605-20.
136. Kitamura, T., et al., *Inactivation of chemokine (C-C motif) receptor 1 (CCR1) suppresses colon cancer liver metastasis by blocking accumulation of immature myeloid cells in a mouse model.* Proc Natl Acad Sci U S A, 2010. **107**(29): p. 13063-8.
137. Van Dyken, S.J. and R.M. Locksley, *Interleukin-4- and interleukin-13-mediated alternatively activated macrophages: roles in homeostasis and disease.* Annu Rev Immunol, 2013. **31**: p. 317-43.
138. Gray, M.J., et al., *Induction of arginase I transcription by IL-4 requires a composite DNA response element for STAT6 and C/EBPbeta.* Gene, 2005. **353**(1): p. 98-106.
139. Bonavita, E., et al., *Phagocytes as Corrupted Policemen in Cancer-Related Inflammation.* Adv Cancer Res, 2015. **128**: p. 141-71.
140. Tannahill, G.M., et al., *Succinate is an inflammatory signal that induces IL-1beta through HIF-1alpha.* Nature, 2013. **496**(7444): p. 238-42.
141. Colegio, O.R., et al., *Functional polarization of tumour-associated macrophages by tumour-derived lactic acid.* Nature, 2014. **513**(7519): p. 559-63.
142. Corzo, C.A., et al., *HIF-1alpha regulates function and differentiation of myeloid-derived suppressor cells in the tumor microenvironment.* J Exp Med, 2010. **207**(11): p. 2439-53.

143. Ceradini, D.J., et al., *Progenitor cell trafficking is regulated by hypoxic gradients through HIF-1 induction of SDF-1.* Nat Med, 2004. **10**(8): p. 858-64.
144. Muller, A., et al., *Involvement of chemokine receptors in breast cancer metastasis.* Nature, 2001. **410**(6824): p. 50-6.
145. Bingle, L., N.J. Brown, and C.E. Lewis, *The role of tumour-associated macrophages in tumour progression: implications for new anticancer therapies.* J Pathol, 2002. **196**(3): p. 254-65.
146. Zhang, Q.W., et al., *Prognostic significance of tumor-associated macrophages in solid tumor: a meta-analysis of the literature.* PLoS One, 2012. **7**(12): p. e50946.
147. Pollard, J.W., *Tumour-educated macrophages promote tumour progression and metastasis.* Nat Rev Cancer, 2004. **4**(1): p. 71-8.
148. Condeelis, J. and J.W. Pollard, *Macrophages: obligate partners for tumor cell migration, invasion, and metastasis.* Cell, 2006. **124**(2): p. 263-6.
149. Klimp, A.H., et al., *Expression of cyclooxygenase-2 and inducible nitric oxide synthase in human ovarian tumors and tumor-associated macrophages.* Cancer Res, 2001. **61**(19): p. 7305-9.
150. Biswas, S.K., et al., *A distinct and unique transcriptional program expressed by tumor-associated macrophages (defective NF-kappaB and enhanced IRF-3/STAT1 activation).* Blood, 2006. **107**(5): p. 2112-22.
151. Sica, A., et al., *Autocrine production of IL-10 mediates defective IL-12 production and NF-kappa B activation in tumor-associated macrophages.* J Immunol, 2000. **164**(2): p. 762-7.
152. Porta, C., et al., *Tolerance and M2 (alternative) macrophage polarization are related processes orchestrated by p50 nuclear factor kappaB.* Proc Natl Acad Sci U S A, 2009. **106**(35): p. 14978-83.
153. Greten, F.R., et al., *IKKbeta links inflammation and tumorigenesis in a mouse model of colitis-associated cancer.* Cell, 2004. **118**(3): p. 285-96.
154. Pikarsky, E., et al., *NF-kappaB functions as a tumour promoter in inflammation-associated cancer.* Nature, 2004. **431**(7007): p. 461-6.
155. Ziegler-Heitbrock, L., *The p50-homodimer mechanism in tolerance to LPS.* J Endotoxin Res, 2001. **7**(3): p. 219-22.
156. Lin, E.Y., et al., *Macrophages regulate the angiogenic switch in a mouse model of breast cancer.* Cancer Res, 2006. **66**(23): p. 11238-46.
157. Hotchkiss, K.A., A.W. Ashton, and E.L. Schwartz, *Thymidine phosphorylase and 2-deoxyribose stimulate human endothelial cell migration by specific activation of the integrins alpha 5 beta 1 and alpha V beta 3.* J Biol Chem, 2003. **278**(21): p. 19272-9.
158. Cho, M.S., et al., *Autocrine Effects of Tumor-Derived Complement.* Cell Reports, 2014. **6**(6): p. 1085-1095.
159. Kitamura, T., B.Z. Qian, and J.W. Pollard, *Immune cell promotion of metastasis.* Nat Rev Immunol, 2015. **15**(2): p. 73-86.

160. Wyckoff, J.B., et al., *Direct visualization of macrophage-assisted tumor cell intravasation in mammary tumors.* Cancer Res, 2007. **67**(6): p. 2649-56.
161. DeNardo, D.G., et al., *CD4(+) T cells regulate pulmonary metastasis of mammary carcinomas by enhancing protumor properties of macrophages.* Cancer Cell, 2009. **16**(2): p. 91-102.
162. DeNardo, D.G., et al., *Leukocyte complexity predicts breast cancer survival and functionally regulates response to chemotherapy.* Cancer Discov, 2011. **1**(1): p. 54-67.
163. Lu, T., et al., *Tumor-infiltrating myeloid cells induce tumor cell resistance to cytotoxic T cells in mice.* J Clin Invest, 2011. **121**(10): p. 4015-29.
164. Kondo, A., et al., *Interferon-gamma and tumor necrosis factor-alpha induce an immunoinhibitory molecule, B7-H1, via nuclear factor-kappaB activation in blasts in myelodysplastic syndromes.* Blood, 2010. **116**(7): p. 1124-31.
165. Wan, S., et al., *Tumor-associated macrophages produce interleukin 6 and signal via STAT3 to promote expansion of human hepatocellular carcinoma stem cells.* Gastroenterology, 2014. **147**(6): p. 1393-404.
166. Lu, H., et al., *A breast cancer stem cell niche supported by juxtacrine signalling from monocytes and macrophages.* Nat Cell Biol, 2014. **16**(11): p. 1105-17.
167. Jinushi, M., et al., *Tumor-associated macrophages regulate tumorigenicity and anticancer drug responses of cancer stem/initiating cells.* Proc Natl Acad Sci U S A, 2011. **108**(30): p. 12425-30.
168. Ginhoux, F., et al., *New insights into the multidimensional concept of macrophage ontogeny, activation and function.* Nat Immunol, 2016. **17**(1): p. 34-40.
169. Glass, C.K. and G. Natoli, *Molecular control of activation and priming in macrophages.* Nat Immunol, 2016. **17**(1): p. 26-33.
170. Mitchem, J.B., et al., *Targeting tumor-infiltrating macrophages decreases tumor-initiating cells, relieves immunosuppression, and improves chemotherapeutic responses.* Cancer Res, 2013. **73**(3): p. 1128-41.
171. Mantovani, A. and P. Allavena, *The interaction of anticancer therapies with tumor-associated macrophages.* J Exp Med, 2015. **212**(4): p. 435-45.
172. Loberg, R.D., et al., *Targeting CCL2 with systemic delivery of neutralizing antibodies induces prostate cancer tumor regression in vivo.* Cancer Res, 2007. **67**(19): p. 9417-24.
173. Lu, X. and Y. Kang, *Chemokine (C-C motif) ligand 2 engages CCR2+ stromal cells of monocytic origin to promote breast cancer metastasis to lung and bone.* J Biol Chem, 2009. **284**(42): p. 29087-96.

174. Li, X., et al., *Targeting of tumour-infiltrating macrophages via CCL2/CCR2 signalling as a therapeutic strategy against hepatocellular carcinoma.* Gut, 2015.
175. Bonapace, L., et al., *Cessation of CCL2 inhibition accelerates breast cancer metastasis by promoting angiogenesis.* Nature, 2014. **515**(7525): p. 130-3.
176. Halama, N., et al., *Tumoral Immune Cell Exploitation in Colorectal Cancer Metastases Can Be Targeted Effectively by Anti-CCR5 Therapy in Cancer Patients.* Cancer Cell, 2016. **29**(4): p. 587-601.
177. Goswami, S., et al., *Macrophages promote the invasion of breast carcinoma cells via a colony-stimulating factor-1/epidermal growth factor paracrine loop.* Cancer Res, 2005. **65**(12): p. 5278-83.
178. Pyonteck, S.M., et al., *CSF-1R inhibition alters macrophage polarization and blocks glioma progression.* Nat Med, 2013. **19**(10): p. 1264-72.
179. Javeed, A., et al., *Paclitaxel and immune system.* Eur J Pharm Sci, 2009. **38**(4): p. 283-90.
180. D'Incalci, M. and C.M. Galmarini, *A review of trabectedin (ET-743): a unique mechanism of action.* Mol Cancer Ther, 2010. **9**(8): p. 2157-63.
181. D'Incalci, M., et al., *Trabectedin, a drug acting on both cancer cells and the tumour microenvironment.* Br J Cancer, 2014. **111**(4): p. 646-50.
182. Allavena, P., et al., *Trabectedin: A drug from the sea that strikes tumor-associated macrophages.* Oncoimmunology, 2013. **2**(6): p. e24614.
183. Kodumudi, K.N., et al., *A novel chemoimmunomodulating property of docetaxel: suppression of myeloid-derived suppressor cells in tumor bearers.* Clin Cancer Res, 2010. **16**(18): p. 4583-94.
184. Beatty, G.L., et al., *CD40 agonists alter tumor stroma and show efficacy against pancreatic carcinoma in mice and humans.* Science, 2011. **331**(6024): p. 1612-6.
185. Cuzick, J., et al., *Estimates of benefits and harms of prophylactic use of aspirin in the general population.* Ann Oncol, 2015. **26**(1): p. 47-57.
186. Trinchieri, G., *Innate inflammation and cancer: Is it time for cancer prevention?* F1000 Med Rep, 2011. **3**: p. 11.
187. Obermajer, N., et al., *PGE(2)-driven induction and maintenance of cancer-associated myeloid-derived suppressor cells.* Immunol Invest, 2012. **41**(6-7): p. 635-57.
188. Luan, B., et al., *CREB pathway links PGE2 signaling with macrophage polarization.* Proc Natl Acad Sci U S A, 2015. **112**(51): p. 15642-7.
189. DiDonato, J.A., F. Mercurio, and M. Karin, *NF-kappaB and the link between inflammation and cancer.* Immunol Rev, 2012. **246**(1): p. 379-400.
190. Bonizzi, G. and M. Karin, *The two NF-kappaB activation pathways and their role in innate and adaptive immunity.* Trends Immunol, 2004. **25**(6): p. 280-8.

191. Dieguez-Gonzalez, R., et al., *Genetic variation in the nuclear factor kappaB pathway in relation to susceptibility to rheumatoid arthritis.* Ann Rheum Dis, 2009. **68**(4): p. 579-83.
192. Sethi, G., B. Sung, and B.B. Aggarwal, *Nuclear factor-kappaB activation: from bench to bedside.* Exp Biol Med (Maywood), 2008. **233**(1): p. 21-31.
193. Abdulamir, A.S., et al., *Severity of asthma: the role of CD25+, CD30+, NF-kappaB, and apoptotic markers.* J Investig Allergol Clin Immunol, 2009. **19**(3): p. 218-24.
194. Spehlmann, M.E. and L. Eckmann, *Nuclear factor-kappa B in intestinal protection and destruction.* Curr Opin Gastroenterol, 2009. **25**(2): p. 92-9.
195. Kurylowicz, A. and J. Nauman, *The role of nuclear factor-kappaB in the development of autoimmune diseases: a link between genes and environment.* Acta Biochim Pol, 2008. **55**(4): p. 629-47.
196. Hagemann, T., et al., *Regulation of macrophage function in tumors: the multifaceted role of NF-kappaB.* Blood, 2009. **113**(14): p. 3139-46.
197. Kawai, T. and S. Akira, *Signaling to NF-kappaB by Toll-like receptors.* Trends Mol Med, 2007. **13**(11): p. 460-9.
198. Ghosh, S., M.J. May, and E.B. Kopp, *NF-kappa B and Rel proteins: evolutionarily conserved mediators of immune responses.* Annu Rev Immunol, 1998. **16**: p. 225-60.
199. May, M.J. and S. Ghosh, *Rel/NF-kappa B and I kappa B proteins: an overview.* Semin Cancer Biol, 1997. **8**(2): p. 63-73.
200. Silverman, N. and T. Maniatis, *NF-kappaB signaling pathways in mammalian and insect innate immunity.* Genes Dev, 2001. **15**(18): p. 2321-42.
201. Malek, S., et al., *IkappaBbeta, but not IkappaBalpha, functions as a classical cytoplasmic inhibitor of NF-kappaB dimers by masking both NF-kappaB nuclear localization sequences in resting cells.* J Biol Chem, 2001. **276**(48): p. 45225-35.
202. Jacobs, M.D. and S.C. Harrison, *Structure of an IkappaBalpha/NF-kappaB complex.* Cell, 1998. **95**(6): p. 749-58.
203. Ghosh, S. and M. Karin, *Missing pieces in the NF-kappaB puzzle.* Cell, 2002. **109 Suppl**: p. S81-96.
204. Rothwarf, D.M. and M. Karin, *The NF-kappa B activation pathway: a paradigm in information transfer from membrane to nucleus.* Sci STKE, 1999. **1999**(5): p. RE1.
205. Oeckinghaus, A. and S. Ghosh, *The NF-kappaB family of transcription factors and its regulation.* Cold Spring Harb Perspect Biol, 2009. **1**(4): p. a000034.
206. Alcamo, E., et al., *Targeted mutation of TNF receptor I rescues the RelA-deficient mouse and reveals a critical role for NF-kappa B in leukocyte recruitment.* J Immunol, 2001. **167**(3): p. 1592-600.

207. Dejardin, E., et al., *The lymphotoxin-beta receptor induces different patterns of gene expression via two NF-kappaB pathways.* Immunity, 2002. **17**(4): p. 525-35.
208. Xiao, G., A. Fong, and S.C. Sun, *Induction of p100 processing by NF-kappaB-inducing kinase involves docking IkappaB kinase alpha (IKKalpha) to p100 and IKKalpha-mediated phosphorylation.* J Biol Chem, 2004. **279**(29): p. 30099-105.
209. Ruland, J. and T.W. Mak, *From antigen to activation: specific signal transduction pathways linking antigen receptors to NF-kappaB.* Semin Immunol, 2003. **15**(3): p. 177-83.
210. Karin, M., *Nuclear factor-kappaB in cancer development and progression.* Nature, 2006. **441**(7092): p. 431-6.
211. Shishodia, S. and B.B. Aggarwal, *Nuclear factor-kappaB activation: a question of life or death.* J Biochem Mol Biol, 2002. **35**(1): p. 28-40.
212. Bates, R.C. and A.M. Mercurio, *Tumor necrosis factor-alpha stimulates the epithelial-to-mesenchymal transition of human colonic organoids.* Mol Biol Cell, 2003. **14**(5): p. 1790-800.
213. Luo, J.L., et al., *Nuclear cytokine-activated IKKalpha controls prostate cancer metastasis by repressing Maspin.* Nature, 2007. **446**(7136): p. 690-4.
214. Giri, D.K. and B.B. Aggarwal, *Constitutive activation of NF-kappaB causes resistance to apoptosis in human cutaneous T cell lymphoma HuT-78 cells. Autocrine role of tumor necrosis factor and reactive oxygen intermediates.* J Biol Chem, 1998. **273**(22): p. 14008-14.
215. Krappmann, D., et al., *Molecular mechanisms of constitutive NF-kappaB/Rel activation in Hodgkin/Reed-Sternberg cells.* Oncogene, 1999. **18**(4): p. 943-53.
216. Inoue, J., et al., *I kappa B gamma, a 70 kd protein identical to the C-terminal half of p110 NF-kappa B: a new member of the I kappa B family.* Cell, 1992. **68**(6): p. 1109-20.
217. Cao, S., et al., *NF-kappaB1 (p50) homodimers differentially regulate pro- and anti-inflammatory cytokines in macrophages.* J Biol Chem, 2006. **281**(36): p. 26041-50.
218. Baer, M., et al., *Tumor necrosis factor alpha transcription in macrophages is attenuated by an autocrine factor that preferentially induces NF-kappaB p50.* Mol Cell Biol, 1998. **18**(10): p. 5678-89.
219. Saccani, A., et al., *p50 nuclear factor-kappaB overexpression in tumor-associated macrophages inhibits M1 inflammatory responses and antitumor resistance.* Cancer Res, 2006. **66**(23): p. 11432-40.
220. Larghi, P., et al., *The p50 subunit of NF-kappaB orchestrates dendritic cell lifespan and activation of adaptive immunity.* PLoS One, 2012. **7**(9): p. e45279.

221. Wu, W.C., et al., *Circulating hematopoietic stem and progenitor cells are myeloid-biased in cancer patients.* Proc Natl Acad Sci U S A, 2014. **111**(11): p. 4221-6.
222. He, D., et al., *IL-17 promotes tumor development through the induction of tumor promoting microenvironments at tumor sites and myeloid-derived suppressor cells.* J Immunol, 2010. **184**(5): p. 2281-8.
223. Zamarron, B.F. and W. Chen, *Dual roles of immune cells and their factors in cancer development and progression.* Int J Biol Sci, 2011. **7**(5): p. 651-8.
224. Zhu, X., et al., *IL-17 expression by breast-cancer-associated macrophages: IL-17 promotes invasiveness of breast cancer cell lines.* Breast Cancer Res, 2008. **10**(6): p. R95.
225. Ivanov, II, et al., *The orphan nuclear receptor RORgammat directs the differentiation program of proinflammatory IL-17+ T helper cells.* Cell, 2006. **126**(6): p. 1121-33.
226. Yang, X.O., et al., *T helper 17 lineage differentiation is programmed by orphan nuclear receptors ROR alpha and ROR gamma.* Immunity, 2008. **28**(1): p. 29-39.
227. Manel, N., D. Unutmaz, and D.R. Littman, *The differentiation of human T(H)-17 cells requires transforming growth factor-beta and induction of the nuclear receptor RORgammat.* Nat Immunol, 2008. **9**(6): p. 641-9.
228. Hueber, A.J., et al., *Mast cells express IL-17A in rheumatoid arthritis synovium.* J Immunol, 2010. **184**(7): p. 3336-40.
229. Taylor, P.R., et al., *Activation of neutrophils by autocrine IL-17A-IL-17RC interactions during fungal infection is regulated by IL-6, IL-23, RORgammat and dectin-2.* Nat Immunol, 2014. **15**(2): p. 143-51.
230. Mangelsdorf, D.J., et al., *The nuclear receptor superfamily: the second decade.* Cell, 1995. **83**(6): p. 835-9.
231. Solt, L.A. and T.P. Burris, *Action of RORs and their ligands in (patho)physiology.* Trends Endocrinol Metab, 2012. **23**(12): p. 619-27.
232. Jetten, A.M., *Recent advances in the mechanisms of action and physiological functions of the retinoid-related orphan receptors (RORs).* Curr Drug Targets Inflamm Allergy, 2004. **3**(4): p. 395-412.
233. Jetten, A.M., *Retinoid-related orphan receptors (RORs): critical roles in development, immunity, circadian rhythm, and cellular metabolism.* Nucl Recept Signal, 2009. **7**: p. e003.
234. Meissburger, B., et al., *Adipogenesis and insulin sensitivity in obesity are regulated by retinoid-related orphan receptor gamma.* EMBO Mol Med, 2011. **3**(11): p. 637-51.
235. Wittke, A., et al., *Vitamin D receptor-deficient mice fail to develop experimental allergic asthma.* J Immunol, 2004. **173**(5): p. 3432-6.
236. Oh, T.G., et al., *The Nuclear Receptor, RORgamma, Regulates Pathways Necessary for Breast Cancer Metastasis.* EBioMedicine, 2016. **6**: p. 59-72.

237. Eberl, G., et al., *An essential function for the nuclear receptor RORgamma(t) in the generation of fetal lymphoid tissue inducer cells.* Nat Immunol, 2004. **5**(1): p. 64-73.
238. Eberl, G. and D.R. Littman, *The role of the nuclear hormone receptor RORgammat in the development of lymph nodes and Peyer's patches.* Immunol Rev, 2003. **195**: p. 81-90.
239. Jetten, A.M. and J.H. Joo, *Retinoid-related Orphan Receptors (RORs): Roles in Cellular Differentiation and Development.* Adv Dev Biol, 2006. **16**: p. 313-355.
240. Chen, Z., A. Laurence, and J.J. O'Shea, *Signal transduction pathways and transcriptional regulation in the control of Th17 differentiation.* Semin Immunol, 2007. **19**(6): p. 400-8.
241. Duez, H. and B. Staels, *The nuclear receptors Rev-erbs and RORs integrate circadian rhythms and metabolism.* Diab Vasc Dis Res, 2008. **5**(2): p. 82-8.
242. Takeda, Y., et al., *RORgamma directly regulates the circadian expression of clock genes and downstream targets in vivo.* Nucleic Acids Res, 2012. **40**(17): p. 8519-35.
243. Tinahones, F.J., et al., *The retinoic acid receptor-related orphan nuclear receptor gamma1 (RORgamma1): a novel player determinant of insulin sensitivity in morbid obesity.* Obesity (Silver Spring), 2012. **20**(3): p. 488-97.
244. Wang, J., et al., *ROR-gamma drives androgen receptor expression and represents a therapeutic target in castration-resistant prostate cancer.* Nat Med, 2016. **22**(5): p. 488-96.
245. Vacca, M., et al., *Nuclear receptors in regenerating liver and hepatocellular carcinoma.* Mol Cell Endocrinol, 2013. **368**(1-2): p. 108-19.
246. Kurebayashi, S., et al., *Retinoid-related orphan receptor gamma (RORgamma) is essential for lymphoid organogenesis and controls apoptosis during thymopoiesis.* Proc Natl Acad Sci U S A, 2000. **97**(18): p. 10132-7.
247. Zhang, F., G. Meng, and W. Strober, *Interactions among the transcription factors Runx1, RORgammat and Foxp3 regulate the differentiation of interleukin 17-producing T cells.* Nat Immunol, 2008. **9**(11): p. 1297-306.
248. Miyahara, Y., et al., *Generation and regulation of human CD4+ IL-17-producing T cells in ovarian cancer.* Proc Natl Acad Sci U S A, 2008. **105**(40): p. 15505-10.
249. Chu, S., et al., *The expression of Foxp3 and ROR gamma t in lung tissues from normal smokers and chronic obstructive pulmonary disease patients.* Int Immunopharmacol, 2011. **11**(11): p. 1780-8.

250. Ciree, A., et al., *Expression and activity of IL-17 in cutaneous T-cell lymphomas (mycosis fungoides and Sezary syndrome).* Int J Cancer, 2004. **112**(1): p. 113-20.
251. Steiner, G.E., et al., *Expression and function of pro-inflammatory interleukin IL-17 and IL-17 receptor in normal, benign hyperplastic, and malignant prostate.* Prostate, 2003. **56**(3): p. 171-82.
252. Slominski, A.T., et al., *RORalpha and ROR gamma are expressed in human skin and serve as receptors for endogenously produced noncalcemic 20-hydroxy- and 20,23-dihydroxyvitamin D.* FASEB J, 2014. **28**(7): p. 2775-89.
253. Huang, Q., et al., *Retinoic acid-related orphan receptor C isoform 2 expression and its prognostic significance for non-small cell lung cancer.* J Cancer Res Clin Oncol, 2016. **142**(1): p. 263-72.

Chapter 2

2. Outline of the thesis

"Emergency" hematopoiesis is defined as a modification of the magnitude and composition of the hematopoietic output that occurs during immunological stress, including tumor progression, to ensure proper supply of immune cells to increased demand. Myeloid cells, in particular, abundantly expand in tumor bearers and infiltrate almost all solid cancers, where microenvironmental signals promote their transcriptional reprogramming towards a tumor-promoting phenotype. Although dynamic changes in myeloid cell functions have been reported to parallel tumor progression, a large gap remains in our understanding of the molecular pathways guiding this cancer-driven "emergency" myelopoiesis.

Recent studies reveal that tumor associated macrophages (TAMs) and myeloid derived suppressor cells (MDSCs), the two major myeloid populations associated with cancer development, differentiate from a common myeloid progenitor (CMP) into functionally altered myeloid cells. These populations display functional plasticity and are considered to have a major impact on the orchestration of cancer-related inflammation, promoting the construction of a protumor microenvironment and a protumor host macroenvironment associated with increased serum hematopoietic colony-stimulating activity and "emergency" hematopoiesis.

Myeloid cell plasticity is exemplified in the M1 vs M2 extremes of macrophage polarization, which respectively express different anti- vs pro- inflammatory functional outcomes in response to polarizing signals, including cytokines. Moreover, polarized macrophages (either M1 or M2) reprogram their responses towards a subsequent exposure to Th1 (IFN-γ) or Th2 (IL-4) cytokines.

Cancer fuels myeloid cells heterogeneity by promoting sustained myelopoiesis. Investigation of signaling pathways controlling hematopoiesis revealed that G-CSF-induced "emergency" granulopoiesis is mediated through the transcription factors c-EBPβ and STAT3, whereas M-CSF supports monocyte differentiation

through activation of the transcription factors PU.1 and IRF8. Of relevance, GM- CSF and M-CSF respectively represent prototypical M1 vs M2 polarizing signals, thus affecting both differentiation and polarization of myeloid cells. Thus, investigation of the molecular networks dictating reciprocal regulation of macrophage versus neutrophil/granulocyte differentiation appears to be crucial, as it may affect tissue homeostasis during cancerogenesis.

In this scenario, also IL-17 is becoming of great interest, since in response to inflammation or infection it promotes G-CSF-mediated neutrophilia and supports G-CSF-driven "emergency" granulopoiesis. Interestingly, it was also shown that IL-17 is required for the development of MDSCs in tumor-bearing mice and that TAMs and MDSCs produce the Th17-driving cytokines TGFβ and IL-6; moreover, IL-17-expressing cells with macrophage morphology have been described in cancer patients.

Although in literature it is well described that retinoic-acid-related orphan receptor gamma (RORγ) full-length protein (RORC1) and the RORCγt splice variant (RORC2) are master regulators of IL-17A gene transcription and of Th17 response, the signaling pathways that drive IL-17-producing innate immune cells have been poorly investigated. These observations led us to hypothesize that IL-17 and RORC, might be involved in mediating both expansion and transcriptional reprogramming of MDSCs and TAMs, through modulation of granulo- vs mono/macrophage-lineage commitment, thereby contributing to tumor growth. Hence, our challenge is to clarify the role of RORC1 in driving myeloid lineage commitment in cancer bearers, in order to generate clinically translatable strategies preventing the protumoral commitment of myeloid cells.

Both the recruitment and activation of tumor associated myeloid cells may be considered putative targets for therapeutic intervention; accordingly, because of their unique role in linking the innate and adaptive immunity, macrophage-based immunotherapy is widely considered in clinical trials with cancer patients. In particular, current therapeutic approaches affecting TAMs

compartment are aimed either at reeducating their functional activation to an antitumor, M1-like, phenotype or inhibiting their recruitment and/or survival in tumors. Several evidences indicate that massive presence of TAMs in solid tumor correlates with a poor prognosis. TAMs favor tumor growth and progression through the production of anti-inflammatory cytokines that suppress anti-tumor adaptive immunity. Moreover, they help invasion, angiogenesis and metastasis since they produce pro-angiogenic factors and matrix remodelling agents. Hence, modulating the recruitment of TAMs in tumors could be important to improve anti-tumor therapies.

We previously reported that, during cancer progression massive nuclear, accumulation of p50 NF-κB in TAMs results in the lack of responsiveness to M1 polarizing signals, including LPS and TNF α, along with an increased capacity to express M2 genes in response to the M2 polarizing cytokines, correlating with impaired inflammatory functions and tumor promotion. Interestingly, similar to the TAMs, p50 NF-κB accumulation in monocytes/macrophages is essential for endotoxin tolerance as well as for M2 polarized activation. Yet, little is known about the forces that drive the recruitment of TAMs into tumors, or more generally, of M2 polarized macrophages into sites of inflammation. Hence, the challenge is to identify new potential anti-tumor targets by studying the mechanisms underlying differentiation and recruitment of myeloid cells in neoplastic tissue. Given the importance of p50 NF-κB in driving the phenotype of tolerant macrophages, we investigated whether p50 controls differentiation and/or recruitment and pathogenic roles of macrophage subsets to inflamed tissues, including the tumor microenvironment.

Chapter 3

Homing regulation of distinct macrophage subsets in infection and cancer

Unpublished results

Francesca Maria Consonni[1], Maria Grazia Totaro,[2] Chiara Porta,[1] Marco Fabbri[3] and Antonio Sica [1,2,*]

[1]Department of Pharmaceutical Sciences, Università del Piemonte Orientale "Amedeo Avogadro," Via Bovio 6, 28100 Novara, Italy.

[2]Department of Inflammation and Immunology, Humanitas Clinical and Research Center, 20089 Rozzano, Milan, Italy.

[3]European Commission, Joint Research Centre (JRC), Institute for Health and Consumer Protection (IHCP), Nanobiosciences (NBS) Unit, via E. Fermi 2749, 21027 Ispra, Varese, Italy .

*Correspondence: antonio.sica@humanitasresearch.it

Abstract

Tumor associated macrophages (TAMs) share a typical M2-skewed phenotype with lipopolysaccharide- (LPS-) tolerant macrophages. Both populations display impaired capacity to mount an effective M1 inflammatory response and this phenotype, often referred to as "tolerance", is driven by nuclear accumulation of p50 NF-κB inhibitory homodimers. It's widely accepted that TAMs recruitment into tumors correlates with poor prognosis, however, the detailed mechanisms underlying the recruitment of M2-like macrophages to inflamed tissues, including the tumor microenvironment, are not fully understood. Given the importance of p50 NF-κB in driving macrophage's tolerance, we investigated whether nuclear accumulation of p50 may also mediate the recruitment of M2-like macrophages to inflamed tissues. This study demonstrates that p50 NF-κB accumulation is a necessary event guiding the chemotactic responsiveness of tolerant macrophages to complement anaphylatoxins C3a and C5a. By using an in vivo model of LPS-tolerance, we demonstrate a differential recruitment into the inflammatory sites of distinct F4/80^{+} macrophage subsets characterized by different expression levels of F4/80 and the C5aR (CD88), respectively defined as F4/80^{high}CD88^{high} and F4/80^{low}CD88^{low}. Of relevance, we observed systemic accumulation (blood) of the CD88^{high} mono/macrophage population only in tolerant conditions (LPS-tolerance and sepsis), both in mouse and human, strengthening the idea that p50-dependent induction of systemic tolerance is required for the systemic expansion of F4/80^{high}CD88^{high} mono/macrophages. Differential expansion of the F4/80^{low}CD88^{low} and F4/80 ^{high}CD88^{high} populations was confirmed also in the preclinical MN/MCA1 fibrosarcoma model, supporting a direct link with conditions of emergency hematopoiesis. Consistent with the LPS-tolerance model, ablation of p50 NF-κB resulted in significant impairment of F4/80^{high}CD88^{high} TAMs accumulation in primary tumors, which correlated with inhibition of tumor growth and vascularization. Moreover, transcriptome

analysis proved that F4/80^{high} and F4/80^{low} TAMs express different genetic programs, supporting putative different roles in tumor progression. Thus, our study provides evidence that distinct macrophage subset, arise during infection- and cancer-driven inflammation, in a p50 NF-κB-dependent manner and that complement-mediated pathways drives their infiltration of inflammatory sites, including solid tumors. Future studies will provide the functional characterization and roles of these populations in infection and cancer.

Introduction

Leukocyte migration is an indispensable process occurring in several physiological and pathological events. Accordingly, inflammatory and immune responses mostly involve the recruitment of circulating monocytes into specific tissues [1]. Myeloid cells, in particular, abundantly expand in tumor bearers and infiltrate almost all solid cancers, where microenvironmental signals promote their transcriptional reprogramming towards a tumor-promoting phenotype [2, 3]. Tumor associated macrophages (TAMs) are the major component of leucocytes infiltrating tumors and extensive presence of TAMs correlate with poor prognosis in a widely variety of human carcinomas [4-6]. Indeed, in established cancers, TAMs entail pro-tumor functions, since they express an M2-skewed phenotype, associated with suppression of adaptive immune functions and promotion of angiogenesis and invasion [3]. However, due to their well known functional plasticity, these cells can also express an M1 phenotype, associated with anti-tumor activities [7-9]. M1 and M2 functional phenotypes are the extremes of a continuum of diverse activation states [10], hence, in response to the complex tissue-derived signals that macrophages receive, cells in different functional states or with a mixed phenotype can coexist in the same tumor [11]. We previously reported that during cancer progression nuclear accumulation of p50 NF-κB in TAMs results in the lack of responsiveness to M1 polarizing signals (e.g. IFNγ) along with an increased capacity to express M2 genes in response to the M2 polarizing cytokines (e.g. IL-4, IL-10), correlating with impaired inflammatory functions and tumor promotion [12]. Prompted by these evidences, current macrophage-centered therapeutic approaches are aimed either at activating their antitumor activity or inhibiting their recruitment in tumors [13-15]. Chemoattractants involved in monocyte recruitment include chemokines (e.g. CCL2, CCL5, CXCL4) [16-18], colony-stimulating factor-1 (CSF-1) [19, 20], and members of the VEGF family [21]. Recently, genetic evidence in the mouse suggested that complement

components play also an important role in accumulation and functional polarization of TAMs [22, 23]. Nevertheless, the detailed mechanisms underlying the recruitment of M2-like macrophages to inflamed tissues, including tumor microenvironment, are not fully understood.

TAMs share nuclear overexpression of p50 NF-κB and the anti-inflammatory M2 phenotype with lipopolysaccharide- (LPS-) tolerant macrophages. LPS-tolerance is a state of hypo-responsiveness acquired after prolonged exposure of macrophages to inflammatory agents, including bacterial products such as LPS. Tolerant macrophages enter into a transient unresponsive state and are unable to respond to further stimulation with endotoxin, but still produce high level of anti-inflammatory cytokines involved in wound healing, clearing of cell debris and pathogens, dampening of the inflammatory response. This phenomenon has been observed both *in vitro* and *in vivo* in animal models, as well as in humans, and is mainly mediated by nuclear accumulation of p50 NF-κB homodimers [24-26]. Accordingly, acquisition of a tolerant phenotype could be important in protecting the host from a prolonged inflammation and in the resolution of the inflammatory response and the ability to recruit tolerant macrophages would ameliorate the outcome of pathologies characterized by chronic inflammation. Thus, we speculate that more detailed insights into the M2-like macrophages-recruitment factors in infection and cancer will provide new opportunities for therapeutic intervention.

By using *in vivo* LPS-tolerance and tumor mouse models, we study new mechanisms underling tolerant macrophages recruitment in infection and cancer and we demonstrated that nuclear accumulation of p50 NF-κB promotes the recruitment of specific $F4/80^{+}$ macrophage subset, expressing high level of F4/80 and complement receptor factors (C5aR and C3aR), into inflammatory sites, including solid tumors. Strikingly, we showed that defect in the accumulation of $F4/80^{high}$ population in the tumor microenvironment correlates with an impaired tumor growth.

Materials and methods

Ethics statement. The study was designed in compliance with: Italian Governing Law (Legislative Decree 116 of Jan. 27, 1992); EU directives and guidelines (EEC Council Directive 86/609, OJ L 358, 12/12/1986); Legislative Decree September 19, 1994, n. 626 (89/391/CEE, 89/654/CEE, 89/655/CEE, 89/656/CEE, 90/269/CEE, 90/270/CEE, 90/394/CEE, 90/679/CEE); the NIH Guide for the Care and Use of Laboratory Animals (1996 edition); Authorization n. 11/2006-A issued January 23, 2006 by Ministry of Health. The study was approved by the scientific board of Humanitas Clinical and Research Center. Mice have been monitored daily and euthanized when displaying excessive discomfort. Septic patients were enrolled in the study after signing Cancer Research Center Humanitas IRB-approved consent.

Mice. C57BL/6 mice were purchased from Charles River (Calco, Italy). p50 NF-κB deficient mice on the C57BL/6J background were available in the laboratory [12]. Homozygous C3 mutant mice (B6;129S4-*C3*^{tm1Crr}/J) were obtained from Jackson Laboratories (Bar Harbor, Maine, USA).

MN/MCA1 tumor model. 8 weeks old mice were injected intramuscularly in the left leg with 10^5 cells of murine fibrosarcoma (MN/MCA1). Tumor growth was monitored three times a week with a caliper, starting from day 14.

Cell Culture and Reagents. Thioglycollate-elicited peritoneal exudate cells (PEC) were isolated from healthy mice as previously described [26]. Briefly, mice were injected I.P. with 1 ml of 3% (wt/vol) with thioglycollate medium (Difco). Peritoneal exudate cells were harvested 4-5 days after injection. PEC were incubated in RPMI medium 1640, containing 10% FBS, 2 mM glutamine, and 100 U/mL of penicillin–streptomycin. The concentrations for the different treatments were as follows: LPS (100 ng/mL) (LPS from Salmonella Abortus

Equi S-form; Alexis). To induce LPS tolerance, cells were incubated in the presence of LPS for 20 h, washed, and maintained in RPMI medium for 2 h and then rechallenged with LPS for 4 h (L/L). To induce M1 activation, cells were incubated in medium for 20 h, washed, left in medium for 2 h, and finally stimulated with LPS for 4 h (M/L). Control cells (M/M) were cultured in medium for the entire period of the experiment.

TAMs were isolated from tumor bearing mice as previously described [27]. Briefly, when tumors reached a volume of about 2 cm^3 (indicatively 3 weeks after tumor implantation), mice were sacrified and tumors were processed with Trypsin 0,125%. Cell suspension was plated in incomplete RPMI, substituted after one hour with RPMI containig 10% serum.

The concentrations for the different treatments *in vitro* were as follows: C5a and C3a (R&D System) were used 100ng/ml, CCL5, CCL2 and MCSF (Peprotech) were used 100ng/ml.

Analysis on tumor-infiltrated cells was performed as follow: tumor tissues were cut into small pieces and treated with collagenase (type IV, 1 mg/mL, Sigma-Aldrich) for 30 min at 37°C. Cell suspensions were stained with the following mixture of antibodies.

Flow cytometry. 0.5-1*10^6 cells were re-suspended in HBSS (Hank's balanced salt solution, Lonza) supplemented with 0.5% BSA (Sigma). Staining was performed at 4°C for 20 minutes, with the following antibodies: anti-mouse/human CD11b (clone M1/70), anti-mouse CD45 (clone 30-F11), anti-mouse CD88 (clone 20/70), anti-mouse CD115 (clone AFS98), anti-mouse CCR5 (clone HM-CCR5), anti-mouse CCR2 (clone SA203G11), anti-mouse CD31 (clone MEC 13.3), anti-human CD88 (clone S5/1), anti-human Tie2 (clone 33.1), anti-human CD14 (clone M5E2) (Biolegend San Diego, CA), anti-mouse Ly6C (clone HK1.4), anti-mouse Tie2 (clone TEK4) (eBioscience San Diego, CA), anti-human CD15 (clone HI98) (BD biosciences, San Diego, CA), anti-mouse HO-1 (clone HO-1-2) (Enzo Life Sciences). Further we used

unconjugated rabbit monoclonal anti-mouse C3aR (clone D-20, Santa Cruz Biotechnology) followed by incubation with secondary goat anti rabbit Alexa Fluor® 647 conjugated antibody (Invitrogen, Molecular Probes, Carlsbad, CA). For intracellular staining Cytofix/Cytoperm and Permwash staining kit (BD Pharmigen) were used. Cells were detected using the BD FACS Canto II cytofluorimeter and analyzed with Flowjo Software.

F4/80^{high} and F4/80^{low} TAMs sorting. TAMs were isolated from tumor as previously described and were enriched by positive selection with CD11b microbeads, according to manufacturer's instruction (MACS, Miltenyi). CD11b^{+} cells were stained with CD45, F4/80 and CD88 antibodies and sorted with cell sorting BD FACS Aria to obtain CD45^{+}F4/80^{high}CD88^{high} population and CD45^{+}F4/80^{low}CD88^{low} population.

Migration assay. PEC and TAMs migration was evaluated using a chemotaxis microchamber technique as described previously [28]. Briefly, 30 ∝l of chemoattractant solution (CCL2, CCL5, MCSF, C5a or C3a 100ng/ml in RPMI 1640 with 1% FBS) or control medium (RPMI 1640 with 1% FBS) was added to the lower wells of a chemotaxis Boyden chamber (Neuroprobe) and a polycarbonate filter (PVP treated, 5 ∝m pore size; Neuroprobe) was placed into the wells and covered with a silicon gasket. The correct concentration for each cytokines used was determinated by a dose-response assay both for wt and p50$^{-/-}$ cells (Fig. S1A). 50 ∝l of cell suspension (4*10 ^{6}/ml) were seeded in the upper wells and the chamber was incubated at 37°C for 4 hours. At the end of this period, filters were removed and stained with Diff- Quik (Baxter) and 10 high-power oil immersion fields were counted.

Real-Time PCR. Total RNA was extracted with TRIzol (Invitrogen) according to the manufacturer's instructions. 1 μg of total RNA was reverse-transcribed by

the High Capacity cDNA Reverse Transcription kit (Applied Biosystems), amplified using Fast Syber Green Master Mix (Applied Biosystems), and detected by the 7900HT Fast Real-Time System (Applied Biosystems). The sequences of gene-specific primers are available upon request. Data were processed using SDS2.2.2 software (Applied Biosystems). Results were normalized to the expression of the housekeeping gene β-actin and then expressed as fold up-regulation with respect to the control cell population.

Microarray expression profiling. PEC from three independent experiments were stimulated as described above with LPS for 4 or 24 hours. F4/80 ^{high} and F4/80^{low} TAMs were sorting from three biological replicates. The RNA was purified from PEC and TAMs using the RNeasy Plus Mini Kit, following standard RNA isolation protocol (Qiagen, Italy), and quantified with ND-1000 UV–Vis Spectrophotometer (NanoDropTechnologies, USA). All the cRNA synthesis/sample-labelling, hybridization, washing, and scanning steps were conducted following the manufacturer's specifications (Agilent Technologies Inc., Italy). After hybridization, the slides were washed and then scanned with the Agilent G2565BA Microarray Scanner. The fluorescence intensities of scanned images were extracted and pre-processed by Agilent Feature Extraction Software (v10.5.1.1). Expression measures were computed using robust multiarray average. Principal component analysis was carried out on all genes analyzed to assign the general variability in the data to a reduced set of variables called principal components. PCA (analysis was applied to the complete dataset) is a mathematical algorithm that reduces the dimensionality of the data. It accomplishes this reduction by identifying directions, called principal components, along which the variation in the data is maximal [29]. In PCA, we obtain a set of orthogonal axes oriented in the directions of largest variance within a set of data points in a high-dimensional space. The first principal component is a vector in the direction of greatest variance, the second principal component is a vector in the direction of greatest variance orthogonal to this,

and so on. These vectors are in fact eigenvectors of the empirical data covariance matrix. Values on the *x*- and *y*-axis express a two-dimensional representation of greatest variance vectors. Genes were defined as regulated when characterized by a fold change ≥4 and p value ≤ 0.05. We performed enrichment analyses using the databases GO (Biological Process and Molecular Function), and KEGG pathways.

Immunoblotting. After the indicated treatments, PEC or TAMs were lysed in 50 µL of lysis buffer (20 mM Tris-HCl, pH 8; 137 mM NaCl; 10% glycerol (vol/vol); 1% Triton X-100 (vol/vol); 1 mM Na_3VO_4; 2 mM EDTA; 1 mM PMSF; 20 µM leupeptin; and 0.15 U/mL aprotinin) for 20 minutes at 4°C. The lysates were centrifuged at 13000g at 4°C for 15 minutes and the supernatants were run on a 10% (wt/vol) sodium dodecyl sulphate (SDS)-polyacrylamide gel electrophoresis (SDS-PAGE; 30 µg protein/lane). Separated proteins were transferred onto a nitrocellulose membrane (1 h at 125 mA) and immunoblotted for specific antibodies as per manufacturer's instructions. Blocking was done with 5% (wt/vol) bovine serum albumin (BSA) in TBS-0.1% Tween (TBST) for 1 hour at room temperature. All antibody dilutions were prepared in 5% (wt/vol) BSA-TBST. Primary antibody was used at 1:2000 dilution for overnight at 4°C. HRP-conjugated anti-rabbit secondary antibody (Amersham, USA) was used at 1:4000 dilution for 1 hour at room temperature. Blots were visualized using an enhanced chemiluminescence (ECL) kit (Amersham, USA). The antibodies used were: rabbit anti-mouse Phospho-p44/42 MAPK (Erk1/2) antibody (Cell Signalling Technologies Inc, MA); goat anti-mouse vinculin antibody (Santa Cruz Biotechnology).

Confocal microscopy. Frozen tissues in OCT were sectioned (8 µm), mounted on positively charged slides, air-dried for 30 minutes and fixed with 4% PFA for 10 minutes at room temperature. Sections were blocked with PBS 0.1% Triton-X100 (Sigma-Aldrich) plus 5% normal goat serum (Dako Cytomation,

Carpinteria, CA USA) and 2% BSA, (Amersham Biosciences, Piscataway Township, NJ USA) for 1 hour. Slides were then incubated with the following antibodies: rabbit anti-mouse/human HO-1, rat anti-mouse F4/80 (AbD Serotec), rabbit anti-mouse CD31 (PECAM-1, Pharmingen, San Diego, CA). After 1h of incubation, the detection antibodies goat anti-rabbit IgG Alexa® 488 and goat anti-rat IgG Alexa® 647 (Invitrogen, Molecular Probes) were used. Nuclei were counterstained with DAPI (Invitrogen, Molecular Probes). Samples were mounted with FluorPreserve Reagent (Calbiochem San Diego, CA USA) and analyzed with an Olympus Fluoview FV1000 laser scanning confocal microscope.

In vivo treatments. When the tumor became palpable (day 14), wt mice were injected with CSFR1 antagonist (kindly donated by Dr. Carola Ries, Roche Diagnostic Gmbh, Penzberg, Germany) as an initial dose of 60mg/kg followed by two doses of 30 mg/kg two times a week for a total of 2 weeks.
To induce LPS tolerance *in vivo*, 6 to 8-week-old wt and $p50^{-/-}$ mice were injected intraperitoneally with 200 µg of LPS. After 24 hours we collected blood and PEC for flow cytometry analysis.

Air pouch model. The air pouch model was performed as described elsewhere [30]. Briefly, wt and $CD88^{-/-}$ mice were subcutaneously injected on the back with sterile air (day 0: 5ml; day 3: 3ml). Mice induced tolerant were injected on day 5 I.P. with 200 ∝g of LPS. On day 6, 200 ng of LPS (SIGMA) dissolved in 1ml carboxymethylcellulose (CMC, SIGMA; 0,5% in PBS) were injected into the air pouch. After 24 hours, the animal were sacrified and the pouches were washed with 2 ml of PBS to recover the infiltrating cells. Cells were washed twice to eliminate CMC and used for flow cytometry analysis.

Adoptive transfer. $CD45^{+}F4/80^{high}CD88^{high}$ and $CD45^{+}F4/80^{low}CD88^{low}$ cells were sorted from wt tumor bearing mice and immediately injected together with MN tumor cells into the hind leg of wt or p50$^{-/-}$ animals (10^5 tumor cells + 2*10^5 $F4/80^{high}$ or $F4/80^{low}$ per mouse). Tumors were measured three times a week with a caliper.

Patients. Peripheral blood was collected from healty donors and septic patients (n = 20 patients and 15 controls) and was analyzed within 3 hours after collection by FACS-analysis (see section Flow Cytometry).

Statistics. Statistical significance was determined by two-tailed Student's t test. *p value< 0.05; **p value< 0.01; ***p value< 0.001.

Results

p50 NF-κB modulates macrophage migratory behaviour. We previously reported that nuclear accumulation of p50 NF-κB is a key event guiding macrophage reprogramming towards an immunosuppressive M2-like phenotype [12, 26]. As macrophage functions are dependent on their homing capacity in response to chemotactic signals, we decided to investigate the putative role of p50 NF-κB on monocyte/macrophage migration. *In vitro* migration assay, performed in a Boyden chamber, demonstrated that $p50^{-/-}$ peritoneal macrophages (PEC) migrate significantly less than their wt counterparts towards canonical chemotactic stimuli (i.e. CCL2, CCL5, C5a, C3a) (Fig. 1A-S1A). Of note, flow cytometry analysis (FACS) on wt and $p50^{-/-}$ PEC revealed no differences in the level of expression of the specific chemotactic receptors (Fig. S1B). Since a major pathway involved in myeloid cells migration includes the MAPkinases [31], we checked the levels of ERK1/2 phosphorylation in wt and $p50^{-/-}$ PEC after stimulation with the chemotactic agents. We observed that in response to each different stimulus, including the positive control LPS [32], ERK1/2 phopshorylation in $p50^{-/-}$ cells was impaired, as compared to wt cells (Fig. 1B). Based on this, we next investigated whether and how nuclear accumulation of p50 NF-κB, as occurring in LPS-tolerant macrophages [26] (Fig. S1C) could affect their chemotactic ability. *In vitro* migration assay demonstrated that PEC activated with LPS for 4 hours (ML) failed to migrate in response to several stimuli, including CCL2 [28]. Notably, we observed that macrophages undergoing LPS-tolerance (LL) were able to recover their chemotactic response towards the complement factors C5a and C3a, while their migration in response to CCL2 and CCL5 remained impaired (Fig. 1C). In agreement, western blot analysis confirmed that LPS-tolerant macrophages phosphorylate ERK1/2 only in response to complement factors (C3a and C5a) (Fig. 1D). Altogether, these data indicate that lack of p50 NF-κB impairs

macrophage chemotactic responsiveness and that LPS-tolerant macrophages migrate only in response to complement factors (C5a and C3a).

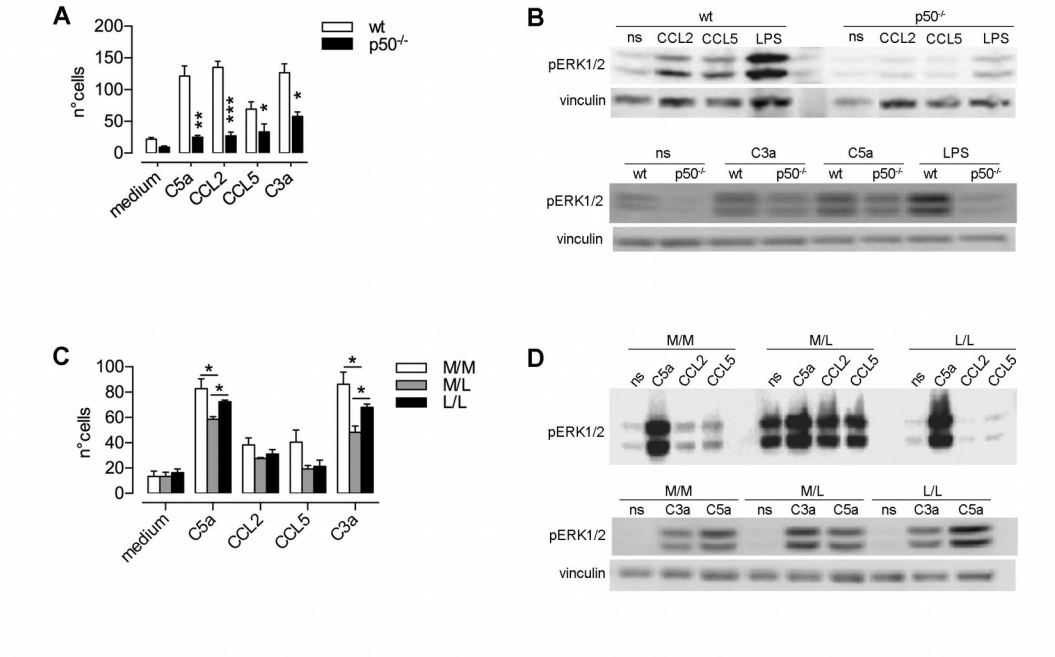

Fig. 1: Role of p50 NF-κB in macrophage migration. (A) Wt and p50$^{-/-}$ peritoneal macrophages (PEC) were used to assemble an *in vitro* chemotaxis assay in a Boyden chamber, in the presence of 100ng/ml of each chemotactic stimulus. (B) Wt and p50 $^{-/-}$ PEC were stimulated with different chemotactic agonists (all used 100ng/ml) for 3 minutes and with LPS (positive control) for 15 minutes. Protein lysates were immunoblotted with an antibody against phospho-ERK1/2 (p44/42) (Thr202/Tyr204). Vinculin was used as loading control. (C) PEC from wt mice were stimulated or not *in vitro* with LPS (MM=medium; ML=20 hrs medium plus 4 hrs LPS (activated macrophages); LL= 20 hrs LPS plus 4 hrs restimulation with LPS (tolerant macrophages)). Next, cells were harvested and put into a Boyden chamber, in the presence of different chemotactic stimuli (all used 100ng/ml). (D) Protein lysates from wt PEC (M/M; M/L and L/L) restimulated or not with different chemotactic agents for 3 minutes, were immunoblotted with anti phospho-ERK antibody. Vinculin was used as loading control. Data are expressed as the mean +/- SEM. Graphs are representative of 3 independent experiments.*p < 0.05 **p < 0.01 ***p < 0.001.

Distinct macrophage subsets are differentially recruited to sites of inflammation during systemic LPS-tolerance. To assess the chemotactic response of M2-polarized macrophages also *in vivo*, we performed an air-pouch assay in LPS-tolerant wt mice, treated systemically with LPS (10mg/kg), according to the scheme described in Fig. S2A. We divided mice in four groups: A) ctrl mice injected with only air into the air pouch; B) mice injected with LPS (200ng/ml) into the air pouch; C) LPS-tolerant mice (injected I.P. with LPS); D) LPS tolerant mice injected with LPS into the air pouch. As expected, FACS analysis of the cellular infiltrate collected from the air pouches of the different groups revealed that mice treated with LPS into the pouch (group B and D) displayed increased number of $CD45^{+}$ myeloid cells, compared to control mice (Fig. S2B). Interestingly, we observed a differential regulation in the accumulation of distinct $F4/80^{+}$ macrophage subsets. In particular, $F4/80^{+}$ macrophages recruited to the inflammatory site were composed by two subsets characterized by different expression levels of F4/80 and CD88, respectively defined as $F4/80^{high}CD88^{high}$ and $F4/80^{low}CD88^{low}$. Of note, $F4/80^{high}CD88^{high}$ macrophages were specifically and exclusively recruited during LPS-tolerance (group C and D); in fact, into the air pouches of non-tolerant mice (group A and B) we observed only the presence of $F4/80^{low}CD88^{low}$ (Fig. 2A-B). Because LPS-tolerant macrophages respond chemotactically to the complement factors C3a and C5a (Fig. 1C), we performed an air-pouch assay also in $CD88^{-/-}$ mice. Strikingly, the air pouches of $CD88^{-/-}$ mice showed decreased accumulation of $F4/80^{high}CD88^{high}$ cells associated with an increased recruitment of $F4/80^{low}CD88^{low}$ macrophages (group D), compared to wt (Fig. 2C). Thus, a specific subset of macrophages expressing high level of F4/80 and CD88 migrate to sites of inflammation in tolerant conditions.

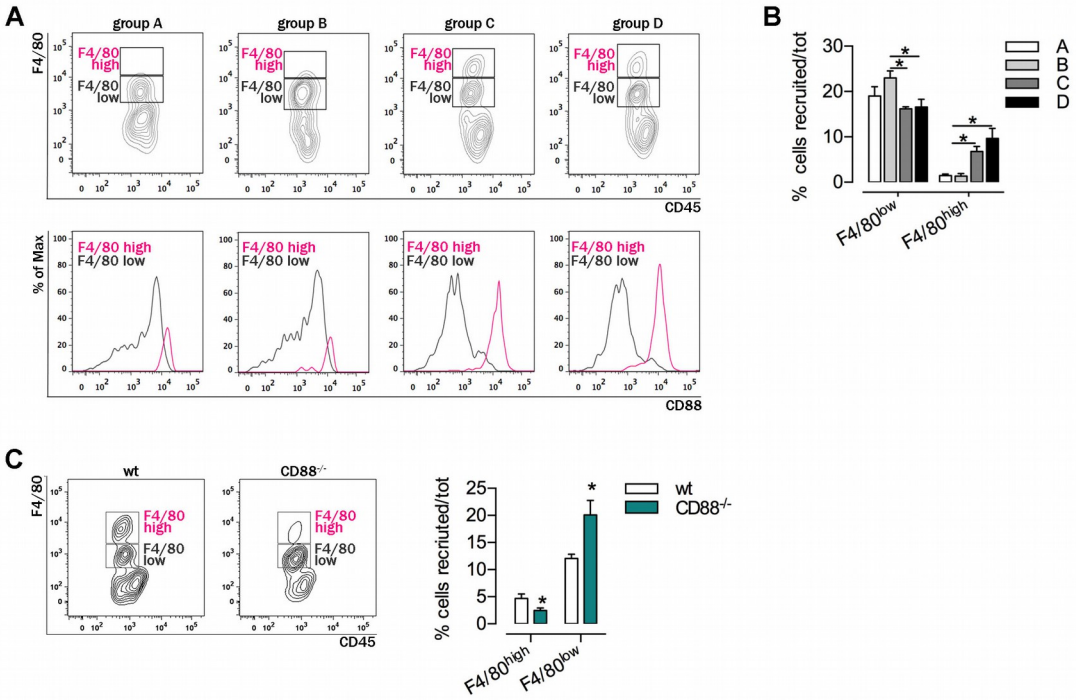

Fig. 2: F4/80^{high}CD88^{high} macrophages migrate to sites of inflammation during LPS-tolerance. (A) Flow cytometry analysis of CD45^{+}F4/80^{+} cells collected from the air pouches of the different groups of wt mice. Group A: ctrl mice injected with only air into the air pouch; Group B: mice injected with LPS into the air pouch; Group C: LPS-tolerant mice (injected IP with LPS 10mg/kg); Group D: LPS tolerant mice injected with LPS into the air pouch. (B) Percentage of F4/80 ^{high} and F4/80 ^{low} cells recruited into the air pouch in the different groups. (C) Flow cytometry analysis and percentage of F4/80 ^{high} and F4/80^{low} cells recruited into the air pouches of group D, in wt and CD88 $^{-/-}$ mice. Data are expressed as the mean +/- SEM (n = 4-5 mice per group). *p < 0.05

p50 NF-κB drives CD88 expression and recruitment of F4/80^{high}CD88^{high} cells during tolerance. Additional analysis demonstrated that CD88 expression is upregulated in concomitance with the induction of tolerance *in vivo*, in a p50-dependent manner. In fact, FACS analysis on PEC purified from wt and p50 $^{-/-}$ mice at different time points (4, 8, 16 and 24 hours) after I.P. injection with LPS, showed that while in wt PEC the expression of CD88 increases in parallel with the induction of systemic tolerance, macrophages p50 $^{-/-}$ are unable to up-regulate CD88, even after long exposure to LPS (24 hours) (Fig. 3A). Further, specific recruitment of F4/80 ^{high}CD88^{high} subset during systemic LPS-tolerance was observed at the site of inflammation (air pouch, Fig. 2). In order to investigate whether the F4/80^{high}CD88^{high} population could also increase systemically, we performed FACS analysis of blood from both wt and p50 $^{-/-}$ mice, at different time points (4, 8, 16 and 24 hours) after I.P. injection with LPS (10mg/kg). Notably, the F4/80 ^{high} population was detectable in the blood of wt mice only after LPS injection. As already reported [26], p50-deficient mice do not develop systemic LPS-tolerance. In agreement, these mice did not show accumulation of the F4/80 ^{high} population in the blood of p50 $^{-/-}$ mice after prolonged LPS treatment (16-24 hours) (Fig. 3B), suggesting that p50-mediated tolerance is required to recruit this population. Interestingly, as compared to the F4/80^{low}CD88^{low} macrophages, the F4/80^{high}CD88^{high} population was characterized by higher levels of expression of Tie2, CCR2 and Ly6C (Fig. 3C-S3B), that increased with similar a kinetic, both *in vivo* (Fig. 3C) and *in vitro* (Fig. S3A).

During the course of human sepsis, neutrophils down-regulate the levels of CD88 expression [33, 34]. Strikingly, while we confirmed the CD88 downregulation on peripheral neutrophils of septic patients, their blood monocytes showed a significant upregulation of CD88 and Tie2, as compared to healthy controls (Fig. 3D), indicating the expansion of the human CD88^{high}Tie2^{high} monocytic population in condition of systemic infection.

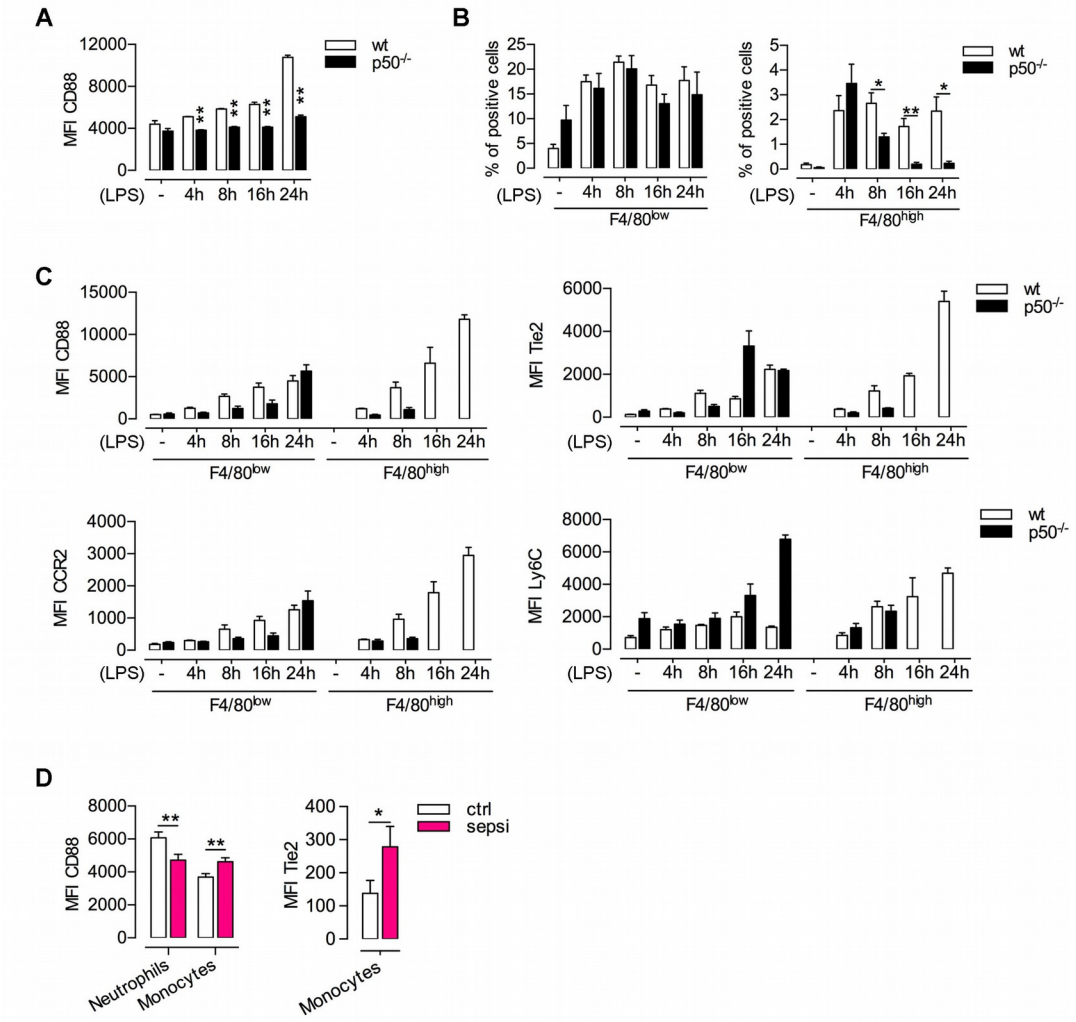

Fig. 3: p50 NF-κB controls expansion and recruitment of F4/80^{high}CD88^{high} cells during tolerance. (A) Wt and p50$^{-/-}$ mice were injected I.P. with saline or LPS (10mg/kg) and PEC were recovered 4-8-16-24 hours after injection. CD88 expression was analyzed by FACS as mean of fluorescence intensity (MFI). (B) Blood from wt and p50 $^{-/-}$ mice injected with LPS I.P. was recovered at different time points (4-8-16-24 hours)after LPS administration and analyzed by FACS for the presence of F4/80 ^{high} and F4/80^{low} populations and (C) for the expression of CD88 and Tie2. Data are expressed as the mean +/- SEM (n = 4 mice per group). (D) Neutrophils and monocytes from blood of septic patients were analyzed by FACS for the expression of CD88 and Tie2. Healthy donors were used as a control. Data are expressed as the mean +/- SEM (n = 20 patients and 15 controls). *p < 0.05 **p < 0.01.

Detection of F4/80^{high}CD88^{high} and F4/80^{low}CD88^{low} TAMs populations in primary tumors and metastasis. We already published that similarly with LPS-tolerant macrophages, tumor associated macrophages (TAMs) display high nuclear accumulation of p50 inhibitory homodimers [12]. Based on this, we functionally and phenotypically analyzed TAMs populations *in vitro* and *in vivo* in the transplantable MN/MCA1 murine model of fibrosarcoma. First, *in vitro* chemotaxis assay demonstrated that, similarly with LPS-tolerant macrophages, TAMs show chemotactic responsiveness towards the complement factors C5a and C3a (Fig. 4A-B), associated with similar levels of ERK1/2 phosphorylation (data not shown). Furthermore, in analogy with LPS-tolerant macrophages (Fig. 1A), p50$^{-/-}$ TAMs showed decreased migration capacity to C5a and C3a, as compared to wt TAMs (Fig. 4B).

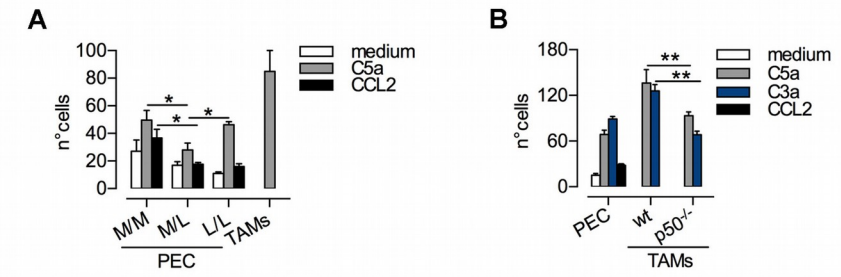

Fig. 4: TAMs recapitulate the chemotactic behavior of LPS-tolerant macrophages. TAMs from wt (A) or wt and p50$^{-/-}$ mice (B) were used to assemble an *in vitro* chemotaxis assay, in comparison with untreated, LPS activated or LPS tolerant peritoneal macrophages. Data are expressed as the mean +/- SEM. Graphs are representative of at least 2 independent experiments. ***p < 0.001.

To assess the phenotypic similarities between TAMs and LPS-tolerance macrophages also *in vivo*, we performed flow cytometry analysis of TAMs purified from the MN/MCA1 fibrosarcoma. To this aim, 10^5 MN/MCA1 tumor cells were injected in the hind leg of wt mice and after 4 weeks primary tumors and lung metastasis were recovered, smashed to obtain single cell

suspension and stained for FACS analysis. We observed that similarly with the macrophage populations detected in LPS-tolerant mice (Fig. 2A), TAMs from both primary tumors and lung metastasis were composed by two distinct F4/80^{high}CD88^{low} and F4/80^{low}CD88^{low} populations (Fig. 5A). In further support of this similarity, the F4/80^{high}CD88^{high} subset also expressed higher levels of Tie2 (Fig. 5B). Of note, analysis of TAMs populations in wt tumor bearing mice subcutaneously injected with B16F10 melanoma cells resulted in similar phenotype (Fig. S4A).

Next, we investigated the role of p50 in the recruitment of TAMs subsets. FACS staining on infiltrating TAMs demonstrated that genetic ablation of p50 strongly affects F4/80^{high} recruitment in both primary MN/MCA1 tumors and metastasis (Fig. 5C-D). To further assess the *in vivo* importance of p50 NF-κB in macrophage migration, we generated a p50 NF- κB conditional knockout mice with selective depletion of p50 in the myeloid compartment (p50flox/floxLyzCre), by intercrossing p50 NF- κB floxed mice with LyzM-Cre mice. Strikingly, we observed that compared to littermate controls, myeloid-specific ablation of p50 resulted in significant impairment of F4/80^{high} TAMs recruitment in primary tumors, both in MN/MCA1 and B16 model; while, the recruitment of F4/80^{low} TAMs was unaffected (Fig. S4B).

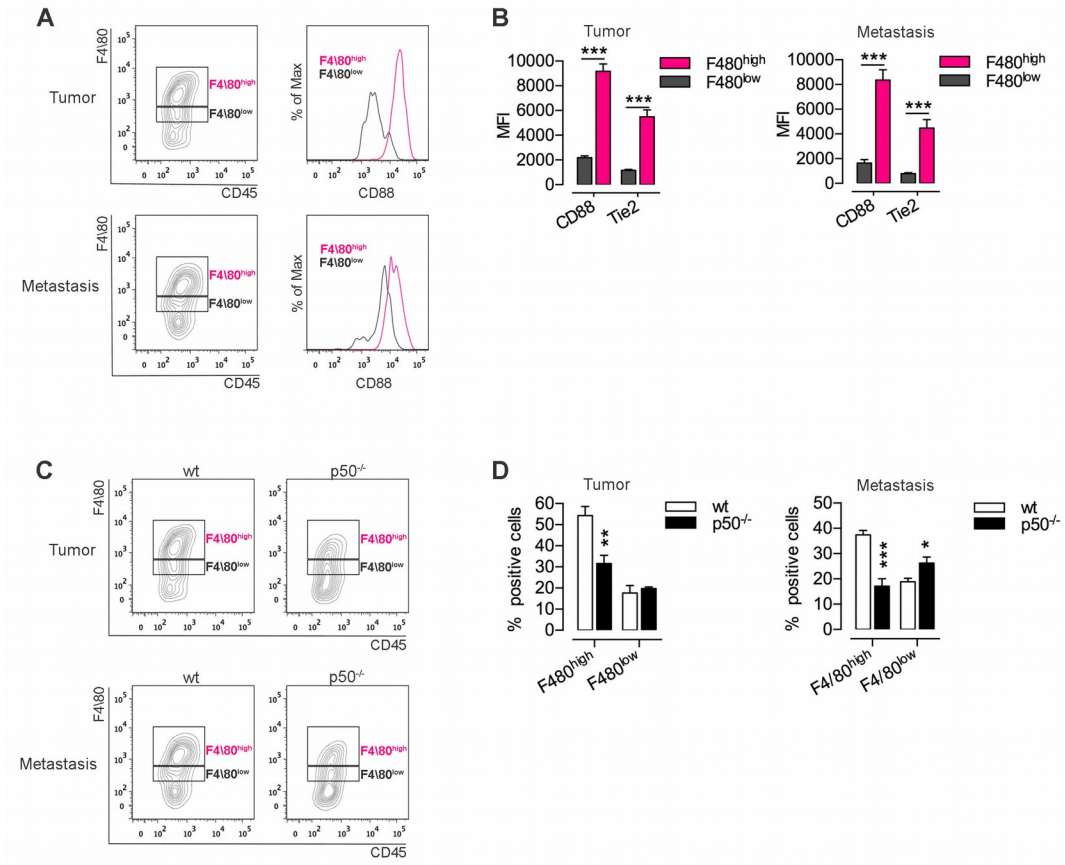

Fig. 5: Distinct roles of p50 in the recruitment of the F4/80 ^{high}CD88^{high} and F4/80^{low}CD88^{low} TAMs populations, in primary tumors and metastasis. (A-B) MN/MCA1 fibrosarcoma primary tumors and metastasis from wt mice were analyzed by flow cytometry analysis for the expression of CD88, Tie2 and F4/80 positive cells. (C-D) Percentage of F4/80^{high} and F4/80^{low} populations in MN/MCA1 primary tumors and metastasis from wt and p50$^{-/-}$ mice. Graphs are representative of at least 2 independent experiments. Data are expressed as the mean +/- SEM (n = 5 mice per group). *p < 0.05 **p < 0.01 ***p < 0.001.

The complement factor C3a controls the selective recruitment of F4/80^{high}CD88^{high} TAMs and support tumor development. Additional FACS analysis showed that the F4/80^{high}CD88^{high} and F4/80^{low}CD88^{low} TAMs populations also differ for the expression of several chemotactic receptors. In particular, the F4/80^{high}CD88^{high} TAMs expressed higher levels of the C3aR, cd115 (M-CSF receptor), CCR2 and CCR5 (Fig.6A-B). Differential expression of these chemotactic receptors was functionally associated with increased chemotactic responsiveness to specific chemotactic agonists. In particular, we observed that F480^{high}CD88^{high} TAMs displayed higher chemotactic ability than F4/80^{low} in response to C5a, C3a and MCSF (Fig. 6C).

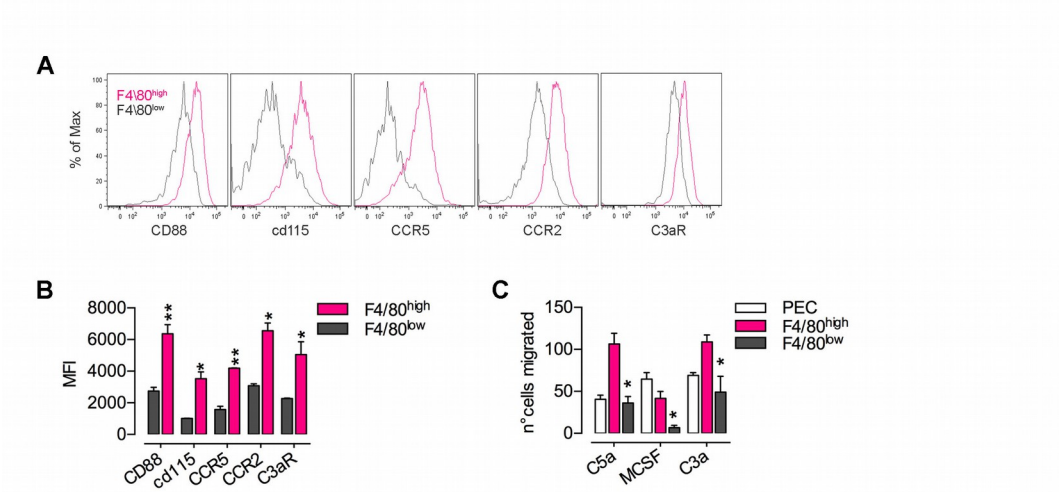

Fig.6: Chemotacitc response of F4/80 ^{high}CD88^{high} and F4/80^{low}CD88^{low} TAMs. (A-B) TAMs were stained with an anti-F4/80 antibody, along with several antibodies recognizing different chemokine receptors. CD88, CD115, CCR5, CCR2 and C3aR expression are indicated as MFI. (C) F4/80 ^{high}CD88^{high} and F4/80 ^{low}CD88^{low} TAMs were sorted from MN/MCA1 tumors for F4/80 and CD88 expression and used for an *in vitro* chemotaxis assay. All the chemotactic stimuli were used at a concentration of 100ng/ml. Figures are representative of 2 independent experiments. Data are expressed as the mean +/- SEM. *$p < 0.05$ **$p < 0.01$.

It was proposed that M-CSF regulates the recruitment and survival of "resident" macrophages involved in tissue homeostasis and several studies indicate that CSF-1 inhibition reduces the number of tissue macrophages, including TAMs [20, 35, 36]. Based on this, we wondered whether antibodies against M-CSFR could selectively affect TAMs subsets. To this aim, wt mice were injected with 10^5 MN/MCA1 tumor cells in the hind leg and 2 weeks later were treated I.P. twice a week with vehicle or anti-CSFR1 blocking antibody. During the treatment regimen, an initial dose of 60mg/kg was followed by two doses of 30 mg/kg. Administration of anti-CSFR1 antibody resulted in severe inhibition of tumor growth and reduced TAMs accumulation, with a predominant impairment of the $F480^{high}CD88^{high}$ subset (Fig. 7A-B). Of relevance, treatment with anti-CSFR antibody significantly reduced the percentage of CD31 expressing cells in tumors (Fig. 7C), indicating that the ratio between the TAMs subsets may be relevant in tumor angiogenesis and tumor growth. Hence, we also investigated whether, in addition to M-CSF1, the complement factors C3a and C5a could play a role in the selective recruitment of TAMs subsets *in vivo*. Of note, injection of MN/MCA1 cells in C3 deficient mice resulted in significant impairment of $F4/80^{high}CD88^{high}$ TAMs accumulation, in both primary tumor and lung metastasis, while the recruitment of $F4/80^{low}$ TAMs was unchanged. In addition, C3 deficient mice displayed reduced tumor growth and lung metastasis formation, as compared to wt mice (Fig. 7D-E).

Angiogenesis represents a critical process during tumor initiation and progression; however, unlike physiological angiogenesis, blood vessel development in solid tumors is not tightly controlled but rather occurs relentlessly. Consequently, tumor vessels are heterogeneous, branch chaotically and are aberrant in almost all aspects of their structure and function [37, 38]. Thus, we decided to checked tumor vascularization, in order to further characterize the effects of impairing $F4/80^{high}$ cells recruitment on tumor growth. Primary tumor lesions from C3 deficient mice displayed impaired

tumor vascularization, assessed as reduced $CD31^+$ cells density and vessels length (Fig. 7F).

Surprisingly, MN/MCA1 tumor growth, metastasis formation and recruitment of $F480^{high}CD88^{high}$ and $F480^{low}CD88^{low}$ subsets were not affected in $CD88^{-/-}$ mice, (Fig. S5A-B).

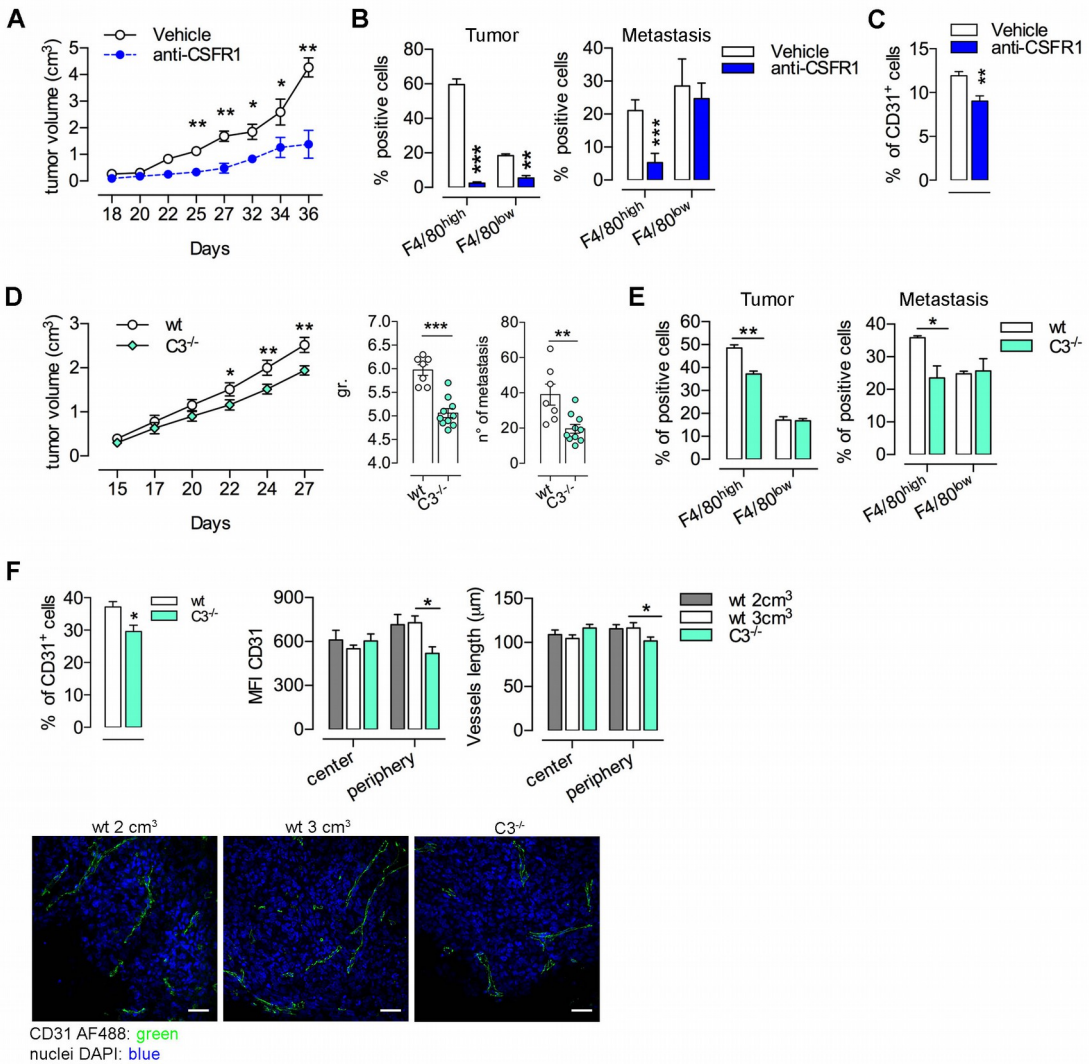

Fig.7: Defective recruitment of F4/80 $^{high}CD88^{high}$ TAMs correlates with inhibition of tumor growth and tumor angiogenesis. (A) MN/MCA1 tumor-bearing wt mice were treated twice a week with vehicle or anti-CSFR1 blocking antibody as indicated. (B) Data on $F4/80^{high}CD88^{high}$ and $F4/80^{low}CD88^{low}$ TAMs in primary tumors (left) and metastasis (right) are

shown. (C) Tumors from vehicle or anti-CSFR1 treated mice were analyzed by FACS for the presence of $CD31^+$ cells. (D) MN/MCA1 tumor cells were injected in $C3^{-/-}$ mice and tumor growth was measured 3 times a week starting from day 15 after cells injection. Tumor weights (left) and number of macroscopic lung metastasis (right) are shown. (E) Mean percentage +/- SEM of $F4/80^{high}CD88^{high}$ and $F4/80^{low}CD88^{low}$ TAMs in primary tumors (left) and metastasis (right) from wt and $C3^{-/-}$ tumor bearers. (F) Mean percentage +/- SEM of $CD31^+$ cells of primary tumors from wt and $C3^{-/-}$ tumor bearers (left). Frozen tumor slides from wt ($2cm^3$ and $3cm^3$) and $C3^{-/-}$ mice were analyzed by confocal microscopy for the expression of CD31 (green). Analysis of vessels length is also performed. Nuclei were counterstained with DAPI (blue). Representative images are shown (scale bars are 10 ∝m). Graphs are representative of at least 2 independent experiments. Data are expressed as the mean +/- SEM (n = 5 mice per group). *p < 0.05 **p < 0.01 ***p < 0.001.

$F4/80^{high}CD88^{high}$ and $F4/80^{low}CD88^{low}$ TAMs play different roles in tumor progression. To investigate the specific roles of TAMs subsets, $F4/80^{high}CD88^{high}$ and $F4/80^{low}CD88^{low}$ TAMs were sorted from MN/MCA1 tumors and adoptively transferred, together with MN/MCA1 tumor cells, in the hind leg of wt mice (10^5 tumor cells + 2*10^5 TAMs per mouse). Interestingly, as compared to mice receiving only tumor cells, adoptive transfer of $F4/80^{low}CD88^{low}$ TAMs significantly inhibited tumor growth and lung metastasis formation (Fig. 8A), as opposed to decreased vessels length (Fig. 8B). Conversely, mice adoptively transferred with $F4/80^{high}CD88^{high}$ TAMs displayed increased metastasis formation (Fig. 8A), along with increased tumor vessels density and length (Fig. 8B).

Because ablation of p50 NF-κB in tumor bearing mice resulted in decreased accumulation of $F4/80^{high}CD88^{high}$ TAMs in both primary tumors and metastasis, we perform adoptive transfer experiments also in $p50^{-/-}$ mice. As expected [12], $p50^{-/-}$ mice implanted with MN/MCA1 cells displayed both reduced tumor growth and metastasis number as compared to wt mice. Strikingly, transfer of wt $F4/80^{high}CD88^{high}$ TAMs in $p50^{-/-}$ tumor bearing mice resulted in restoration of tumor growth, increased metastasis formation and increased tumor vessels density and length (Fig. 8C-D). Our results indicate a differential pro- vs antitumor functions of $F4/80^{high}CD88^{high}$ and

F4/80^{low}CD88^{low} subsets respectively, with the F4/80^{high}CD88^{high} TAMs strongly supporting tumor angiogenesis.

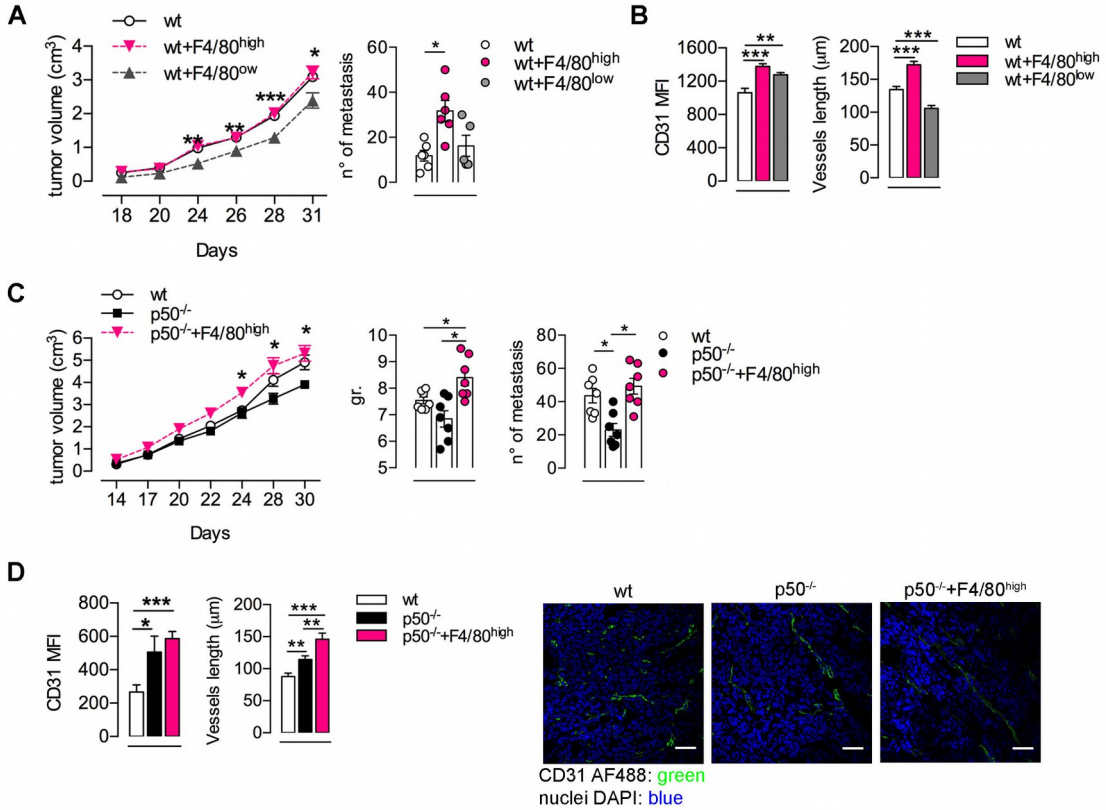

Fig.8: F4/80^{high}CD88^{high} and F4/80^{low}CD88^{low} TAMs play different roles in tumor progression. (A) F4/80^{high} and F4/80^{low} cells were sorted for F4/80 and CD88 expression from wt tumor bearing mice and next injected together with MN/MCA1 tumor cells into wt mice (10^5 tumor cells + 2*10^5 F4/80^{high}CD88^{high} and F4/80^{low}CD88^{low} TAMs per mouse). (B) Frozen tumor sections were analyzed by confocal microscopy for the expression of CD31. Analysis of vessels length is also shown. (C) F4/80 ^{high} cells sorted from wt tumor-bearing mice were injected together with MN/MCA1 tumor cells into p50 $^{-/-}$ mice. Tumor weights (center) and number of metastasis (right) are shown. (D) Frozen tumor sections were analyzed by confocal microscopy for the expression of CD31 (green). Analysis of vessels length is also performed. Nuclei were counterstained with DAPI (blue). Representative images are shown (scale bars are 10 ∝m). Graphs are representative of at least 2 independent experiments. Data are expressed as the mean +/- SEM (n = 5 mice per group). *p < 0.05 **p < 0.01 ***p < 0.001.

F4/80^{high}CD88^{high} and F4/80^{low}CD88^{low} TAMs express distinct transcriptional programs. As macrophage polarization plays a crucial role in tumor development [7] and since we observed distinct roles of the F4/80^{high}CD88^{high} and F4/80^{low}CD88^{low} TAMs subsets, we performed genome wide analysis through the Agilent DNA microarray platform, comparing global gene profiling of F4/80 ^{high} TAMs, F4/80 ^{low} TAMs, PEC untreated (M/M), LPS-activated PEC (M/L) and LPS-tolerant PEC (L/M). To identify sources of variability among these entire databases, a PCA was performed [29]. The results showed that F4/80^{high} and F4/80^{low} TAMs are distinct in terms of global gene expression. Moreover, their global profiling is closer to that of L-M than M-L PEC (Fig. 9A). Real Time qPCR analysis confirmed the differential expression of several pro- and anti-inflammatory cytokines by these two populations of TAMs. Indeed, F4/80^{high}CD88^{high} TAMs express for example CXCL10, IL10, MsrII (Macrophage scavenger receptor II), at higher levels as compared to F480^{low}CD88^{low} TAMs. On the contrary, F4/80 ^{low}CD88^{low} TAMs express Arg1, GrzB (Granzyme B) at higher levels (Fig. S6A).

Interestingly, gene ontology analysis showed that F480^{high}CD88^{high} TAMs preferentially expressed clusters of genes involved in immunity, inflammation, leukocyte migration and activation. In contrast, F4/80^{low}CD88^{low} TAMs expressed preferentially clusters of genes involved in metabolism/catabolism and regulation of apoptosis (Fig. 9B), confirming profound differences in the gene expression profiles. Strikingly, we showed differential expression of genes involved in iron metabolism, by both gene ontology (Fig. 9C) and Real Time qPCR analysis (Fig. 9D).

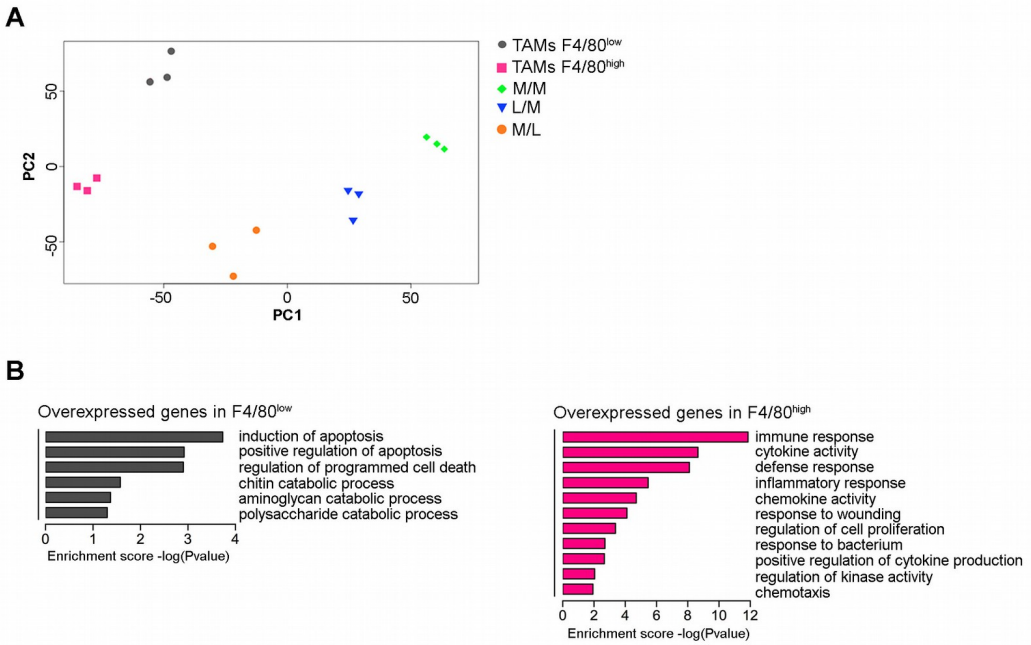

C

Gene Symbol	Description	FC F4/80low	FC F4/80high	Biological Function
Cp	ceruloplasmin	0,30	2,85	iron oxidation
Sfxn1	sideroflexin 1	-0,09	-1,12	mitochondria iron transport
Hfe	hemochromatosis	-1,93	0,09	iron absorption, regulation of interaction transferrin-transferrin R
Hp	haptoglobin	3,23	-1,45	binding free hemoglobin
Lcn2	lipocalin 2	7,00	1,54	binding iron-containing siderophores, antimicorbial
Ltf	lactotransferrin	5,40	0,44	iron transport, antimicrobial
Trf	transferrin	-2,94	-1,04	iron binding, control of free iron
Tfrc	transferrin receptor	1,95	-1,47	iron import into cells
Slc40a1	ferroportin	2,42	-0,27	iron export outside cells
Hamp	hepcidin antimicrobial peptide	0,31	1,92	inhibits ferroportin (iron transport)

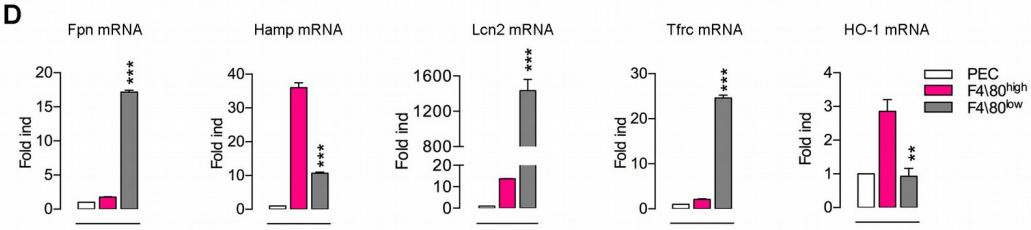

Fig.9: F4/80^{high}CD88^{high} and F4/80^{low}CD88^{low} TAMs express distinct transcriptional profiles. (A) mRNA was prepared from F480^{high}CD88^{high} and F480^{low}CD88^{low} TAMs sorted from MN/MCA1 tumors and was analyzed by the Agilent DNA microarray platform, in comparison with untreated, LPS activated and LPS tolerant PEC. Global gene profiling comparison performed among the TAMs and PEC dataset by PCA is shown . (B) Gene ontology [39] enrichment analysis of differentially expressed genes. (left) Top enriched GO terms for genes with higher expression in F4/80^{low} TAMs versus F4/80^{high} TAMs. (right) Top enriched GO terms for genes with higher expression in F4/80^{high} TAMs versus F4/80^{low}

TAMs. Enrichment score (-log(Pvalue)) is shown. (C) Iron related gene expression analysis of F4/80^{high} and F4/80^{low} TAMs. Results (mean of three independent experiments) are fold-increase relative to unstimulated PEC. (D) mRNA expression levels of selected cytokines were analyzed by real-time PCR. Wt PEC were used as a control cells. Graphs are representative of at least 3 independent experiments. Data are expressed as the mean +/- SEM. **p < 0.01 ***p < 0.001.

Of relevance, F4/80^{high}CD88^{high} TAMs expressed high levels of the heme oxygenase-1 gene (HO-1 encoded by *HMOX1*), which encodes for a heme-catabolizing enzyme with cytoprotective and antiapoptotic properties. HO-1 acts by extracting iron from protoporphyrin and generates equimolar amounts of biliverdin and CO, and is high expression in different tumor cells (e.g. prostate cancers, brain tumors, adenocarcinoma, squamous carcinoma, melanoma and pancreatic carcinoma) is associated with tumor progression and increased tumor angiogenesis [40, 41]. High expression of HO-1 in F4/80^{high}CD88^{high} TAMs was confirmed by both Real Time qPCR (Fig. 9D) and FACS analysis (Fig. 10A). Due to the preferential expression of HO-1 by the F4/80^{high}CD88^{high} TAMs population, we used this enzyme to evaluate the preferential localization of TAMs subsets into the tumor lesions. Confocal microscopy analysis on MN/MCA1 tumor thick-sections stained with anti-HO-1 and anti-F4/80 antibodies indicated that F4/80 $^{+}$HO-1^{+} TAMs were specifically enriched at the tumor margin, while F4/80^{+}HO-1^{-} TAMs localized preferentially in the inner areas of tumors (Fig. 10B).

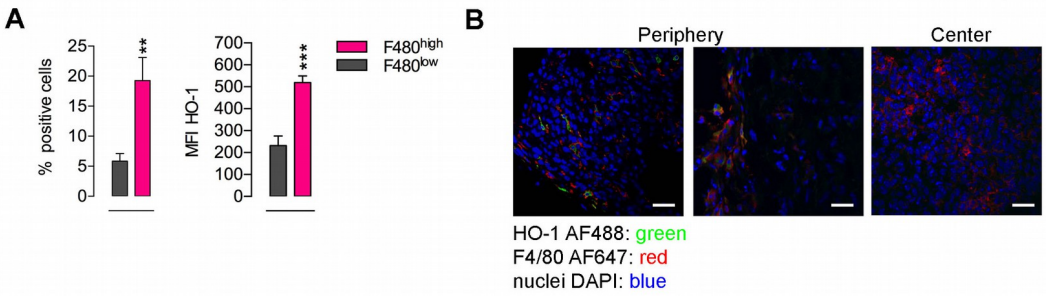

Fig.10: HO-1 is specifically expressed by F4/80^{high}CD88^{high} TAMs and preferentially localize at the peripheral margin of tumors. (A) F4/80 ^{high}CD88 ^{high} and F4/80^{low}CD88^{low} TAMs were stained with an anti-HO-1 antibody and analyzed by FACS. (B) Frozen wt MN/MCA1 tumor sections were analyzed by confocal microscopy for the expression of F4/80 (red) and HO-1 (green). Nuclei were counterstained with DAPI (blue). Representative images are shown (scale bars are 10 ∝m). Graphs are representative of at least 2 independent experiments. Data are expressed as the mean +/- SEM (n = 5 mice per group). **p < 0.01 ***p < 0.001.

Discussion

Inflammatory and immune responses mostly involve the recruitment of circulating monocytes to specific contexts. In particular, macrophages infiltrating tumors are a major leukocyte component of many cancer types and extensive evidence indicates that TAMs recruitment into tumors correlates with a poor prognosis [2, 42-45]. Thus, strategies aimed either to "re-educate" TAMs towards an M1 phenotype or to inhibit their recruitment in tumors represent attractive anti-tumor approaches. This work has identified p50 NF-κB also as an important regulator of macrophage migration. In particular we demonstrated that lack of p50 NF-κB impairs macrophage chemotactic responsiveness. Accordingly, nuclear accumulation of p50 NF-κB not only drives phenotypic traits of TAMs and LPS-tolerant macrophages, including the expression of anti-inflammatory M2 polarized genes [26], but also promotes their chemotactic response to complement anaphylatoxins C5a and C3a. Our group already published that monocytes stimulated with LPS for short periods (till 6 hours) display a dramatic drop in migration in response to CCL2, due to the inactivation of CCR2 function [28]. We demonstrated here that tolerant macrophages are able to migrate only in response to complement factors C5a and C3a, while migration to CCL2 remained impaired.

Distinct F4/80^{+} macrophage subsets characterized by different expression levels of F4/80 and the C5aR (CD88), respectively defined as F4/80 ^{high}CD88^{high} and F4/80^{low}CD88^{low}, differentially accumulate into the inflammatory sites, in *in vivo* model of LPS-tolerance. Of relevance, p50-dependent induction of systemic tolerance [26] is a necessary event driving systemic accumulation of F4/80^{high}CD88^{high} mono/macrophages, both in mouse and human. This result, along with the differential expansion of the F4/80^{low}CD88^{low} and F4/80^{high}CD88^{high} populations, observed also in the preclinical MN/MCA1 fibrosarcoma and B16 melanoma model, indicates that expansion of F4/80^{high}CD88^{high} macrophages is promoted through emergency hematopoiesis.

Moreover, in line with the LPS-tolerance model, ablation of p50 NF-κB resulted in significant impairment of F4/80 ^{high}CD88^{high} TAMs accumulation in primary tumors, which correlated with inhibition of tumor growth [12] and vascularization.

Consistent with other reports where lack of complement factors (C3 or C5aR) in tumor bearers resulted in impaired MDSCs accumulation, as well as in resistance to tumor development and metastasis formation [46-50], we observed that reduced fibrosarcoma growth and lung metastasis formation in C3 $^{-/-}$ mice, as compared to wt mice, was paralleled by significant impairment recruitment of F4/80^{high} TAMs, in both primary tumor and lung metastasis. This result was mimicked by treatment with an anti-CSFR1 antibody, indicating that blocking accumulation of F4/80 ^{high} macrophages in the tumor microenvironment impairs tumor growth and tumor angiogenesis.

Strikingly, adoptive transfer of F4/80 ^{low} TAMs in wt tumor bearing mice resulted in inhibition of tumor growth and in reduced formation of lung metastasis, while, conversely, transfer of wt F4/80^{high} TAMs in p50$^{-/-}$ tumor bearing mice caused restoration of tumor growth and increased metastasis formation. Accordingly, transfer of F4/80high TAMs also increased tumor vessels density and length, indicating that the ratio between the F4/80^{high} and F4/80^{low} TAMs critically controls the angiogenic switch in growing tumors [51].

A distinct role of F4/80 ^{high} and F4/80 ^{low} TAMs in tumor development was also confirmed by analysis of their transcriptomes, showing that distinct gene profiles characterize the transcriptional programs of these populations. These data are in line with findings that macrophages in different functional states or with a mixed phenotype can coexist in the same tumor and that they could preferentially localize in different tumor regions [52-54].

Thus, we show that distinct macrophage subsets with different functions arise during infection- and cancer-driven inflammation, in a p50 NF-κB-dependent manner and that complement-mediated pathways selectively drive their infiltration of inflammatory sites, including solid tumors. Interestingly, we

describe a novel role of p50 NF-kB in guiding expansion, recruitment and the tumor promoting functions of the M2-like F4/80^{high} TAMs subset.

References

1. Eltzschig, H.K. and P. Carmeliet, *Mechanisms of Disease: Hypoxia and Inflammation.* New England Journal of Medicine, 2011. **364**(7): p. 656-665.
2. Mantovani, A., et al., *Cancer-related inflammation.* Nature, 2008. **454**(7203): p. 436-44.
3. Mantovani, A. and A. Sica, *Macrophages, innate immunity and cancer: balance, tolerance, and diversity.* Curr Opin Immunol, 2010. **22**(2): p. 231-7.
4. De Palma, M. and C.E. Lewis, *Macrophage regulation of tumor responses to anticancer therapies.* Cancer Cell, 2013. **23**(3): p. 277-86.
5. Johansson, M., D.G. DeNardo, and L.M. Coussens, *Polarized immune responses differentially regulate cancer development.* Immunological Reviews, 2008. **222**: p. 145-154.
6. Bingle, L., N.J. Brown, and C.E. Lewis, *The role of tumour-associated macrophages in tumour progression: implications for new anticancer therapies.* J Pathol, 2002. **196**(3): p. 254-65.
7. Mantovani, A., et al., *Macrophage polarization: tumor-associated macrophages as a paradigm for polarized M2 mononuclear phagocytes.* Trends Immunol, 2002. **23**(11): p. 549-55.
8. Sica, A., et al., *Macrophage polarization in tumour progression.* Semin Cancer Biol, 2008. **18**(5): p. 349-55.
9. Qian, B.Z. and J.W. Pollard, *Macrophage diversity enhances tumor progression and metastasis.* Cell, 2010. **141**(1): p. 39-51.
10. Biswas, S.K. and A. Mantovani, *Macrophage plasticity and interaction with lymphocyte subsets: cancer as a paradigm.* Nat Immunol, 2010. **11**(10): p. 889-96.
11. Sica, A. and A. Mantovani, *Macrophage plasticity and polarization: in vivo veritas.* J Clin Invest, 2012. **122**(3): p. 787-95.
12. Saccani, A., et al., *p50 nuclear factor-kappaB overexpression in tumor-associated macrophages inhibits M1 inflammatory responses and antitumor resistance.* Cancer Res, 2006. **66**(23): p. 11432-40.
13. Mantovani, A. and P. Allavena, *The interaction of anticancer therapies with tumor-associated macrophages.* J Exp Med, 2015. **212**(4): p. 435-45.
14. Noy, R. and J.W. Pollard, *Tumor-Associated Macrophages: From Mechanisms to Therapy (vol 41, pg 49, 2014).* Immunity, 2014. **41**(5): p. 866-866.

15. Casazza, A., et al., *Impeding Macrophage Entry into Hypoxic Tumor Areas by Sema3A/Nrp1 Signaling Blockade Inhibits Angiogenesis and Restores Antitumor Immunity.* Cancer Cell, 2013. **24**(6): p. 695-709.
16. Movahedi, K. and J.A. Van Ginderachter, *The Ontogeny and Microenvironmental Regulation of Tumor-Associated Macrophages.* Antioxid Redox Signal, 2016.
17. Qian, B.Z., et al., *CCL2 recruits inflammatory monocytes to facilitate breast-tumour metastasis.* Nature, 2011. **475**(7355): p. 222-5.
18. Weitzenfeld, P. and A. Ben-Baruch, *The chemokine system, and its CCR5 and CXCR4 receptors, as potential targets for personalized therapy in cancer.* Cancer Letters, 2014. **352**(1): p. 36-53.
19. Chitu, V. and E.R. Stanley, *Colony-stimulating factor-1 in immunity and inflammation.* Curr Opin Immunol, 2006. **18**(1): p. 39-48.
20. Hume, D.A. and K.P.A. MacDonald, *Therapeutic applications of macrophage colony-stimulating factor-1 (CSF-1) and antagonists of CSF-1 receptor (CSF-1R) signaling.* Blood, 2012. **119**(8): p. 1810-1820.
21. Linde, N., et al., *Vascular endothelial growth factor-induced skin carcinogenesis depends on recruitment and alternative activation of macrophages.* J Pathol, 2012. **227**(1): p. 17-28.
22. Bonavita, E., et al., *Phagocytes as Corrupted Policemen in Cancer-Related Inflammation.* Adv Cancer Res, 2015. **128**: p. 141-71.
23. Cho, M.S., et al., *Autocrine Effects of Tumor-Derived Complement.* Cell Reports, 2014. **6**(6): p. 1085-1095.
24. Fan, H. and J.A. Cook, *Molecular mechanisms of endotoxin tolerance.* J Endotoxin Res, 2004. **10**(2): p. 71-84.
25. Medvedev, A.E., K.M. Kopydlowski, and S.N. Vogel, *Inhibition of lipopolysaccharide-induced signal transduction in endotoxin-tolerized mouse macrophages: dysregulation of cytokine, chemokine, and toll-like receptor 2 and 4 gene expression.* J Immunol, 2000. **164**(11): p. 5564-74.
26. Porta, C., et al., *Tolerance and M2 (alternative) macrophage polarization are related processes orchestrated by p50 nuclear factor kappaB.* Proc Natl Acad Sci U S A, 2009. **106**(35): p. 14978-83.
27. Biswas, S.K., et al., *A distinct and unique transcriptional program expressed by tumor-associated macrophages (defective NF-kappaB and enhanced IRF-3/STAT1 activation).* Blood, 2006. **107**(5): p. 2112-22.
28. Sica, A., et al., *Bacterial lipopolysaccharide rapidly inhibits expression of C-C chemokine receptors in human monocytes.* J Exp Med, 1997. **185**(5): p. 969-74.
29. Jolliffe, I.T. and J. Cadima, *Principal component analysis: a review and recent developments.* Philosophical Transactions of the Royal Society a-Mathematical Physical and Engineering Sciences, 2016. **374**(2065).

30. Romano, M., et al., *Carrageenan-induced acute inflammation in the mouse air pouch synovial model. Role of tumour necrosis factor.* Mediators Inflamm, 1997. **6**(1): p. 32-8.
31. Beinke, S., et al., *Lipopolysaccharide activation of the TPL-2/MEK/extracellular signal-regulated kinase mitogen-activated protein kinase cascade is regulated by IkappaB kinase-induced proteolysis of NF-kappaB1 p105.* Mol Cell Biol, 2004. **24**(21): p. 9658-67.
32. Waterfield, M.R., et al., *NF-kappaB1/p105 regulates lipopolysaccharide-stimulated MAP kinase signaling by governing the stability and function of the Tpl2 kinase.* Mol Cell, 2003. **11**(3): p. 685-94.
33. Furebring, M., et al., *Expression of the C5a receptor (CD88) on granulocytes and monocytes in patients with severe sepsis.* Critical Care, 2002. **6**(4): p. 363-370.
34. Markiewski, M.M., R.A. DeAngelis, and J.D. Lambris, *Complexity of complement activation in sepsis.* Journal of Cellular and Molecular Medicine, 2008. **12**(6a): p. 2245-2254.
35. Ries, C.H., et al., *Targeting tumor-associated macrophages with anti-CSF-1R antibody reveals a strategy for cancer therapy.* Cancer Cell, 2014. **25**(6): p. 846-59.
36. Zhu, Y., et al., *CSF1/CSF1R Blockade Reprograms Tumor-Infiltrating Macrophages and Improves Response to T-cell Checkpoint Immunotherapy in Pancreatic Cancer Models.* Cancer Research, 2014. **74**(18): p. 5057-5069.
37. Ziyad, S. and M.L. Iruela-Arispe, *Molecular mechanisms of tumor angiogenesis.* Genes Cancer, 2011. **2**(12): p. 1085-96.
38. Chung, A.S., J. Lee, and N. Ferrara, *Targeting the tumour vasculature: insights from physiological angiogenesis.* Nat Rev Cancer, 2010. **10**(7): p. 505-14.
39. Abdulamir, A.S., et al., *Severity of asthma: the role of CD25+, CD30+, NF-kappaB, and apoptotic markers.* J Investig Allergol Clin Immunol, 2009. **19**(3): p. 218-24.
40. Nemeth, Z., et al., *Heme oxygenase-1 in macrophages controls prostate cancer progression.* Oncotarget, 2015. **6**(32): p. 33675-33688.
41. Hjortso, M.D. and M.H. Andersen, *The Expression, Function and Targeting of Haem Oxygenase-1 in Cancer.* Current Cancer Drug Targets, 2014. **14**(4): p. 337-347.
42. Coussens, L.M., *Neutralizing tumor-promoting chronic inflammation: A magic bullet? (vol 339, pg 286, 2013).* Science, 2013. **339**(6127): p. 1522-1522.
43. Hanahan, D. and R.A. Weinberg, *Hallmarks of cancer: the next generation.* Cell, 2011. **144**(5): p. 646-74.

44. Mantovani, A., P. Allavena, and A. Sica, *Tumour-associated macrophages as a prototypic type II polarised phagocyte population: role in tumour progression.* Eur J Cancer, 2004. **40**(11): p. 1660-7.
45. Balkwill, F. and A. Mantovani, *Inflammation and cancer: back to Virchow?* Lancet, 2001. **357**(9255): p. 539-45.
46. Vadrevu, S.K., et al., *Complement C5a Receptor Facilitates Cancer Metastasis by Altering T-Cell Responses in the Metastatic Niche.* Cancer Research, 2014. **74**(13): p. 3454-3465.
47. Markiewski, M.M., et al., *Modulation of the antitumor immune response by complement.* Nature Immunology, 2008. **9**(11): p. 1225-1235.
48. Corrales, L., et al., *Anaphylatoxin C5a Creates a Favorable Microenvironment for Lung Cancer Progression.* Journal of Immunology, 2012. **189**(9): p. 4674-4683.
49. Gunn, L., et al., *Opposing Roles for Complement Component C5a in Tumor Progression and the Tumor Microenvironment.* Journal of Immunology, 2012. **189**(6): p. 2985-2994.
50. Wang, Y., et al., *Autocrine Complement Inhibits IL10-Dependent T-cell-Mediated Antitumor Immunity to Promote Tumor Progression.* Cancer Discovery, 2016. **6**(9): p. 1022-1035.
51. Lin, E.Y. and J.W. Pollard, *Tumor-associated macrophages press the angiogenic switch in breast cancer.* Cancer Res, 2007. **67**(11): p. 5064-6.
52. Movahedi, K., et al., *Different tumor microenvironments contain functionally distinct subsets of macrophages derived from Ly6C(high) monocytes.* Cancer Res, 2010. **70**(14): p. 5728-39.
53. Tymoszuk, P., et al., *In situ proliferation contributes to accumulation of tumor-associated macrophages in spontaneous mammary tumors.* Eur J Immunol, 2014. **44**(8): p. 2247-62.
54. Hughes, R., et al., *Perivascular M2 Macrophages Stimulate Tumor Relapse after Chemotherapy.* Cancer Research, 2015. **75**(17): p. 3479-3491.

Supplemental data

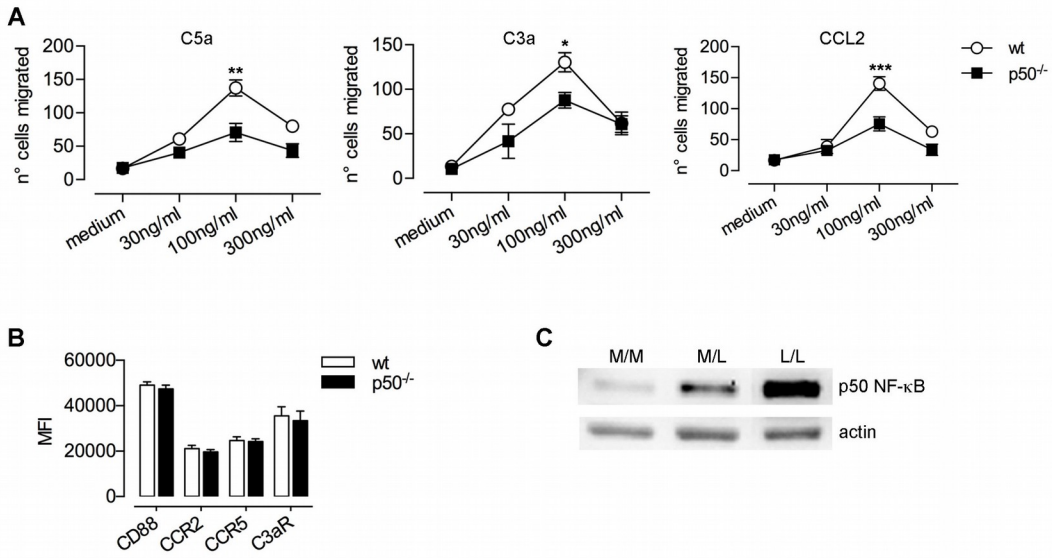

Fig. S1. (A) Wt and p50$^{-/-}$ PEC were used to assemble an *in vitro* dose-response chemotaxis assay in a Boyden chamber, in the presence of different indicated concentrations of each chemotactic stimulus. Data are expressed as the mean +/- SEM. (B) Wt and p50$^{-/-}$ PEC were stained with several antibodies recognizing different chemokine receptors. CD88, CD115, CCR5, CCR2 and C3aR expression are indicated as MFI. (C) Protein lysates from wt PEC (M/M; M/L and L/L) were immunoblotted with anti p50 NF-κB antibody. Actin was used as loading control. Graphs are representative of 3 independent experiments.*$p < 0.05$ **$p < 0.01$ ***$p < 0.001$.

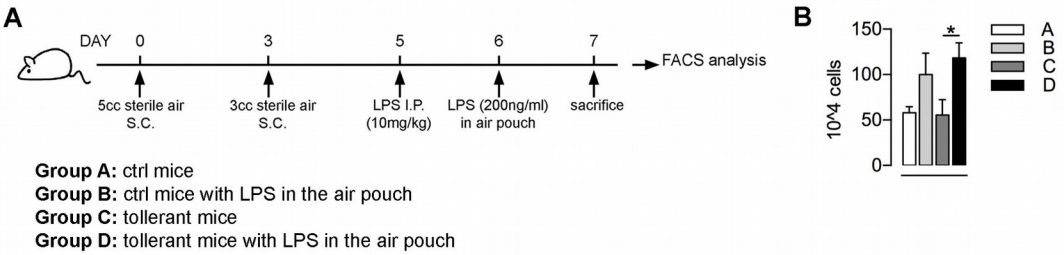

Fig. S2. (A) Air pouch model scheme: wt mice were injected at day 0 subcutaneously with 5cc of sterile air. The injection was repeated at day 3. 48 hrs after the second injection of air, mice belonging to groups C and D were injected IP with LPS 10mg/Kg to induce systemic LPS-tolerance. After additional 24 hrs mice from group B and D were injected with LPS 200ng/ml into the air pouch. At day 7 cells recruited into the air pouch were collected and analyzed by flow cytometry. (B) Number of total CD45^{+} cells recruited into the air pouch in the different groups is shown. Data are expressed as the mean +/- SEM (n = 4-5 mice per group). *$p < 0.05$.

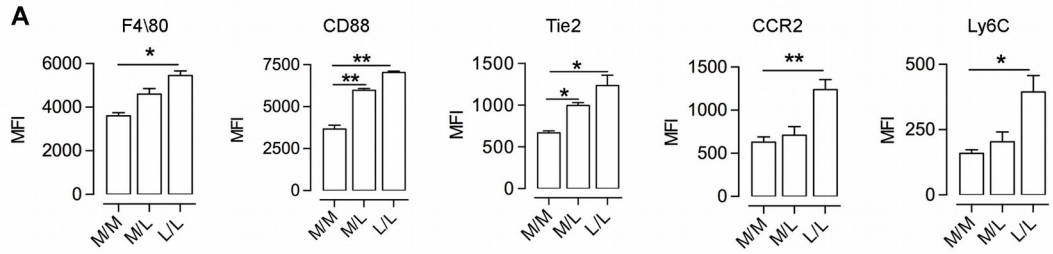

Fig. S3. (A) PEC from wt mice were stimulated or not *in vitro* with LPS (MM=medium; ML=20 hrs medium plus 4 hrs LPS (activated macrophages); LL= 20 hrs LPS plus 4 hrs restimulation with LPS (tolerant macrophages)); after stimulation cells were harvested and analyzed by flow cytometry for the expression (MFI) of F4\80, CD88, Tie2, CCr2 and Ly6C.
Data are expressed as the mean +/- SEM. Graphs are representative of 3 independent experiments. *p < 0.05 **p < 0.01.

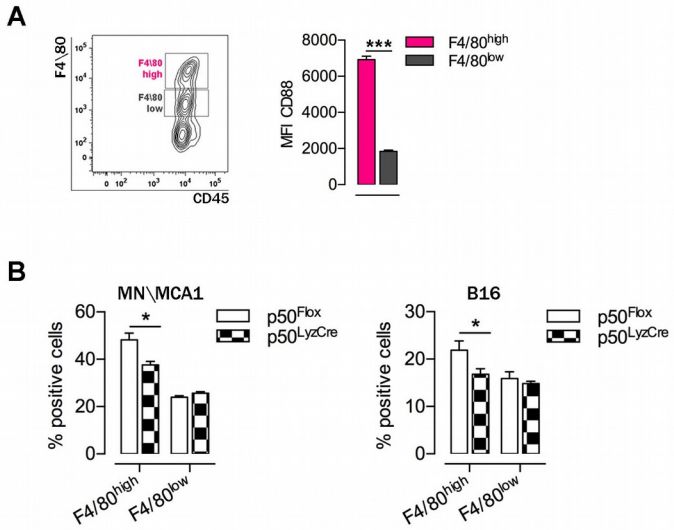

Fig. S4. (A) B16 melanoma tumors from wt tumor-bearing mice were analyzed by FACS for the presence of F4/80^{high} and F4/80^{low} populations and for expression of CD88. (B) Mean percentage of F4/80 ^{high}CD88^{high} and F4/80 ^{low}CD88^{low} TAMs in primary tumors from p50 ^{Flox} and p50^{LyzCre} tumor bearers (MN/MCA1 (left) and B16 (right)). Data are expressed as the mean +/- SEM (n = 4-5 mice per group). *p < 0.05.

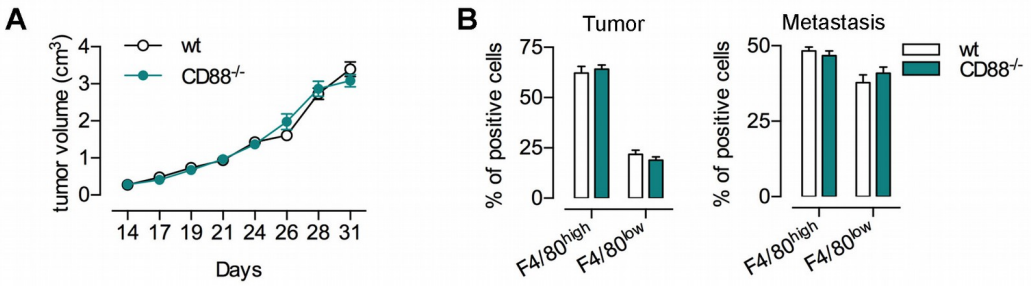

Fig. S5. (A) MN/MCA1 tumor cells were injected in CD88$^{-/-}$ mice and tumor growth was measured 3 times a week starting from day 14 after cells injection. (B) Mean percentage of F4/80^{high}CD88^{high} and F4/80^{low}CD88^{low} TAMs in primary tumors (left) and metastasis (right) from wt and CD88 $^{-/-}$ tumor bearers. Data are expressed as the mean +/- SEM (n = 4-5 mice per group).

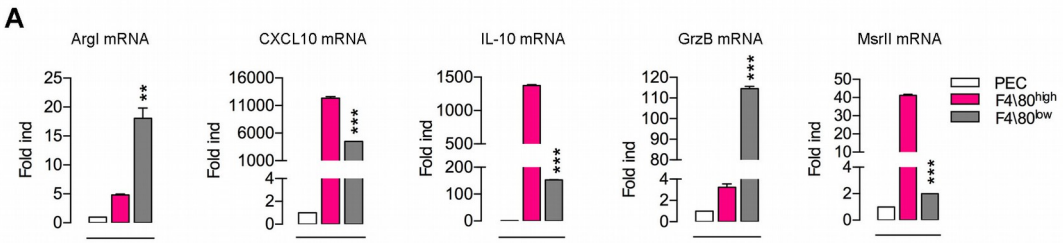

Fig. S6: (A) Total RNA was prepared from F4/80^{high}CD88^{high} and F4/80^{low}CD88^{low} TAMs sorted from MN/MCA1 tumors. mRNA expression levels of seleceted cytokines were analyzed by real-time PCR. Wt PEC were used as a control cells. Graphs are representative of at least 3 independent experiments. Data are expressed as the mean +/- SEM. ***p < 0.001.

Supplemental materials and methods

Mice. The targeting construct to generate a NFKB1flox/flox (p50 ^{Flox}) mice was designed as follows: the eighth exon of NFKB1 gene was flanked with loxP sites and the neomycin resistance gene, flanked with Flippase Recognition Target (FRT) sites to permit its excision, was inserted in the seventh intron. This construct was introduced by electroporation into mouse ES cells. Homologous recombination was confirmed by southern blot and ES cells carrying NFKB1fl-neo allele were injected into C57 blastocysts to generate germ-line chimeras. The neomycin resistance cassette in the targeting construct was removed by crossing heterozygous NFKB1+/fl-neo mice with mice carrying the FLP recombinase under the control of the actin promoter (kindly provided by Rolf Sprengel) to produce mice carrying the NFKB1 floxed allele (p50F/F mice). p50^{Flox} mice were crossed with B6.129P2-Lyz2tm1(cre)Ifo/J mice (Jackson Laboratories, Bar Harbor, Maine, USA) to generate p50fl/fl; LyzCre mice. Homozygous CD88 (C5aR1) mutant mice were kindly donated by Dr. J.D. Lambris (Pathology and Laboratory Medicine, University of Pennsylvania, USA).

B16 tumor model. 8 weeks old wt, p50^{Flox} and p50^{LyzCre} mice were injected subcutaneously with 5*10^5 cells of melanoma (B16)/200∝l saline solution into the right flank. Tumor growth was monitored 3 times a week with a caliper, starting from day 13.

Chapter 4

RORC1 regulates tumor-promoting "emergency" granulo-monocytopoiesis

Published on Cancer Cell 28, 253–269
August 10, 2015 ©2015 Elsevier Inc.
http://dx.doi.org/10.1016/j.ccell.2015.07.006

Laura Strauss,[1] Sabina Sangaletti,[4] Francesca Maria Consonni,[2] Gabor Szebeni,[1] Sara Morlacchi,[1] Maria Grazia Totaro, [1] Chiara Porta,[2] Achille Anselmo,[1] Silvia Tartari,[1] Andrea Doni,[1] Francesco Zitelli,[2] Claudio Tripodo,[3] Mario P. Colombo,[4] and Antonio Sica [1,2,*]

[1]Department of Inflammation and Immunology, Humanitas Clinical and Research Center, 20089 Rozzano, Milan, Italy. [2]Department of Pharmaceutical Sciences, Universita` del Piemonte Orientale ''Amedeo Avogadro,'' Via Bovio 6, 28100 Novara, Italy. [3]Tumor Immunology Unit, Department of Health Sciences, University of Palermo, Via del Vespro 129, 90127 Palermo, Italy. [4]Experimental Oncology, Fondazione IRCCS Istituto Nazionale Tumori, 20133 Milan, Italy .
*Correspondence: antonio.sica@humanitasresearch.it

Graphical abstract

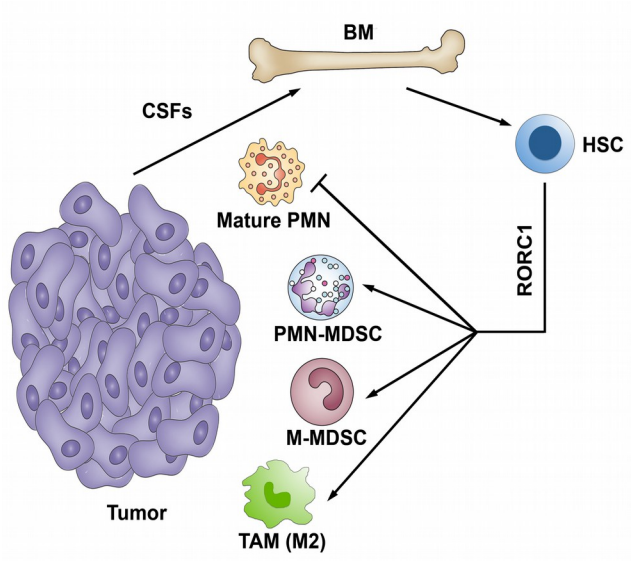

In brief

Strauss et al. show that RORC1 orchestrates myelopoiesis and supports tumor-promoting innate immunity. Importantly, ablation of RORC1 in the myeloid compartment inhibits tumor growth and metastasis, suggesting a cancer therapeutic approach.

Significance

Preclinical data show that MDSCs and TAMs orchestrate tumor-promoting conditions, suggesting these cells as attractive therapeutic targets. MDSCs and TAMs generation is tightly associated with the altered hematopoietic output that occurs in cancer, defined as "emergency hematopoiesis." Here we report that RORC1 is a key driver of emergency hematopoiesis in tumor bearers, in response to colony-stimulating factors (G-CSF, GM-CSF, and M-CSF), and that RORC1-expressing myeloid cells mark advanced cancer inflammation. We demonstrate that ablation of RORC1 in the myeloid compartment impairs tumor development and the generation of suppressive MDSCs while promoting generation of antitumor M1-polarized TAMs. Thus, inhibition of RORC1-dependent myelopoiesis may represent a therapeutic approach to prevent the induction of the tumor-promoting host macro- and microenvironments.

Abstract

Cancer-driven granulo-monocytopoiesis stimulates expansion of tumor promoting myeloid populations, mostly myeloid-derived suppressor cells (MDSCs) and tumor-associated macrophages (TAMs). We identified subsets of MDSCs and TAMs based on the expression of retinoic-acid-related orphan receptor (RORC1/RORγ) in human and mouse tumor bearers. RORC1 orchestrates myelopoiesis by suppressing negative (Socs3 and Bcl3) and promoting positive (C/EBPb) regulators of granulopoiesis, as well as the key transcriptional mediators of myeloid progenitor commitment and differentiation to the monocytic/macrophage lineage (IRF8 and PU.1). RORC1 supported tumor-promoting innate immunity by protecting MDSCs from apoptosis, mediating TAMs differentiation and M2 polarization, and limiting tumor infiltration by mature neutrophils. Accordingly, ablation of RORC1 in the hematopoietic compartment prevented cancer-driven myelopoiesis, resulting in inhibition of tumor growth and metastasis.

Introduction

Immunologic stress, such as infection and cancer, modifies the magnitude and composition of the hematopoietic output, a feature of immune regulation defined as ‘‘emergency’’ hematopoiesis, to guarantee proper supply of immune cells to increased demand [1]. Tumors can reprogram myeloid cells to promote disease progression [2]. However, the molecular pathways guiding cancer-driven ‘‘emer- gency’’ myelopoiesis remain largely unknown. Colony-stimulating factors (CSFs) are major orchestrators of hematopoietic development. Among these, granulocyte CSF (G-CSF) and granulocyte-macrophage CSF (GM-CSF) drive ‘‘emergency’’ myelopoiesis by securing supply of neutrophils and macrophages from bone marrow (BM) and hematopoietic stem cell niches (HSCs) [1, 3]. Further, the macrophage CSF (M-CSF) promotes macrophage differentiation from medullar precursors and differentiation of tissue macrophages involved in tissue homeostasis [4] and tumor progression [5]. Recent studies reveal that monocytic and granulocytic myeloid-derived suppressor cells (M-MDSCs and PMN-MDSCs, respectively) and tumor-associated macrophages (TAMs), the major myeloid populations associated with cancer development [2], differentiate from a common myeloid progenitor (CMP) [6]. Importantly, reciprocal regulation of macrophage versus neutrophil/granulocyte differentiation might control tissue homeostasis. Depletion of tissue macrophages leads to exacerbated G-CSF-mediated granulopoiesis [7, 8], and tissue macrophages regulate HSC niche homeostasis [9, 10]. Thus, investigation of the molecular networks that dictate this reciprocal regulation appears to be crucial, as it may affect tissue homeostasis during cancerogenesis.

G-CSF-induced granulopoiesis is mediated through the transcription factors c-EBPb [11] and STAT3 [12], whereas M-CSF supports monocyte differentiation through the transcription factors PU.1 and IRF8 [13]. Of relevance, interleukin-

17A (IL-17A) promotes G-CSF- and stem-cell-factor-mediated neutrophilia [14] and supports G-CSF-driven ‘‘emergency’’ myelopoiesis [15].

Despite the fact that IL-17 expression in cancer has been so far mainly restricted to the adaptive immunity [16] and its role in cancer remains controversial [17], TAMs and MDSCs produce the Th17-driving cytokines TGFb and IL-6 [18], and IL- 17-expressing cells with macrophage morphology have been described in cancer patients [19]. Although the Th17 response is controlled by the nuclear receptor retinoic-acid-related orphan receptor gamma (RORγ) full-length protein (RORC1) and the RORC γt splice variant (RORC2) [20], the signaling pathways that drive IL-17-producing innate immune cells have been poorly investigated. IL-17A-expressing myeloid cells have been reported in inflammation [19, 21, 22]. In arthritis patients, mast cells express a dual RORC1/IL-17A fingerprint in response to TLR4 ligands [23], and a population of RORγt-expressing neutrophils that produce IL-17 was identified in fungal infection [21]. We explored the role of the IL-17/RORC1 axis in myeloid lineage differentiation and commitment associated with cancer development.

Experimental procedures

More-detailed procedures can be found in the Supplemental Experimental Procedures.

Ethics statement. The study was approved by the scientific board of Humanitas Clinical and Research Center and designed in compliance with Italian governing law, EU directives and guidelines, and the NIH Guide for the Care and Use of Laboratory Animals. Mice have been monitored daily and euthanized when displaying excessive discomfort. Cancer patients were enrolled in the study after signing Cancer Research Center Humanitas IRB-approved consent.

Mice. C57BL/6 mice were purchased from Charles River. RORC1 mutant mice (B6.129P2(Cg)-*Rorctm1Litt*/J) [24] were donated by Dr. Dan Littman (New York University). MMTV-PyMT mice [25] were donated by Professor Guido Forni (University of Turin) and mated with C57BL/6 females to obtain the F1 C57BL/6-MMTV-PyMT strain. IL-17A-deficient mice were donated by Dr. Burkhard Becher (University of Zurich). All animal work was conducted under the approval of the Humanitas Clinical and Research Center, in accordance with Italian and EU directives and guidelines.

BM transplantation. $5*10^6$ CD45.2 RORC1-deficient (*Rorc1*$^{-/-}$), IL-17A$^{-/-}$, or WT BM cells were injected intravenously into 8-week-old lethally irradiated (two doses of 475 cGy) CD45.1 C57BL/6 WT male or C57BL/6-MMTV-PyMT female mice. 8 weeks later, BM engraftment was checked by staining of blood cells with PerCP-conjugated CD45.1 antibody and PE-conjugated CD45.2 antibody (BD Biosciences) and subsequent FACS analysis.

Tumor models. 10^5 murine fibrosarcoma (MN/MCA1) cells were injected intramuscularly in the left hind limb. Tumor growth was monitored three times a week with a caliper, starting from day 14. The models of chemically induce fibrosarcoma and mammary tumor virus-polyoma middle T antigen (MMTV-PyMT) transgenic mice are described in the Supplemental Experimental Procedures.

Cell culture and Reagents. Lineage cell separation from BM, isolation of myeloid cells, and cell-culture conditions are described in the Supplemental Experimental Procedures.

Mixed-Lymphocyte Reaction. Mixed-lymphocyte reaction was performed as previously reported [26] and as described in the Supplemental Experimental Procedures.

Patients. Ten patients with T2 or T3 CRC did not receive radiation or chemotherapy before sample collection.

Flow Cytometry. Detailed conditions and antibodies used in flow cytometry analysis are described in the Supplemental Experimental Procedures

Gating strategy. Gating strategy for the identification of human MDSCs, neutrophils, and mono- cytes is described in the Supplemental Experimental Procedures.

Histopathological analysis. Histopathological analysis was performed on BM and spleens from WT, *Rorc1* $^{-/-}$, and chimeric mice on sections routinely stained with H&E. Single- and double-marker immunohistochemistry on mouse and human tissue spec- imens were performed as previously reported [27] and are described in detail in the Supplemental Experimental Procedures.

Confocal Microscopy. Confocal Microscopy was performed as previously reported [28] and as described in the Supplemental Experimental Procedures.

Statistics. Statistical significance was determined by a two-tailed Student's t test (*p <0.05, ** p <0.01, *** p <0.001).

Results

Divergent RORC1/IL-17A Fingerprint in Tumor-Associated Myeloid Cells.

To clarify the role of IL-17A$^+$ innate immune cells in tumor progression, we screened the myeloid compartment of fibrosarcoma (MN/MCA1)-bearing C57BL/6 mice. A tumor volume of <1.5 cm^3 and few lung metastases (fewer than five), at days 21–23 after tumor cell injection, was defined as early-stage disease (ED), whereas tumors larger than 2 cm^3 and a higher number of lung metastases (more than 15; days 25–28) was defined as advanced-stage disease (AD) (Fig. S1). In AD, few blood and spleen CD45$^+$CD3$^+$ T cells expressed IL-17A (data not shown), whereas IL-17A was significantly expressed by CD45$^+$ CD3$^-$ cells in the blood (30% ± 3%) and spleen (12% ± 1.5%) (Fig. 1A). Few CD45$^+$ CD3$^-$ cells expressed IL-17A in non-tumor bearers (NTs) and ED, suggesting that IL-17A$^+$ myeloid cells mark advanced cancer-associated inflammation. FACS analysis of the CD45$^+$ CD3$^-$ cell pool confirmed that Gr1$^+$CD11b$^+$ MDSCs represent the major splenic myeloid population in AD (Fig. 1B), comprising a predominant polymorphonuclear CD11b$^+$Gr1$^+$Ly6G^{high}Ly6C^{low} (PMN-MDSCs) population and side monocytic CD11b$^+$Gr1$^+$Ly6C^{high}Ly6G^{low} (M-MDSCs) and CD11b$^+$F4/80$^+$ macrophage populations. IL-17A was significantly expressed by PMN-MDSCs in the blood and spleen of AD mice (Fig. 1C), although these cells failed to release IL-17 in response to degranulating signals, including CD16/32 (FCII/III) antibody-mediated cross-linkage and C5a (data not shown) [29]. In contrast, IL-17A was poorly or not expressed by M-MDSCs (Fig. 1C) and CD11b$^+$F4/80$^+$ macrophages (data not shown).

RORC1 and its splice variant RORC2 are master regulators of IL-17A gene transcription in Th17 cells [20], innate lymphocytes [30], γδ T cells [31], and natural killer T cells [32]. Hence, we tested by FACS whether IL-17 expression in myeloid cells was associated with RORC1. In keeping with IL-17A expression, the majority of blood and spleen PMN-MDSCs from AD mice

expressed RORC1, while its expression was restricted to a minor subset of IL-17A M-MDSCs (Fig. 1D, left). Nevertheless, as compared to PMN-MDSCs, M-MDSCs expressed higher levels of RORC1, estimated as mean fluorescence intensity (MFI) (Fig. 1D, right). It is noteworthy that RORC1 was highly expressed by splenic IL-17A $CD11b^{+}F4/80^{+}$ macrophages in AD mice (Fig. 1E), by $F4/80^{+}$ TAMs (>90%) and thyoglicollate-elicited peritoneal macrophages (PECs) from both tumor-free (NT-PEC) and AD (AD-PEC) mice (Fig. 1E).

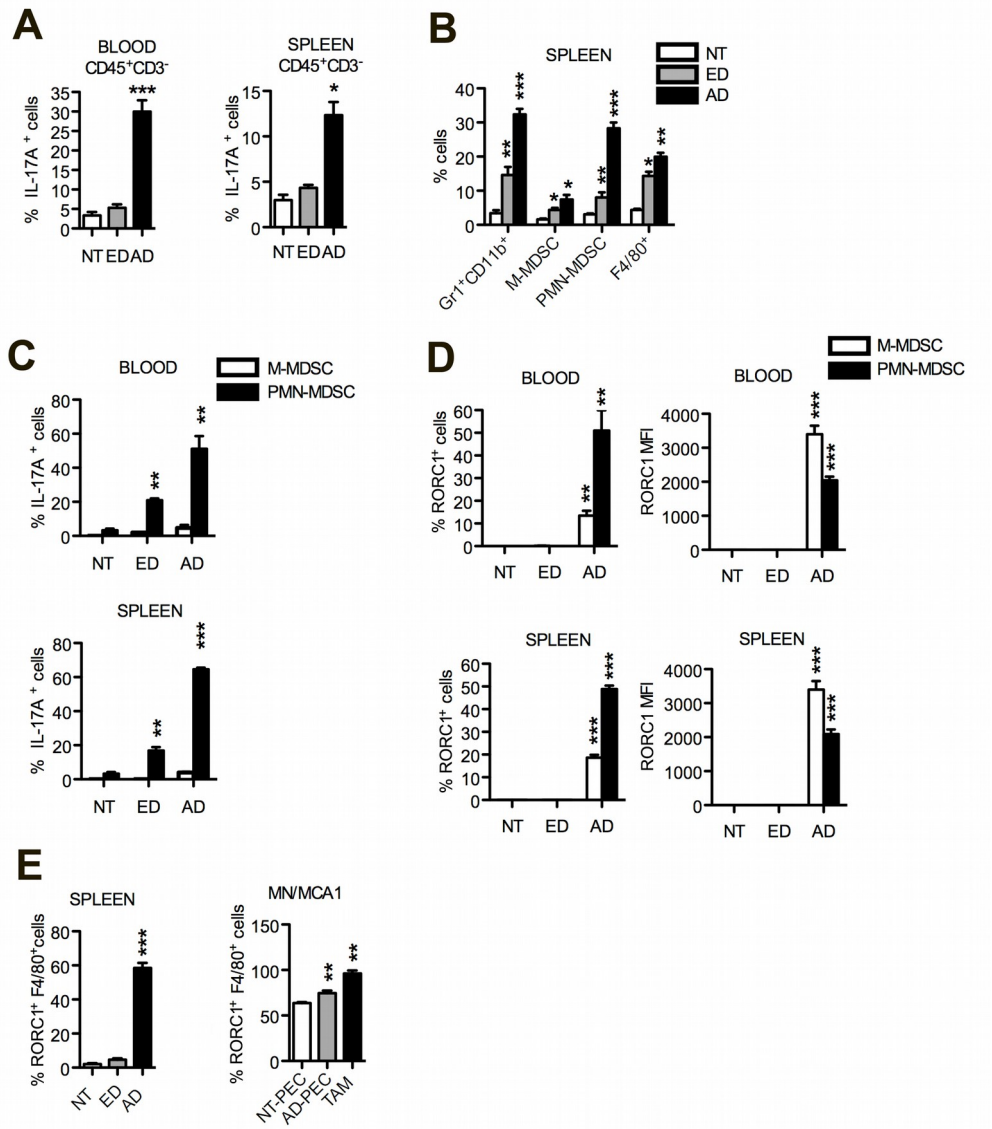

Fig. 1: Myeloid-specific IL-17A $^{+}$/RORC1^{+} cells mark advanced cancer-associated inflammation. (A) Expression of IL-17A by CD45 $^{+}$CD3^{-} hematopoietic cells in blood (left) or spleens (right) from tumor-free (NT) or MN/MCA1-bearing mice, at both early tumor disease (ED) and advanced tumor disease (AD). Mean percentages ± SEM of IL-17A $^{+}$ cells within the CD45^{+}CD4^{-}CD3^{-} gate were measured by fluorescence-activated cell sorting (FACS). (B) Myeloid subsets in spleens from tumor-bearing mice. Mean percentages ± SEM of Gr1 $^{+}$CD11b^{+} (total MDSCs), CD11b $^{+}$Gr1^{+}Ly6C^{high}Ly6G^{low} (M-MDSCs), CD11b $^{+}$Gr1^{+}Ly6G^{+}Ly6C^{low} (PMN-MDSCs) and CD11b^{+}F4/80^{+} cells in spleen from NT, ED, or AD mice measured within the CD45^{+} gate. (C) Mean percentages ± SEM of IL-17A-expressing M-MDSCs and PMN-MDSCs in blood or spleens from NT, ED, or AD mice. (D) Mean percentages and MFI ± SEM of RORC1-expressing M-MDSCs and PMN-MDSCs in blood or spleens from NT or tumor-bearing mice. (E) RORC1-expressing splenic CD11b $^{+}$F4/80^{+} cells obtained from NT, ED, and AD mice (left) or RORC1-expressing PECs obtained from NT (NT-PECs) and AD (AD-PECs) mice and RORC1-expressing TAMs isolated from AD tumors (MN/MCA1) (right). Results are shown as mean percentages ± SEM. Expression of IL-17A and RORC1 in myeloid cells was determined within the CD11b $^{+}$CD45^{+} gate. Results of a representative experiment of six independent experiments with six mice/group are shown. Statistical analysis: *p < 0.05, **p < 0.01, ***p < 0.001 (Student's t test). See also Figure S1.

To corroborate the evidence that ED stages already promote emergency hematopoiesis, we performed histopathological and immunohistochemical analysis of both spleens and BM from mice bearing early- and late-stage tumor (Fig. 2A). Histopathological analysis of the BM parenchyma of wild-type and *Rorc1*$^{-/-}$ tumor-free and tumor-bearing mice (including ED and AD tumor stages) showed a significant expansion of the granulocytic compartment (Fig. 2A, top), which associated with a progressive contraction of the erythroid colonies (blue arrows) and with signs of dysmegakaryopoiesis (i.e., megakaryocytes with bulbous and/or hypolobated nuclei and prominent pleiomorphism; red arrows). Notably, at late time points (AD), the BM granulocytic hyperplasia of tumor-associated emergency hematopoiesis was characterized by the enrichment in immature myeloid precursors (Fig. 2A, top, dashed lines), which were more conspicuous in WT than in *Rorc1* $^{-/-}$ mice. As expected, tumor-free mice showed a normal composition of the hematopoietic parenchyma in the BM with preserved myeloid/erythroid ratio and normal maturation of the myeloid elements. Spleen histopathology performed on the

same animals demonstrated signs of tumor-associated emergency hematopoiesis in the spleen parenchyma of ED and AD tumor-bearing WT and *Rorc1* $^{-/-}$ mice, in the form of red pulp hyperplasia underlying splenomegaly (Fig. 2A, bottom). The enhanced myelopoiesis of WT mice featured the progressive (i.e., from ED to AD) accumulation of clusters of morphologically immature granulocytes (Fig. 2A, bottom, arrows and dashed lines; right H&E insets) that intermingled with erythroid precursor islets, megakaryocytes, and polymorphonuclear granulocytes. Despite a comparable degree of red pulp hyperplasia due to the consistent increase in polymorphonuclear granulocytes, erythroid precursors, and megakaryocyte clusters, *Rorc1*$^{-/-}$ mice showed less clusters of morphologically immature myeloid cells as compared with their WT counterparts (Fig. 2A, bottom, arrows and dashed lines; right H&E insets). Immunohistochemical analysis of the MDSC- associated IL-4R marker highlighted IL-4R^{+} myeloid cells with monocytoid or granulocytic morphology populating the myeloid cell aggregates differently enriched within the expanded red pulp of tumor-bearing WT and *Rorc1*$^{-/-}$ mice (Fig. 2A). Overall, these results demonstrate that *Rorc1*$^{-/-}$ mice effectively instruct BM and splenic emergency hematopoiesis along cancer development while displaying a defective induction of specific MDSC-related myeloid populations. With the gating strategy used to determine IL-17A and RORC1 shown in Fig. 2B, our results suggest that RORC1 expression is uncoupled from IL-17A in the monocytic/macrophage compartment, while it is co-expressed in the granulocytic cells of tumor-bearing mice.

To validate this finding in cancer patients, we analyzed the MDSC populations in PBMCs from healthy donors (HDs; n = 10) or patients with advanced colorectal cancer (CRC; stage II/III; n = 10) using the gating strategy of Fig. 2C. It is noteworthy that the number of RORC1^{+} M-MDSCs (HLA-DR$^{low/-}$ CD14^{+}CD33^{high}) and PMN-MDSCs (HLA-DR $^{low/-}$CD15^{+}CD33^{high}) increased in CRC patients and dominated in the human PMN-MDSC subset (Fig. 2D). Expansion of MDSC populations in cancer patients was paralleled by an

increased number of circulating neutrophils and monocytes (Fig. 2D). Also in analogy to the murine setting (Fig. 1D), the human M-MDSCs population showed higher mean fluorescence intensity of RORC1^{+}. In contrast, IL-17A was detected neither in human blood M-MDSCs nor in PMN-MDSCs (data not shown). These results indicate that expression of RORC1 by myeloid subsets constitutes a hallmark of tumor-promoting ‘‘emergency’’ myelopoiesis.

RORC1 Promotes Expansion of MDSCs and TAMs. To investigate the *in vivo* relevance of RORC1-expressing myeloid cells, we transplanted donor RORC1-deficient BM cells into lethally irradiated C57BL/6 WT recipient mice (*Rorc1*$^{-/-}$ >WT), to be compared to WT>WT mice. Eight weeks later, mice were injected with MN/MCA1 cells and monitored for tumor development. Tumor growth and metastasis were significantly reduced in *Rorc1*$^{-/-}$>WT mice (Fig. 3A). The effect of RORC1 deficiency in BM cells was tested in two additional tumor models. *Rorc1*$^{-/-}$ BM was transplanted into mouse mammary tumor virus-polyoma middle T antigen (MMTV-PyMT; a spontaneous mammary carcinoma) transgenic mice and into C57BL/6 mice that were exposed to methylcholanthrene-induced cancerogenesis and subsequently developed fibrosarcoma [33] (Fig. 3B). Consistently, RORC1 deficiency in the BM resulted in tumor growth inhibition in both models (Fig. 3B). FACS analysis (data not shown) confirmed the IL-17/RORC1 expression pattern observed in the MN/MCA1 model (Fig. 1). *Rorc1*$^{-/-}$>WT tumor-bearing mice showed a significant reduction of splenic M-MDSCs and PMN-MDSCs, in comparison to WT>WT mice (Fig. 3C).

To estimate the suppressive activity of M-MDSCs, we activated cells with IFN-γ [6], loaded them with ovalbumin, and then co-cultured them for 3 days with total splenocytes purified from OT-1 transgenic mice expressing the T cell receptor specific for the ovalbumin antigen. *Rorc1*$^{-/-}$ M-MDSCs displayed reduced suppressive activity, estimated as proliferation of co-cultured OT1

splenocytes (Fig. 3D). It is noteworthy that, at the tumor site, we observed an increase of PMN-MDSCs (Fig. 3E), as opposed to a significant decrease of $CD11b^{+}Ly6C^{low}F4/80^{+}$ TAMs (Fig. 3F).

Histological analysis of spleens from *Rorc1*-deficient tumor bearers showed a dramatic reduction in IL-4R $^{+}$ MDSCs [34] and strongly reduced expression of IL-17A (Fig. 3G) in comparison to WT counterpart. These results are further confirmative of the IL-4R expression analyses on WT and *Rorc1*$^{-/-}$ BM (Fig. 2A) and imply that RORC1 promotes the expansion of splenic MDSCs and TAMs. To confirm this conclusion, we treated tumor-free or MN/MCA1-bearing WT mice with the RORC1 agonist SR1078 [35]. SR1078 increased the AD lung metastatic burden (Fig. S2A), as well as splenic M-MDSCs and PMN-MDSCs (Fig. S2B, left). Despite the fact that CD11b $^{+}F4/80^{+}$ macrophages were not modified (data not shown), SR1078 increased RORC1 expression in splenic macrophages, as well as in M-MDSCs and PMN-MDSCs (Fig. S2B). By contrast, IL-17A expression was selectively induced in PMN-MDSCs (Fig. S2B, right). Of note, SR1078 did not affect steady-state myelopoiesis in tumor-free mice (Fig. S2C), confirming RORC1 as a positive regulator of myelopoiesis in cancer.

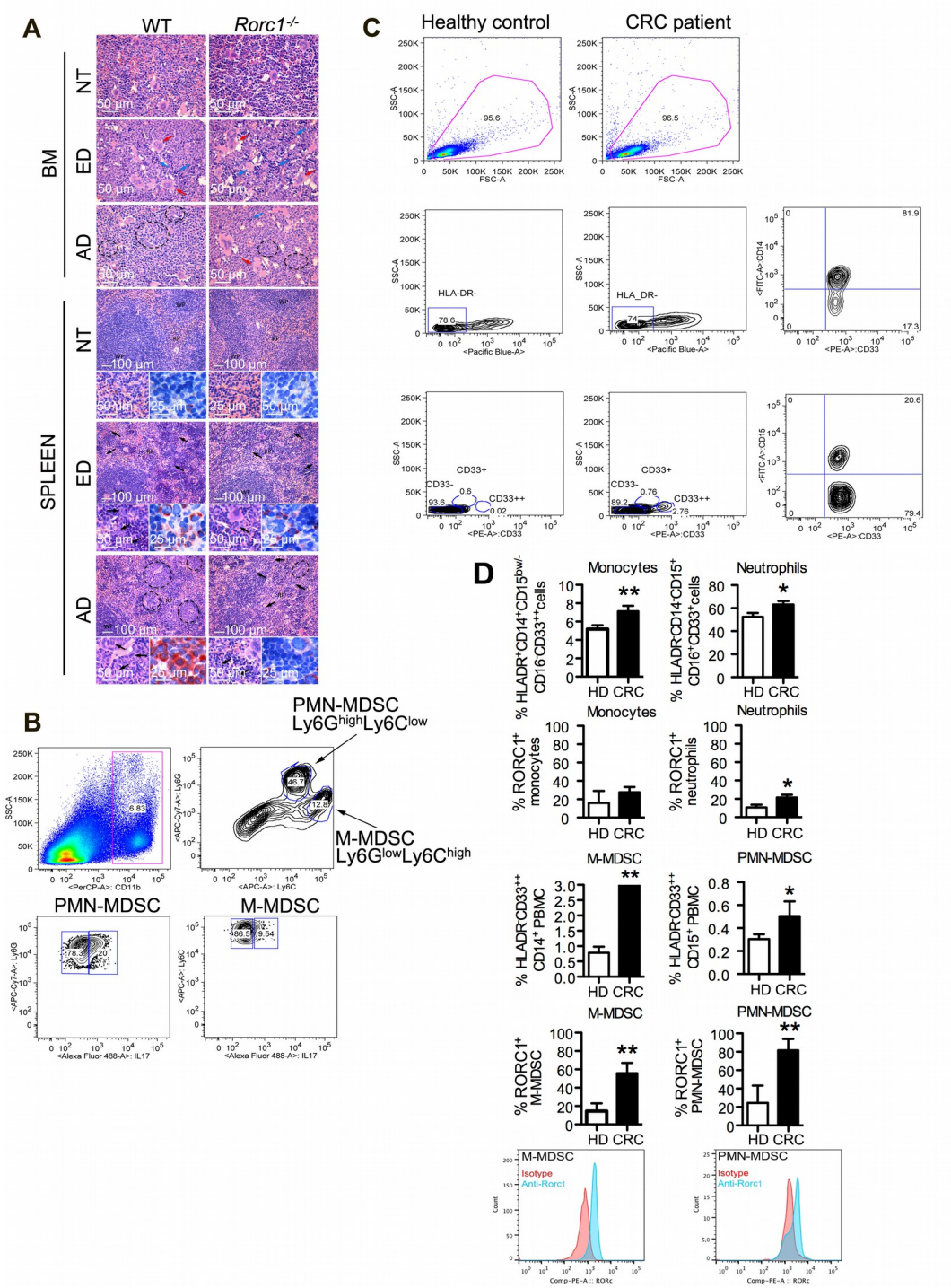

Fig. 2: Effects of RORC1 on emergency hematopoiesis associated with cancer development. (A) Top: BM histopathological analysis of WT (left) and *Rorc1* $^{-/-}$ (right) tumor-free (NT) and tumor-bearing mice with early (ED) and advanced (AD) disease, showing the

progressive changes in BM hematopoietic parenchyma along tumor development in the two strains. While tumor-free mice displayed a normal hematopoietic composition with no detectable differences between WT and *Rorc1*$^{-/-}$ strains, ED and AD BM samples showed a progressive expansion of the myeloid granulocytic lineage, which was paralleled by the contraction of the erythroid (blue arrows) and megakaryocytic (red arrows) compartments and was similarly observed in WT and *Rorc1* $^{-/-}$ mice. In AD samples, the myeloid pool expansion was also characterized by the increase in morphologically immature myeloid cell clusters (dashed lines), which was consistent with the enhanced myelopoietic activitiy of stress-adapted (i.e., cancer-associated) myelopoiesis. The immature myeloid cell clusters characterizing AD samples were more prominent in WT than in *Rorc1*$^{-/-}$ mice. Original magnifications of H&E panels are 3400. Bottom: spleen histopathological analysis of WT (left) and *Rorc1*$^{-/-}$ (right, composite panels) tumor-free (upper panels) and tumor-bearing (ED, middle composite panels; AD, lower composite panels) mice showing the progressive increase in red pulp (RP) hematopoietic function along tumor development in the two strains. In tumor-free mice, white pulp (WP) areas are predominant over RP, the latter being mainly populated by erythroid cells with scattered myeloid and megakaryocytic elements (upper H&E panels and upper H&E insets). In ED and AD samples, RP hyperplasia was evident and consequent to the increase of hematopoietic foci. In particular, the RP WT mice showed an increase in immature myeloid cell figures (left middle and lower H&E panels, arrows and dashed lines) showing granulocytic or monocytoid morphology (left middle and lower H&E insets, arrows), along with an increase in megakaryocyte and erythroid precursor clusters. In *Rorc1* $^{-/-}$ mice, despite a comparable degree of RP hyperplasia mainly consequent to megakaryocyte and polymorphonuclear granulocyte expansion and clustering, foci of morphologically immature myeloid cells were less evident (right middle and lower H&E panels and insets, arrows and dashed lines). Within the RP myeloid cell clusters that were differently expanded in WT and *Rorc1* $^{-/-}$ mice, cells with granulocytic or monocytoid morphology expressing the MDSC marker IL-4R were detected (IHC insets, red signal). (B) Gating strategy used to determine the different mouse myeloid subsets. (C) Gating strategy used to determine the different human myeloid subsets. (D) Cytofluorimetric analysis of RORC1 expression in the circulating MDSC subsets, neutrophils, and monocytes from CRC patients as indicated. MDSC analysis was performed on PBMCs, and analysis of neutrophils and monocytes was carried out in whole blood. Mean percentages ± SEM of M-MDSCs (HLA-DR$^-$ CD33^{2+}CD14$^+$), PMN-MDSCs (HLA-DR$^-$ CD33^{2+}CD15$^+$), monocytes (HLA-DR$^+$CD14$^+$CD15$^{low/-}$CD16$^-$CD33^{2+}), and neutrophils (HLA-DR$^-$CD14$^-$CD15$^+$CD16$^+$CD33$^+$) in blood from healthy donors (HD; n = 10) and CRC patients (n = 10) are shown. Statistical analysis: *p < 0.05, **p < 0.01, ***p < 0.001 (Student's t test). Below, a representative flow-cytometry analysis of RORC1 $^+$ M-MDSCs and RORC1 $^+$ PMN-MDSCs from cancer patients is also shown.

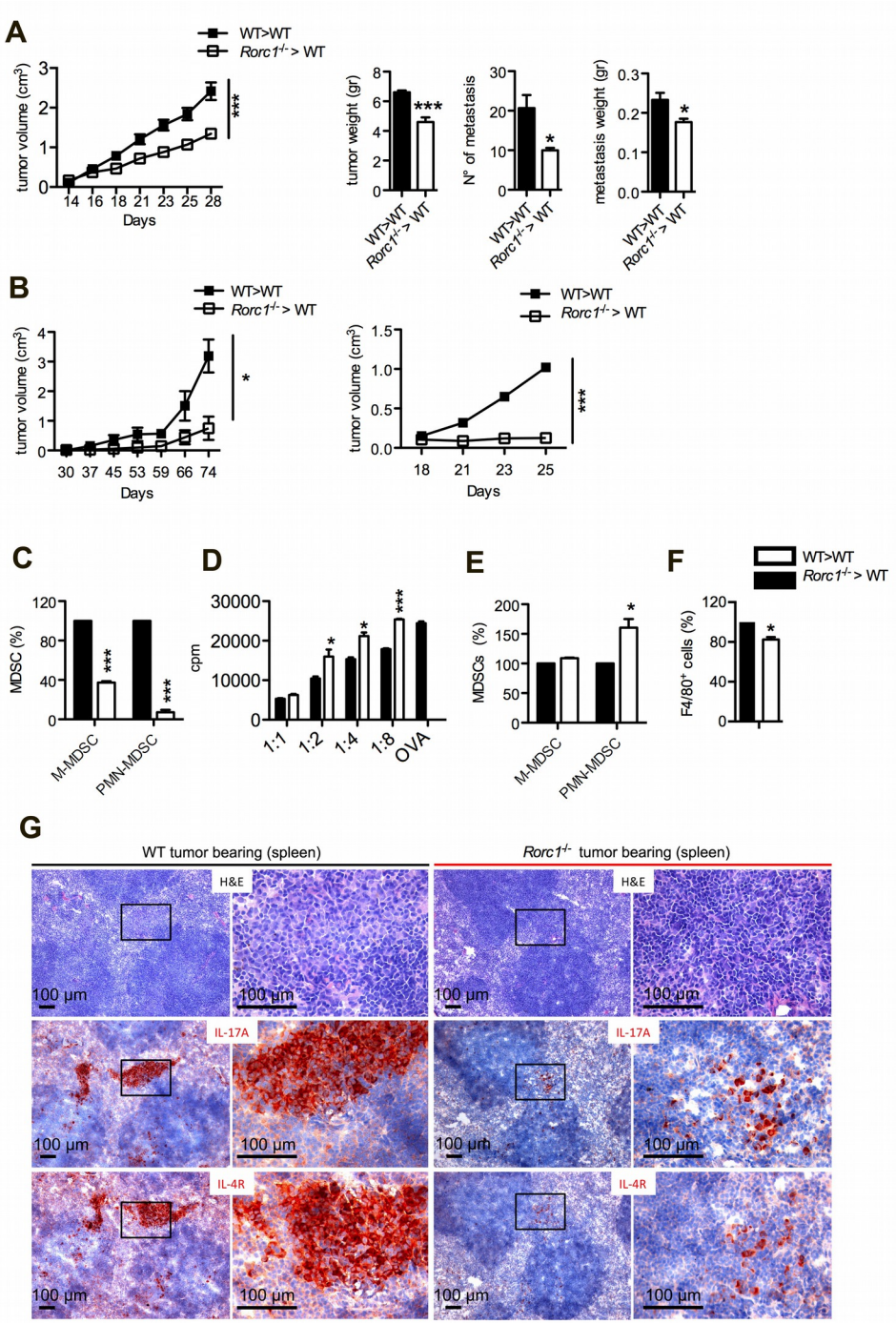

Fig. 3: Role of RORC1 in the expansion of MDSCs and TAMs during tumor-driven emergency myelopoiesis. (A) MN/MCA1 cells were injected into the indicated hematopoietic reconstituted mice. Starting from day 14 after MN/MCA1 cell injection, tumor volume (cm^3) was monitored. At day 28, mice were sacrificed, the weight of the tumors (g) was estimated (left), and the number and weight of macroscopic lung metastases was measured

(right). Data are shown are the mean ± SEM of at least 12 mice/group. Statistical analysis: *p < 0.05, **p < 0.01, ***p < 0.001 (Student's t test). (B) *Rorc1*$^{-/-}$ BM was transplanted into MMTV-PyMT transgenic mice (left) or C57Bl/6 mice, which were subsequently exposed to methylcholanthrene to induce fibrosarcoma (right). Mean tumor volumes (cm^{3}) ± SEM from six WT>WT and *Rorc1*$^{-/-}$>WT chimeras are shown. Statistical analysis: *p < 0.05, **p < 0.01, ***p < 0.001 (Student's t test). (C) Mean percentages ± SEM of M-MDSCs and PMN-MDSCs in spleens from WT>WT and *Rorc1*$^{-/-}$>WT tumor (MN/MCA1) bearers. Statistical analysis: *p < 0.05, **p < 0.01, ***p < 0.001 (Student's t test). (D) Decreased antigen-specific (OVA) suppressive activity of *Rorc1*$^{-/-}$ M-MDSCs in response to IFN- γ at different MDSC:OT1 splenocyte ratios. Data shown are the mean ± SEM of a representative experiment done in triplicate. Statistical analysis: *p < 0.05, **p < 0.01, ***p < 0.001 (Student's t test). (E) Mean percentages ± SEM of M-MDSCs and PMN-MDSCs in primary AD tumors (MN/MCA1) from WT>WT and *Rorc1*$^{-/-}$>WT mice (AD). Statistical analysis: *p < 0.05, **p < 0.01, ***p < 0.001 (Student's t test). (F) Mean percentages ± SEM of F4/80+ TAMs in primary tumors from WT>WT and *Rorc1*$^{-/-}$>WT tumor bearers (MN/MCA1). Myeloid cell percentage in *Rorc1*$^{-/-}$>WT chimeras (white bar) is represented as relative value as compared to WT>WT chimeras (100%) (black bar). Data from a representative experiment, of six independent experiments, with n = 6 mice per group is shown. Statistical analysis: *p < 0.05, **p < 0.01, ***p < 0.001 (Student's t test). (G) Histological analysis of IL-17A^{+} and IL-4R^{+} in the splenic MDSCs population in WT and *Rorc1*$^{-/-}$ tumor-bearing mice.

To explain the reduction of MDSCs in *Rorc1*$^{-/-}$ tumor-bearing mice, we considered two possible mechanisms: RORC1 regulates the differentiation of hematopoietic precursors in the BM (Fig. 4) and/or RORC1 regulates the survival and maturation of MDSCs (Fig. S3). We first analyzed by FACS the commitment of common hematopoietic progenitors in tumor-bearing WT>WT and *Rorc1*$^{-/-}$>WT chimeras. Although in the spleen few Lin^{-}c-kit^{+}Sca-1^{+} (LSK) cells were measured (data not shown), LSK cells were significantly increased in the BM from *Rorc1*$^{-/-}$>WT mice (Fig. 4A). Analysis of myeloid progenitors revealed increased number of CMPs in the BM of *Rorc1*$^{-/-}$>WT chimeras and, in accordance, a decrease of granulocyte/macrophage progenitors (GMPs) (Fig. 4A). These findings reveal a blockage in differentiation of early hematopoietic progenitors in *Rorc1*$^{-/-}$>WT chimeras and suggest a relevance of RORC1 directly in the BM during the early steps of myeloid cell differentiation. Corroborating this hypothesis, RORC1 was expressed by immature (c-kit^{+}) granulocytes and monocytes in the BM of naive mice (Fig. 4B). In the same

myeloid cell subsets, IL-17 was found produced mainly by immature neutrophils (Fig. 4B). Next, we tested the *in situ* expression of IL-17A and RORC1 in BM parenchyma of patients undergoing a biopsy for staging of Hodgkin's lymphoma. Consistently, IL-17A staining was localized within myeloid cells with immature morphology, within the precursor-rich areas lining the bone trabeculae (Fig. 4C, black arrows). By contrast, mature granulocytes with segmented nuclei barely expressed or did not express IL-17A. Indeed, a neat decreasing gradient was observed in IL-17A expression from para-trabecular areas rich in precursors toward inter-trabecular spaces mainly populated by mature elements (Fig. 4C). Notably, double-marker immunohistochemical analysis confirmed that IL-17A $^{+}$ hematopoietic cells did not correspond to Th-17 cells, as they were distinct from the CD3 $^{+}$ T elements populating the BM niche (Fig. 4D, black arrows). Within the same BM hematopoietic parenchyma, RORC1 (ROR γ) expression was detected mostly in myeloid cells with combined cytoplasmatic and nuclear localization (Fig. 4E, black arrows). These results in human samples further support that the RORC1/ IL-17A program takes part in the regulation of the precursor compartment during myelopoiesis. To test whether RORC1 regulates myelopoiesis, lineage-negative [36] cells isolated from WT and *Rorc1* $^{-/-}$ BM were treated in vitro with G-CSF or GM-CSF and tested, 5 days later, for granulocyte or monocyte differentiation by flow cytometry (Fig. 4F). In response to GM-CSF, Lin $^{-}$ cells from *Rorc1* $^{-/-}$ mice failed to differentiate in macrophages, displaying increased differentiation into GR-1^{high} granulocytes. On the contrary, G-CSF treatment resulted in reduced GR-1^{high} granulocyte production by RORC1$^{-/-}$Lin^{-} cells. This contrasts with the steady-state condition, where in absence of any specific stimulus the rate of differentiation of Lin $^{-}$ cells was identical between WT and *Rorc1*$^{-/-}$ BM sources. These results indicated a key role of RORC1 in the myelopoietic activity of G-CSF and GM-CSF. Fig. S3A underlies the different effects of G-CSF and GM-CSF on the differentiation of Ly6G^{+} subsets,

indicating that GM-CSF promotes a larger expansion of double $Ly6G^{+}Ly6C^{+}$ monocytic cells.

We next determined whether RORC1 might control MDSC survival [37] and maturation. Small differences were observed in survival of WT versus *Rorc1* $^{-/-}$ BM-derived MDSCs at steady-state conditions (medium) (Fig. S3B). In contrast, increased $AnxV^{+}$ binding was observed in both M-MDSCs and PMN-MDSCs after 48 hr, which was reduced in the presence of either tumor supernatant (TSN) or combination of GM-CSF/G-CSF in both subsets (Fig. S3B), indicating that RORC1 is crucial for MDSCs survival. The protective role of both TSN and GM-CSF/G-CSF against apoptosis was partially lost in RORC1-deficient M-MDSCs, while RORC1-deficient PMN-MDSCs suffered a massive apoptosis (Fig. S3B). These results confirm the protective role of RORC1 in CSF-mediated M-MSDCs and PMN-MDSCs survival, highlighting a tighter dependence of PMN-MDSCs survival from RORC1 expression levels.

Neutrophil activation and maturation is paralleled by upregulation of the FC γII and FCγIII receptors (CD32 and CD16, respectively) [38] and of the complement C5a receptor (C5aR) [39]. Splenic PMN-MDSCs from WT>WT tumor bearers expressed lower CD16/CD32 and C5aR levels than did PMN-MDSCs from *Rorc1*$^{-/-}$>WT mice (Fig. S3C). Furthermore, WT splenic immature PMN-MDSCs expressed lower levels of CD16/CD32 and C5aR, as opposed to higher RORC1, when compared to mature thioglycollate-elicited neutrophils (Neu-PECs) (Fig. S3D). These observations indicate that RORC1 might suppress neutrophil maturation, favoring immature PMN-MDSCs to support tumor promotion.

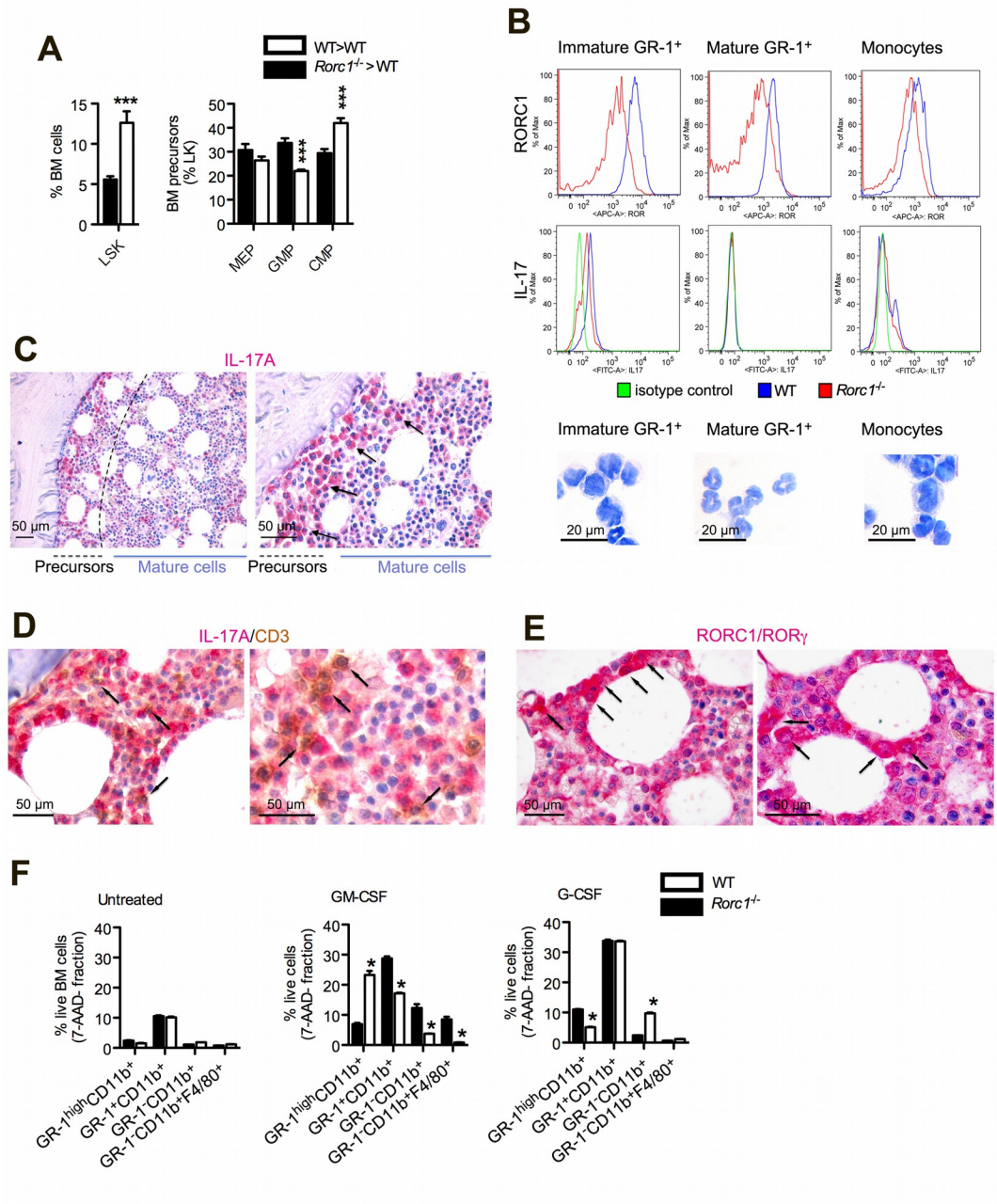

Fig. 4: RORC1 regulates myeloid commitment of BM precursors. (A) Frequency of hematopoietic stem cells (LSK) and myeloid progenitors (CMP, GMP, and MEP) in the BM of WT and *Rorc1* $^{-/-}$ mice. Mean percentages ± SEM is shown. Statistical analysis: *p < 0.05, **p < 0.01, ***p < 0.001 n = 6 (Student's t test). (B) Flow-cytometry analysis for the expression of RORC1 and IL-17 in different myeloid cells identified by staining of BM cells with monoclonal antibodies to CD11b, CD117, GR-1, and F4/80. For RORC1 expression, BM cells from *Rorc1* $^{-/-}$ mice were set as a negative control. Immature granulocytes (myeloblasts) were identified according to their co-expression of GR-1 and c-kit. Mature granulocytes were GR-1 ^{high} and c-kit^{-}, whereas monocytes/macrophages were CD11b^{+}Gr-1^{-}F4/80^{+}. For further checking of their phenotype, these populations were sorted and stained with Giemsa. Representative pictures are

shown. (C–E) In situ expression of IL-17A and RORC1 (ROR γ) within the hematopoietic BM parenchyma of patients undergoing BM biopsy for staining of Hodgkin's lymphoma (HL). Representative pictures show that both IL-17A (C) and RORC1 (E) are produced by immature BM cells lining the endosteal nuche, whereas IL-17A is not expressed by $CD3^+$ cells in the BM (D). (F) Lin^- cells were isolated from the BM of WT and *Rorc1* $^{-/-}$ mice and treated as indicated. The frequency of differentiated myeloid cell subsets was calculated within the gate of viable cells ($7\text{-}AAD^-$). Data shown are the mean ± SEM of two different experiments. Statistical analysis: *$p < 0.05$, **$p < 0.01$, ***$p < 0.001$ (Student's t test). See also Fig. S3.

RORC1 Controls Critical Regulators of Myelopoiesis. To determine the tumor-derived factor/s that activate RORC1, we analyzed MN/MCA1 supernatants from AD mice for myeloid growth factors. TSNs were enriched in G-CSF, GM-CSF, and M-CSF and partially in IL-1b (Fig. 5A). Of note, 48 hr of treatment with either a combination of GM-CSF and G-CSF or TSN induced IL-17A expression in BM-derived PMN-MDSCs and, to a lower extent, in M-MDSCs (Fig. 5B, left). BM-derived M-MDSCs and PMN-MDSCs expressed basal RORC1 levels (Fig. 5B, right), plausibly induced by GM-CSF and G-CSF used for their *in vitro* generation [40], which was increased by combination of GM-CSF and G-CSF (Fig. 5B, right). Confocal microscopy demonstrated that RORC1 expression and nuclear translocation was induced in naive PECs challenged for 72 hr with lipopolysaccharide (LPS), IL- 1b, G-CSF, GM-CSF, and M-CSF, but not by IFN- γ (Fig. 5C) or IL-6 (data not shown). Of note, we found increased levels of G-CSF and GM-CSF in the sera of AD mice (data not shown), as compared to ED mice, suggesting that RORC1-dependent emergency hematopoiesis is controlled by the extent of cancer-associated inflammation.

Finally, we determined the mRNA levels for RORC1 and RORC2 [20, 41] in PECs and in thymocytes [24] from healthy WT mice (Fig. S4A). It is noteworthy that LPS-stimulated (72 hr) PECs expressed *Rorc1* mRNA levels similar to those of WT thymocytes, but not *Rorc2* mRNA. These data confirm that in cancer, the monocyte-macrophage lineage expresses a selective RORC1 fingerprint unlinked from IL-17A, whereas the granulocyte/neutrophil lineage expresses a dual RORC1/IL-17A signature. In support of RORC1 as a key

driver of ‘‘emergency’’ granulo-monocytopoiesis, BM-CD11b^{+}Gr1^{+} granulocytes and BM-CD11b^{+}Ly6C^{+} monocytes from both LPS- and M-CSF-treated mice significantly increased RORC1 expression (Fig. S4B). To determine the *in vivo* role of myeloid growth factor/s, we treated MN/MCA1-bearing mice with neutralizing antibodies to G-CSF, GM-CSF, or the M-CSF receptor (M-CSFR/CSFR1) [4]. Inhibition of G-CSF and GM-CSF limited the accumulation of splenic PMN-MDSCs with no effect on M-MDSCs (Fig. 5D, left). In contrast, the anti-CSFR1 antibody decreased the number of F4/80^{+} spleen macrophages whereas, surprisingly, it induced a strong increase in splenic PMN-MDSCs. At contrast, the anti-G-CSF antibody significantly increased the CD11b $^{+}$F4/80^{+} spleen macrophages. Confirming the relevance of myelopoiesis to cancer inflammation, neutralization of GM-CSF, G-CSF, or M-CSFR resulted in inhibition of tumor growth and metastasis (Fig. 5D, center and right). These findings suggest a reciprocal antagonistic regulation of the polymorphonuclear and monocytic lineages in CSF-driven ‘‘emergency’’ myelopoiesis in cancer.

To shed light on the mechanisms of RORC1-driven emergency myelopoiesis, we evaluated positive and negative transcriptional regulators in BM and spleens from WT>WT and *Rorc1*$^{-/-}$>WT tumor bearers. CCAAT/enhancer binding protein β (C/EBPβ) is a major positive regulator of G-CSF- and GM-CSF-driven ‘‘emergency’’ myelopoiesis [11], whereas C/EBP α appears to be a major regulator of ‘‘steady-state’’ granulopoiesis and cooperates with PU.1 to ‘‘emergency’’ granulo-monocytopoiesis [42, 43]. We observed a mild but significant decrease of mRNA expression of PU.1, C/EBPβ, and C/EBPα in spleens and BM from *Rorc1* $^{-/-}$>WT tumor bearers, paralleled by decreased C/EBPβ protein levels in splenic PMN-MDSCs and M-MDSCs (Fig. 6A). Importantly, BM and spleens from *Rorc1* $^{-/-}$>WT MN/MCA1 tumor bearers displayed increased mRNA levels of the suppressor of cytokine signaling-3 (Socs3) and the transcriptional co-regulator B cell leukemia/lymphoma 3 (Bcl3)

(Fig. 6B), both potent inhibitors of G-CSF-driven granulopoiesis [44, 45]. In agreement with the IFN-γ-mediated inhibition of G-CSF-driven neutrophilia [46], IFN-γ induced a strong increase of Socs3 and Bcl3 mRNA in splenic PMN-MDSCs from *Rorc1*$^{-/-}$ tumor bearers (Fig. 6B, right). Finally, in accordance with the decreased number of macrophages found in spleen and tumor of *Rorc1* $^{-/-}$>WT chimeras (Fig. 6C), we observed a decreased number of IRF8-expressing CD11b^{+}F4/80^{+}CD115^{+} macrophages (Fig. 6D), which was confirmed by confocal microscopy in tumor tissues of *Rorc1*$^{-/-}$>WT chimeras (data not shown). As M-CSFR/CD115 [5] is a marker of terminally differentiated macrophages [47], this result indicates that RORC1 is required for the modulation of cell-fate switching factor(s) driving maturation of macrophages [13].

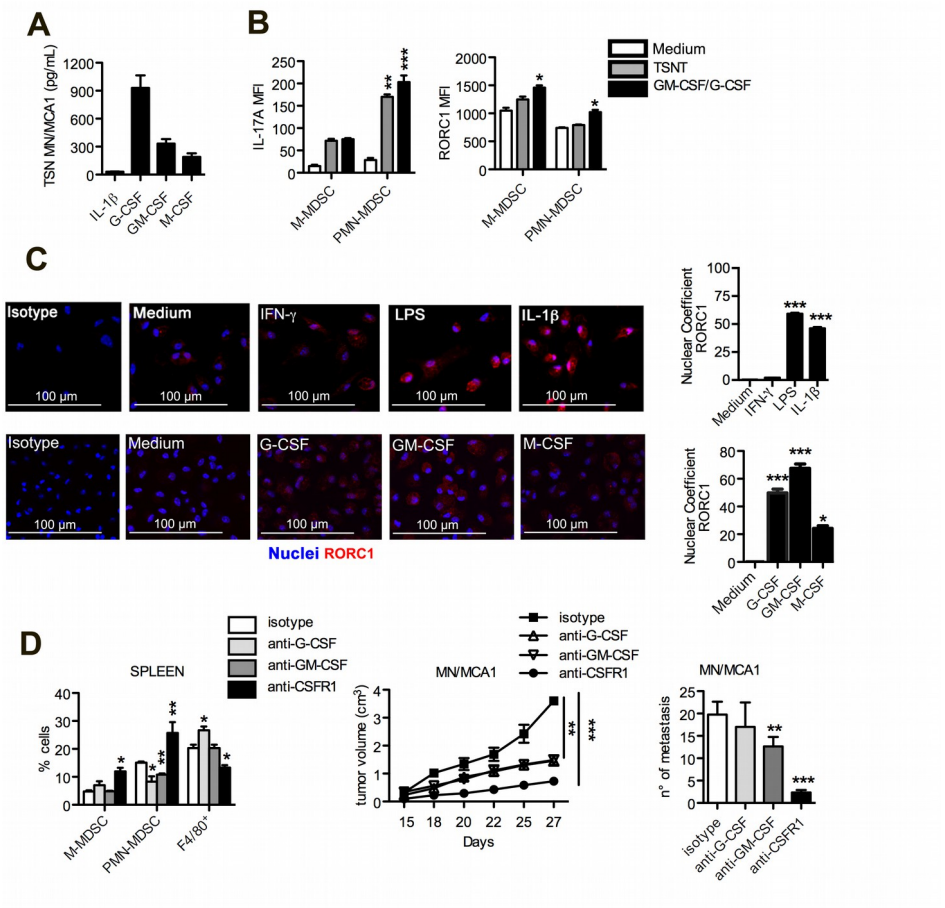

Fig. 5: CSF-, LPS-, and IL-ß-mediated induction of RORC1 in innate immune cells. (A) Expression levels of GM-CSF, G-CSF, M-CSF, and IL-1b in the MN/MCA1 supernatants (TSN) from advanced disease were determined by ELISA. Data shown are the mean ± SEM of three independent experiments.(B) BM-MDSCs were left untreated or were treated with either TSN (MN/MCA1) or a combination of recombinant GM-CSF (40 ng/ml) and G-CSF (40 ng/ml) for 48 hr. Expression of IL-17A and RORC1 in M-MDSCs and PMN-MDSCs was evaluated by FACS analysis. Mean fluorescence intensity (MFI) ± SEM of three representative experiments is shown. Statistical analysis: *p < 0.05, **p < 0.01, ***p < 0.001 (Student's t test). (C) Expression and nuclear translocation of RORC1 in PECs exposed to IFN-g (200 U/ml), LPS (100 ng/ml), IL-1 β (20 ng/ml), G-CSF (40 ng/ml), GM-CSF (40 ng/ml), and M-CSF (40 ng/ml). After 72 hr of *in vitro* activation, PECs were stained with anti-RORC1 antibody (red) or irrelevant rat immunoglobulin G (IgG). Nuclei were counterstained with DAPI (blue). Representative images are shown. Confocal microscopy analysis of RORC1 nuclear fluorescence intensity (nuclear coefficient) is shown on the right. Mean ± SEM from three independent experiments is shown. Statistical analysis: *p < 0.05, **p < 0.01, ***p < 0.001 (Student's t test). (D) MN/MCA1 tumor-bearing mice were treated with blocking antibodies against G-CSF, GM-CSF, M-CSFR/CSFR1, or isotype control antibody as indicated. Data on M-MDSCs, PMN-MDSCs, and CD11b $^{+}$F4/80^{+} cells in spleens from mice with AD within the CD45^{+} gate (left) and primary tumor growth (center) are shown as the mean ± SEM. The number of macroscopic lung metastases (right) is shown as the mean ± SD. A representative experiment with six mice/ group is shown. Statistical analysis: *p < 0.05, **p < 0.01, ***p < 0.001 (Student's t test). See also Figure S4.

RORC1 controls polarization of myeloid cells. M-CSFR signaling modulates macrophage survival and differentiation [5] and induces M2 macrophage polarization, a condition supporting tumor progression [48]. To evaluate RORC1 in the macrophage polarization, we analyzed the mRNA expression of prototypical M1 and M2 genes in AD-PECs, cells displaying an intermediate PEC versus a TAM phenotype and representing a good model to study M1-M2 polarization in cancer [49, 50] from tumor-bearing WT>WT and *Rorc1* $^{-/-}$>WT chimeras. AD-PECs were isolated from tumor- bearing WT>WT and *Rorc1* $^{-/-}$>WT chimeras and treated with 100 ng LPS (M/L) or 200 U/ml IFN- γ for 4 hr to induce M1 polarization or exposed to LPS for 20 hr (L/M) to induce LPS-tolerant M2-like polarization [51]. In addition, spleen PMN- MDSCs were stimulated 4 hr *in vitro* with IFN- γ, LPS, or IFN- γ plus LPS. RORC1-deficient

AD-PECs displayed enhanced expression of M1 (IL-12p40, tumor necrosis factor alpha (TNF-α), IL-1β) and decreased expression of M2 (IL-10, TGFβ, chitinase-3-like protein 3/Ym1) genes under M/L and L/M conditions (Fig 7A). Simiarly, RORC1-deficient PMN-MDSCs showed increased TNF- α and IL-1 β mRNA levels and IL-1β secretion in response to LPS/IFNγ (Fig. 7B). Thus, RORC1 acts as negative regulator of M1 and promoter of M2 cytokine genes. This observation was supported by the increased levels of pro-inflammatory cytokines (TNF-α and IL-1β) and growth factors (G-CSF, GM-CSF, and VEGF) in MN/MCA1 superna- tants from *Rorc1*>WT (Fig. 7C), correlating with marked splenomegalia observed in *Rorc1* $^{-/-}$>WT chimeras bearing the MN/MCA1 and MMTV-PyMT tumors (Fig. 7D). Moreover, we found increased splenic $CD4^{+}IFN\text{-}\gamma^{+}$ and $F4/80^{+}TNF\text{-}\alpha^{+}$ cells in tumor-free and tumor-bearing *Rorc1* $^{-/-}$>WT mice (Fig. S5A), while total $CD45^{+}CD4^{+}$ cells decreased as described (Fig. S5A) [52]. In contrast, tumor-infiltrating $CD4^{+}IFN\text{-}\gamma^{+}$ and total $CD45^{+}CD4^{+}$ T cells increased in *Rorc1* $^{-/-}$>WT chimeras (Fig. S5A). Furthermore, $F4/80^{+}TNF\text{-}\alpha^{+}$ macrophages increased in spleens and tumors from *Rorc1* $^{-/-}$>WT mice (Fig. S5A). Supporting the inhibitory role of RORC1, $CD4^{+}Foxp3^{+}$ T regulatory cells significantly decreased in the spleen from *Rorc1* $^{-/-}$>WT mice (Fig. S5A).

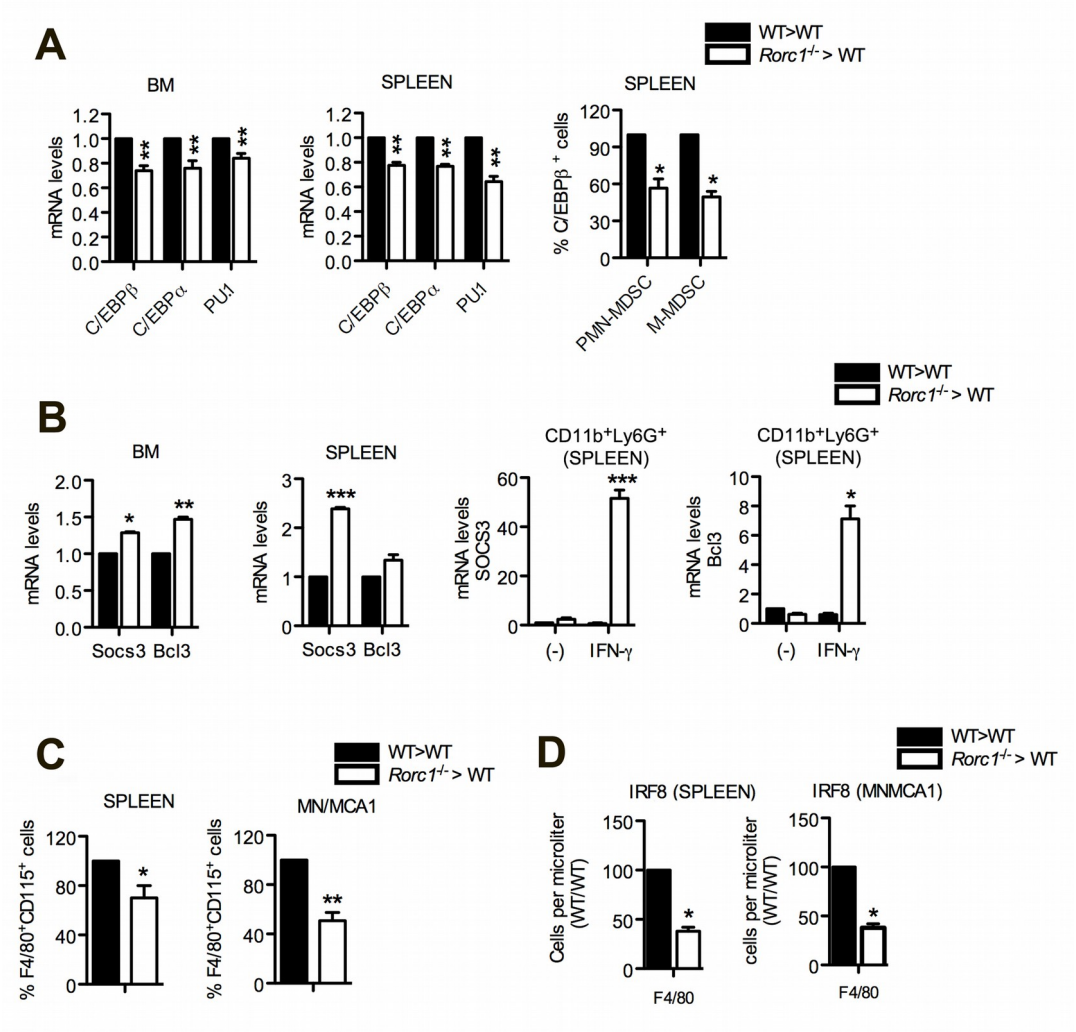

Fig. 6: Influence of RORC1 on the expression of transcriptional regulators of myeloid cell maturation. (A) Total RNA from BM (left) and splenocytes (center) obtained from MN/MCA1-bearing WT>WT and *Rorc1*$^{-/-}$>WT mice was analyzed by RT-PCR for the expression of the C/EBP β, C/EBPα, and PU.1 transcription factors. Results are given as the fold increase over the mRNA level expressed by WT and are representative of at least three different experiments. Mean percentages ± SEM of C/EBP β protein expression in M- and PMN-MDSC subsets in c-kit^{low} BM and splenocytes from WT>WT and *Rorc1* $^{-/-}$>WT tumor-bearing chimeras were measured by FACS analysis (right). The mean ± SD of three independent experiments is shown. (B) mRNA levels of Socs3 and Bcl3 in BM and splenocytes (left) or in unstimulated (-) and IFN-γ-activated PMN-MDSCs (CD11b^{+}Ly6G^{+}) isolated from the spleen (right) obtained from MN/MCA1-bearing WT>WT and *Rorc1*$^{-/-}$>WT mice. Results are shown as the mean ± SEM from triplicate values. (C) Splenic CD11b^{+}F4/80^{+}CD115^{+} macrophages (left) and CD11b^{+}F4/80^{+}CD115^{+} TAMs (right). Macrophage percentage in *Rorc1* $^{-/-}$>WT chimeras (white bar) is represented as relative value as compared to WT>WT chimeras (100%) (black bar). Results are shown as the mean ± SEM from triplicate values. (D) The mean count ± SEM of

IRF8^{+}F4/80^{+} cells in spleens and MN/MCA1 from WT>WT and *Rorc1*$^{-/-}$>WT chimeras analyzed within the CD11b^{+}F4/80^{+} gate is shown. The mean ± SEM of three independent experiments is shown. Statistical analysis: *p < 0.05, **p < 0.01, ***p < 0.001 (Student's t test).

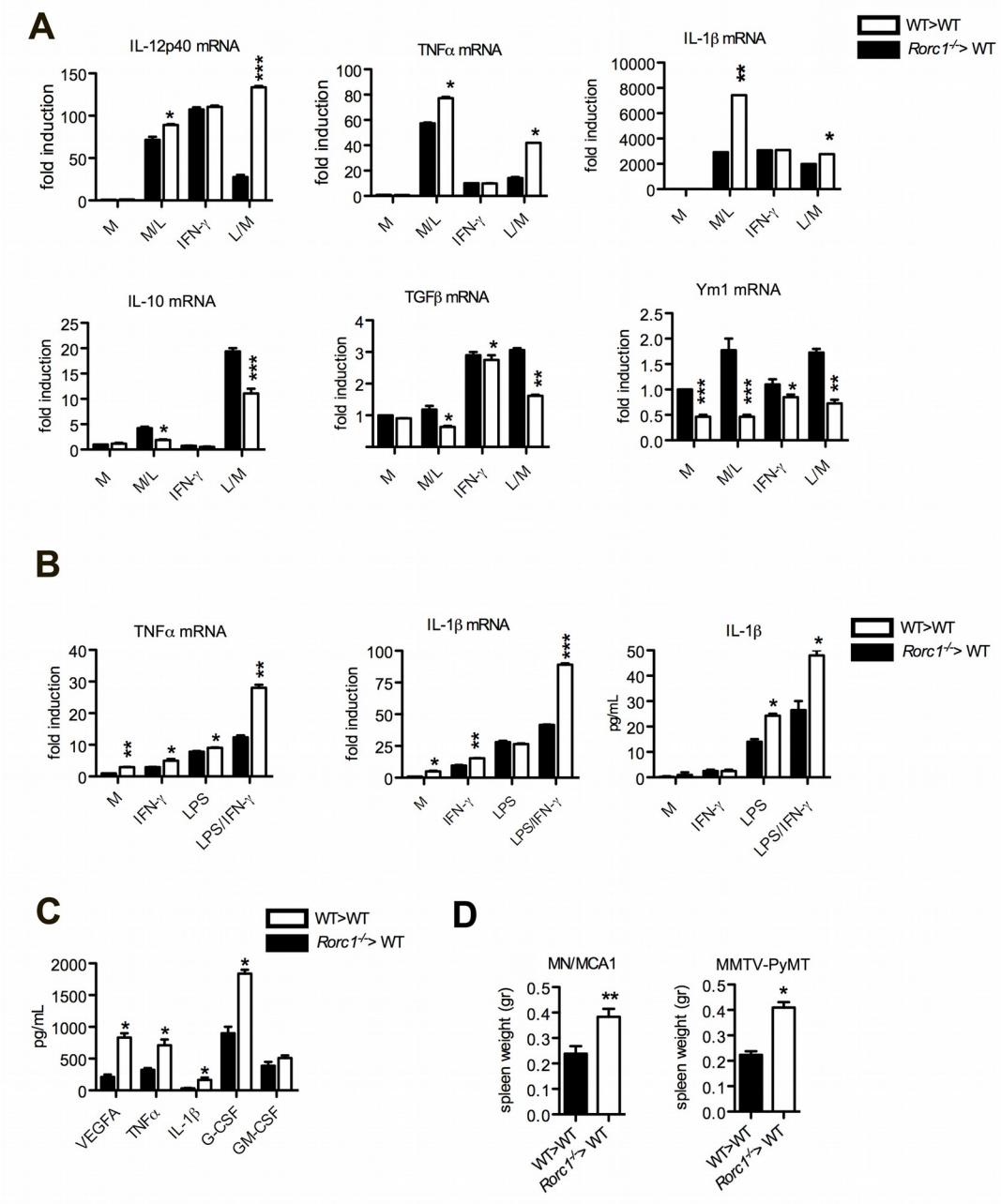

Fig. 7. Effects of RORC1 on macrophage polarization.(A) Total RNA from control (medium), activated (IFN-γ), M1-activated (M/L), and M2-like LPS-tolerant (L/M) AD-PECs

harvested from MN/MCA1 from WT>WT (black bar) or *Rorc1*$^{-/-}$>WT (white bar) chimeras were analyzed by RT-PCR for the expression of representative M1 genes (IL-12p40, TNF-α, and IL-1β) and M2 genes (IL-10, TGF β, and Ym1). Statistical analysis: *p < 0.05, **p < 0.01, ***p < 0.001; n=3 (Student's t test). Results are representative of at least three different experiments and are shown as the mean ± SEM from triplicate values. (B) Total RNA from control (medium) and activated (IFN- γ, LPS, or LPS+IFN- γ) PMN-MDSCs obtained from the spleen from MN/MCA1-bearing WT>WT and *Rorc1*$^{-/-}$>WT chimeras were analyzed by RT-PCR for the expression of representative M1 genes (IL-1β and TNF-α). Secretion of IL-1β (pg/ml) was determined by ELISA. Cells were activated as indicated for 24 hr. Results are given as the fold increase over the mRNA level expressed by untreated cells (medium) and are representative of at least three different experiments; shown are the mean ± SEM from triplicate values. For ELISA, results are the average of three independent experiments ± SD. Statistical analysis: *p < 0.05, **p < 0.01, ***p < 0.001 (Student's t test). (C) Expression levels (pg/ml) of cytokines/growth factors in tumor supernatants (MN/MCA1) harvested from WT>WT and *Rorc1*$^{-/-}$>WT chimeras. Results are the average of three independent experiments ± SEM. Statistical analysis: *p < 0.05, **p < 0.01, ***p < 0.001 (Student's t test). (D) Mean spleen weights (g) ± SEM in MN/MCA1-bearing (n=10) and MMTV-PyMT (n=6) mice. Statistical analysis: *p < 0.05, **p < 0.01, ***p < 0.001 (Student's t test). See also Figure S5.

Antagonistic regulation of the polymorphonuclear and monocytic lineages.

A decreased number of tissue macrophages in tumors from *Rorc1*$^{-/-}$>WT mice (Fig. 3F) correlated with increased PMN-MDSCs infiltration (Fig. 3E), suggesting that pathways leading to terminal differentiation and M2 polarization of TAMs hamper neutrophil accumulation in tumors. To prove this assumption, we treated MN/MCA1-bearing WT mice with an anti-CSFR1 antibody [53], which significantly depleted the CD11b^{+}F4/80^{+}CD115^{+} TAMs population, co-expressing high RORC1 levels (Fig. 8A). Macrophage depletion was paralleled by the inhibition of immature RORC1^{+} M-MDSCs and PMN-MDSCs (Fig. 8B) and increased tumor infiltration of mature (C5a^{high}CD16/32^{high}) (Fig. 8C) RORC1 Ly6G^{high} neutrophils (Fig. 8B). In agreement, RORC1 was highly expressed in F4/80^{+}/CD115^{+} macrophages, in comparison to reduced RORC1 levels in Ly6G^{low} granulocytes and negativity in mature inflammatory Ly6G^{high} granulocytes (Fig. 8D), indicating that TAMs infiltration is accompanied by infiltration of immature MDSC populations, at the expense of mature neutrophils. Of relevance, anti-M-CSF treatment resulted in a similar increase of

$C5a^{high}CD16/32^{high}$ mature neutrophils in the spleen (Fig. S6A), indicating its systemic effects. These results are in agreement with Fig. 5D and together suggest a competition between the monocytic and granulocytic commitment of myeloid precursors. As mature RORC1 PMN-MDSCs display a pronounced inflammatory phenotype (Fig. 7B), their inhibition most likely contributes to maintaining the tumor-promoting microenvironment. Furthermore, while M-CSF induced RORC1 expression in splenic (data not shown) and medullar (Fig. S4B) monocyte precursors, treatment with anti-CSFR1 resulted in reduced monocyte/macrophage precursors (population C + D) and in increased granulocyte progenitors (population A + B) (Fig. 8E). Supporting the role for reciprocal negative regulation of monocytes/macrophages and granulocytes in cancer inflammation, treatment with anti-G-CSF antibody increased the number of splenic $F4/80^{+}TNF\text{-}\alpha^{+}$ M1-like macrophages, paralleled by elevation of $CD4^{+}IFN\text{-}\gamma^{+}$ Th1 cells (Fig. 8F). As the increase in $CD4^{+}IFN\text{-}\gamma^{+}$ and $F4/80^{+}TNF\text{-}\alpha^{+}$ cells observed in *Rorc1* $^{-/-}$ tumor-bearing mice was phenocopied by the anti-G-CSF treatment of MN/MCA1 tumor-bearing mice, we questioned whether G-CSF might work through RORC. To address this question, we treated WT and *Rorc1* $^{-/-}$ tumor-bearing mice with anti-G-CSF and monitored the expansion of both $CD4^{+}IFN\text{-}\gamma^{+}$ and $F4/80^{+}TNF\text{-}\alpha^{+}$ cells. As a result, the anti-G-CSF treatment significantly decreased RORC1 expression in PMN-MDSCs and partially in M- MDSCs and $F4/80^{+}$ macrophages (Fig. S6B). Moreover, the increase of tumor-infiltrating $F4/80^{+}TNF\text{-}\alpha^{+}$ macrophages and $CD4^{+}IFN\text{-}\gamma^{+}$ T cells in response to anti-G-CSF, observed in WT mice, was significantly reduced in *Rorc1* $^{-/-}$ mice (Fig. S6C), strengthening the hypothesis that G-CSF works through the induction of RORC1. Finally, to assess the role of myeloid-specific RORC1 in adaptive immunity against cancer, we depleted $CD4^{+}$ and $CD8^{+}$ T cells in both WT and *Rorc1* $^{-/-}$ tumor-bearing mice. As a result, we observed a significant increase of lung metastasis in *Rorc1* $^{-/-}$ tumor-bearing mice treated with the anti-CD4/anti-CD8 antibodies (Fig. S6D), suggesting that

the protumor activity of RORC1 acts through both the innate and adaptive immunity.

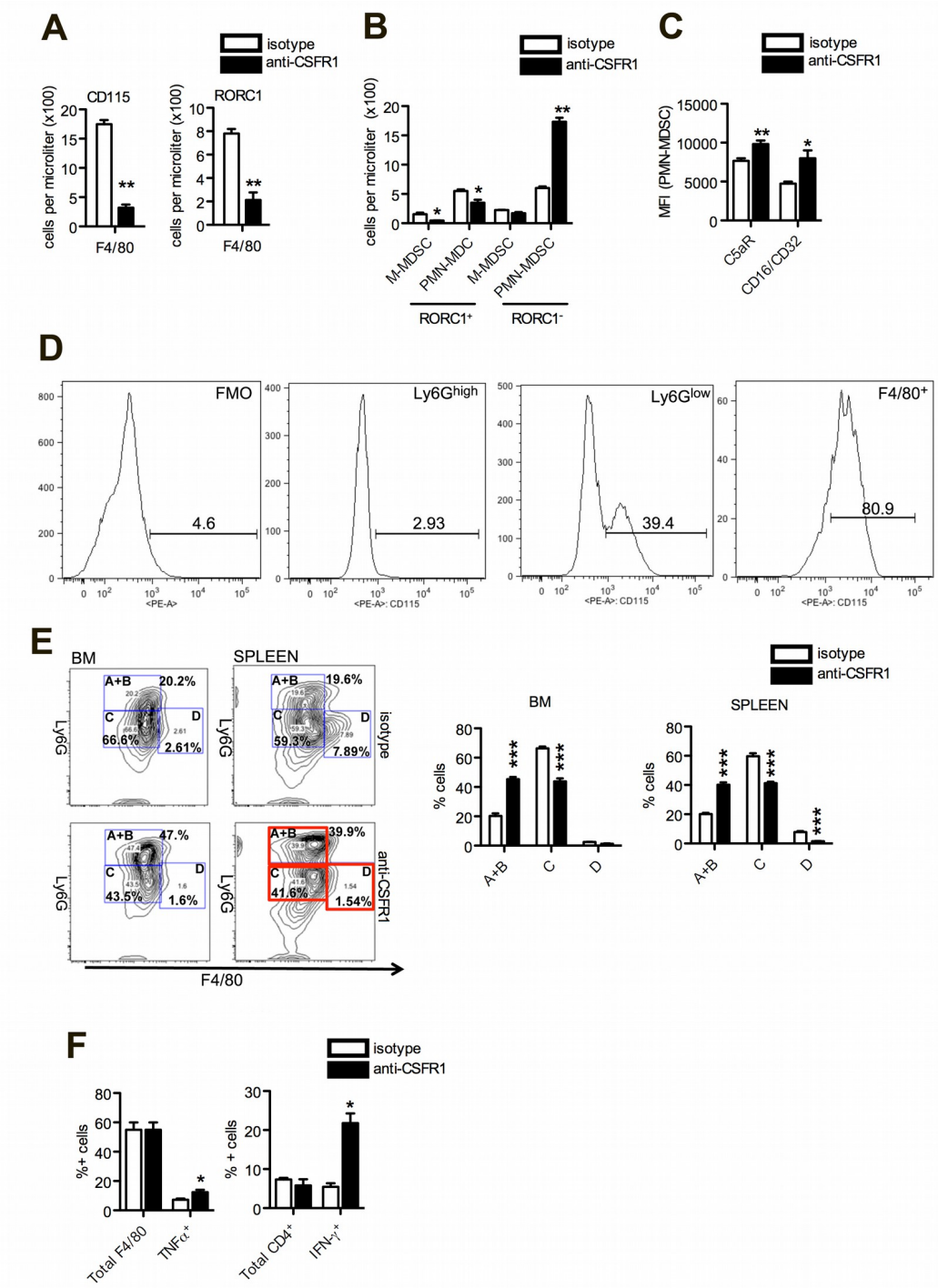

Fig. 8: Reciprocal negative regulation of monocytes/macrophages and granulocytes in cancer-associated inflammation. (A) Mean counts ± SEM of $CD115^-$ and RORC1-expressing $F4/80^+$ macrophages in the MN/MCA1 tissue from untreated (isotype IgG control) and anti-CSFR1-treated tumor-bearing WT mice. (B) Mean counts ± SEM of RORC1+ and RORC1 M-MDSC and PMN-MDSC subsets. (C) Mean fluorescence intensity (MFI) ± SEM for CD16/CD32 and C5aR expression in PMN-MDSCs in MN/MCA1 from WT mice treated with isotype IgG or ant-CSFR1 antibody. (A–C) Statistical analysis: *p < 0.05, **p < 0.01, ***p < 0.001; n = 3 (Student's t test). (D) FACS analysis of RORC1 expression levels in $Ly6G^{high}$ and $Ly6G^{low}$ granulocytes and in $F4/80^+/CD115^+$ macrophages. (E) FACS dot plots for granulocyte (A), monocyte/macrophage (C), and macrophage (D) progenitor subsets in BM and spleen from one representative MN/MCA1- bearing WT mouse treated with IgG isotype and one treated with anti-CSFR1 antibody, both with AD, are shown. The mean ± SD of five mice/experimental group is shown (t test, *p < 0.05; n=5). Statistical analysis: *p < 0.05, **p < 0.01, ***p < 0.001 (Student's t test). (F) Total $CD4^+$ and $CD4^+IFN\text{-}\gamma^+$ and total $F4/80^+$ and $F4/80^+TNF\text{-}\alpha^+$ subsets in MN/MCA1 tumors from tumor-bearing mice treated with isotype control antibody (white bar) or anti-G-CSF antibody (black bars). The mean ± SEM of six mice/experimental group is shown. Statistical analysis: *p < 0.05, **p < 0.01, ***p < 0.001 (Student's t test). See also Figure S6.

Discussion

We demonstrate that RORC1 fuels cancer-promoting inflammation by enhancing survival and expansion of CD16/32^{low}/ C5aR^{low} immature MDSCs, with reduced expression of M1 cytokines (IL-1β and TNF-α) and increased suppressive activity, and promoting terminal macrophage differentiation. Our study indicates that RORC1 impinges on cancer-driven myelopoiesis by suppressing negative (Socs3 and Bcl3) [44, 45] and promoting positive (C/EBPb) [42] transcriptional regulators of ‘‘emergency’’ granulopoiesis, while instating the expression of macrophage-specific tran- scription factors IRF8 and PU.1 [13]. Depletion of RORC1^{+}F4/80^{+}CD115^{+} TAMs with anti-CSFR1 antibody enhanced the recruitment of mature (CD16/CD32^{high}) RORC1 inflammatory neutrophils, with diminished expansion of immature RORC1^{+}(CD16^{low}/CD32^{low}) PMN-MDSCs. This result, along with the observed competition between the commitment of myeloid precursors for the monocytic versus granulocytic lineage, observed with the anti-G-CSF and anti-CSFR1 treatments, respectively, may indicate that blocking M-CSF-dependent myelopoiesis unleashes expansion and maturation of granulocytic cells, which would favor the increase of tumor-infiltrating neutrophils. These events deflect the inflammatory microenvironment to adverse the tumor, increasing infiltration of CD4^{+} IFN-γ^{+} T cells and F4/80^{+}TNF-α^{+} M1 polarized macrophages. Our results indicate that high RORC1 expression acts as pro- resolving mediator of myeloid inflammation and that antagonists to RORC1 might hold the potential to prevent tumor-promoting myeloid differentiation. We also report that IL-17 expression is disjointed from RORC1 in the monocyte/macrophage lineage (M-MDSCs and CD11b^{+}F4/80^{+} TAMs). Wu *et al.* have recently described that tumor-infiltrating inflammatory dendritic cells activate IL-17-producing RORγt^{+} γδT17 cells to secrete IL-8, TNF-α, and GM-CSF cells and sustain the subsequent intratumor accumulation of immunosuppressive PMN-MDSCs in colorectal cancer [54]. Further, an inflammatory cascade encompassing the IL-

1β-mediated production by IL-17 in γδT cells resulted in systemic G-CSF-dependent expansion of suppressive neutrophils and formation of breast cancer metastasis [55]. Our observation that IL-17 is selectively expressed, but not secreted by immature granulocyte/neutrophil subsets, does not support a direct role of myeloid-cell-derived IL-17 in the expansion of MDSCs during cancer development, but rather indicates that IL-17A is a hallmark of immature myeloid responses in cancer bearers. This notion is further supported by the observation that expression of IL-17 and RORC1 localizes within the immature myeloid cells precursor-rich areas lining the bone trabeculae of BM biopsies from patients under diagnosis of Hodgkin's lymphoma. Moreover, in contrast to *Rorc1*$^{-/-}$ BM transplantation, chimeric mice receiving the I*l17a*$^{-/-}$ BM had no defect in developing tumor-associated myeloid cells, in both the BM and spleen (data not shown). It remains to be established whether IL-17A expression by circulating MDSCs is dependent on the disease stage, as we did not observe its expression in blood from T2/T3 CRC patients.

Along with other reports, our observation highlights the relevance of members of the nuclear receptor superfamily in regulation of inflammation [56, 57] and suggests RORC1 as central regulator of cancer associated myelopoiesis and key driver of the protumor differentiation of MDSCs and TAMs.

Author contributions

L.S. and A.S. conceived the ideas and designed the experiments. L.S., S.S., F.M.C., G.S., S.M., M.G.T., C.P., A.A., S.T., A.D., F.Z., and C.T. performed the experiments. L.S., S.S., C.T., M.P.C., and A.S. analyzed the data. L.S. and A.S. wrote the paper.

Acknowledgments

This work was supported by Associazione Italiana Ricerca sul Cancro (AIRC; Program Innovative Tools for Cancer Risk Assessment and Diagnosis, 5 per

mille number 12162 and IG number 2014-15585), Fondazione Cariplo, and Ministero Universita` Ricerca (MIUR).

References

1. Ueha, S., F.H. Shand, and K. Matsushima, *Myeloid cell population dynamics in healthy and tumor-bearing mice.* Int Immunopharmacol, 2011. **11**(7): p. 783-8.
2. Sica, A. and V. Bronte, *Altered macrophage differentiation and immune dysfunction in tumor development.* J Clin Invest, 2007. **117**(5): p. 1155-66.
3. Metcalf, D., *Hematopoietic cytokines.* Blood, 2008. **111**(2): p. 485-91.
4. Hume, D.A. and K.P.A. MacDonald, *Therapeutic applications of macrophage colony-stimulating factor-1 (CSF-1) and antagonists of CSF-1 receptor (CSF-1R) signaling.* Blood, 2012. **119**(8): p. 1810-1820.
5. Qian, B.Z. and J.W. Pollard, *Macrophage diversity enhances tumor progression and metastasis.* Cell, 2010. **141**(1): p. 39-51.
6. Gabrilovich, D.I., S. Ostrand-Rosenberg, and V. Bronte, *Coordinated regulation of myeloid cells by tumours.* Nat Rev Immunol, 2012. **12**(4): p. 253-68.
7. Gordy, C., et al., *Regulation of steady-state neutrophil homeostasis by macrophages.* Blood, 2011. **117**(2): p. 618-29.
8. Goren, I., et al., *A Transgenic Mouse Model of Inducible Macrophage Depletion Effects of Diphtheria Toxin-Driven Lysozyme M-Specific Cell Lineage Ablation on Wound Inflammatory, Angiogenic, and Contractive Processes.* American Journal of Pathology, 2009. **175**(1): p. 132-147.
9. Chow, A., et al., *Bone marrow CD169(+) macrophages promote the retention of hematopoietic stem and progenitor cells in the mesenchymal*

stem cell niche. Journal of Experimental Medicine, 2011. **208**(2): p. 261-271.

10. Winkler, I.G., et al., *Bone marrow macrophages maintain hematopoietic stem cell (HSC) niches and their depletion mobilizes HSCs.* Blood, 2010. **116**(23): p. 4815-4828.
11. Akagi, T., et al., *Impaired response to GM-CSF and G-CSF, and enhanced apoptosis in C/EBP beta-deficient hematopoietic cells.* Blood, 2008. **111**(6): p. 2999-3004.
12. Zhang, H., et al., *STAT3 controls myeloid progenitor growth during emergency granulopoiesis.* Blood, 2010. **116**(14): p. 2462-71.
13. Friedman, A.D., *Transcriptional control of granulocyte and monocyte development.* Oncogene, 2007. **26**(47): p. 6816-28.
14. Liu, B., et al., *IL-17 is a potent synergistic factor with GM-CSF in mice in stimulating myelopoiesis, dendritic cell expansion, proliferation, and functional enhancement.* Exp Hematol, 2010. **38**(10): p. 877-884 e1.
15. Schwarzenberger, P., et al., *Requirement of endogenous stem cell factor and granulocyte-colony-stimulating factor for IL-17-mediated granulopoiesis.* J Immunol, 2000. **164**(9): p. 4783-9.
16. Iwakura, Y., et al., *Functional Specialization of Interleukin-17 Family Members.* Immunity, 2011. **34**(2): p. 149-162.
17. Toomer, K.H. and Z.B. Chen, *Autoimmunity as a double agent in tumor killing and cancer promotion.* Frontiers in Immunology, 2014. **5**: p. 1-14.
18. Zamarron, B.F. and W. Chen, *Dual roles of immune cells and their factors in cancer development and progression.* Int J Biol Sci, 2011. **7**(5): p. 651-8.
19. Zhu, X., et al., *IL-17 expression by breast-cancer-associated macrophages: IL-17 promotes invasiveness of breast cancer cell lines.* Breast Cancer Res, 2008. **10**(6): p. R95.

20. Ivanov, II, et al., *The orphan nuclear receptor RORgammat directs the differentiation program of proinflammatory IL-17+ T helper cells.* Cell, 2006. **126**(6): p. 1121-33.
21. Taylor, P.R., et al., *Activation of neutrophils by autocrine IL-17A-IL-17RC interactions during fungal infection is regulated by IL-6, IL-23, RORgammat and dectin-2.* Nat Immunol, 2014. **15**(2): p. 143-51.
22. Zhuang, Y., et al., *CD8(+) T Cells That Produce Interleukin-17 Regulate Myeloid-Derived Suppressor Cells and Are Associated With Survival Time of Patients With Gastric Cancer.* Gastroenterology, 2012. **143**(4): p. 951-+.
23. Hueber, A.J., et al., *Mast cells express IL-17A in rheumatoid arthritis synovium.* J Immunol, 2010. **184**(7): p. 3336-40.
24. Sun, Z.M., et al., *Requirement for ROR gamma in thymocyte survival and lymphoid organ development.* Science, 2000. **288**(5475): p. 2369-2373.
25. Guy, C.T.C., R.D.; and Muller, W.J., *Induction of mammary tumors by expression of polyomavirus middle T oncogene: a transgenic mouse model for metastatic disease.* Mol Biol Cell, 1992. **12**: p. 954-961.
26. Larghi, P., et al., *The p50 subunit of NF-kappaB orchestrates dendritic cell lifespan and activation of adaptive immunity.* PLoS One, 2012. **7**(9): p. e45279.
27. Tripodo, C., et al., *Stromal SPARC contributes to the detrimental fibrotic changes associated with myeloproliferation whereas its deficiency favors myeloid cell expansion.* Blood, 2012. **120**(17): p. 3541-3554.
28. Moalli, F., et al., *Role of complement and Fc gamma receptors in the protective activity of the long pentraxin PTX3 against Aspergillus fumigatus.* Blood, 2010. **116**(24): p. 5170-5180.

29. Mantovani, A., et al., *Neutrophils in the activation and regulation of innate and adaptive immunity.* Nat Rev Immunol, 2011. **11**(8): p. 519-31.
30. Sawa, S., et al., *Lineage Relationship Analysis of ROR gamma t(+) Innate Lymphoid Cells.* Science, 2010. **330**(6004): p. 665-669.
31. Gray, E.E., K. Suzuki, and J.G. Cyster, *Cutting Edge: Identification of a Motile IL-17-Producing gamma delta T Cell Population in the Dermis.* Journal of Immunology, 2011. **186**(11): p. 6091-6095.
32. Rachitskaya, A.V., et al., *Cutting edge: NKT cells constitutively express IL-23 receptor and ROR gamma t and rapidly produce IL-17 upon receptor ligation in an IL-6-independent fashion.* Journal of Immunology, 2008. **180**(8): p. 5167-5171.
33. Stutman, O., *Tumor development after 3-methylcholanthrene in immunologically deficient athymic-nude mice.* Science, 1974. **183**: p. 534-536.
34. Marigo, I., et al., *Tumor-induced tolerance and immune suppression depend on the C/EBPbeta transcription factor.* Immunity, 2010. **32**(6): p. 790-802.
35. Kojetin, D.J. and T.P. Burris, *REV-ERB and ROR nuclear receptors as drug targets.* Nature Reviews Drug Discovery, 2014. **13**(3): p. 197-216.
36. Markiewski, M.M., et al., *Modulation of the antitumor immune response by complement.* Nature Immunology, 2008. **9**(11): p. 1225-1235.
37. Sinha, P., et al., *Myeloid-derived suppressor cells express the death receptor Fas and apoptose in response to T cell-expressed FasL.* Blood, 2011. **117**(20): p. 5381-5390.
38. Hogarth, P.M., *Fc receptors are major mediators of antibody based inflammation in autoimmunity.* Current Opinion in Immunology, 2002. **14**(6): p. 798-802.
39. Guo, R.F. and P.A. Ward, *Role of C5A in inflammatory responses.* Annual Review of Immunology, 2005. **23**: p. 821-852.

40. Peranzoni, E., et al., *Myeloid-derived suppressor cell heterogeneity and subset definition.* Current Opinion in Immunology, 2010. **22**(2): p. 238-244.
41. Yang, X.O., et al., *T helper 17 lineage differentiation is programmed by orphan nuclear receptors ROR alpha and ROR gamma.* Immunity, 2008. **28**(1): p. 29-39.
42. Hirai, H., et al., *C/EBP beta is required for 'emergency' granulopoiesis.* Nature Immunology, 2006. **7**(7): p. 732-739.
43. Jin, F.L., et al., *PU.1 and C/EBP alpha synergistically program distinct response to NF-kappa B activation through establishing monocyte specific enhancers.* Proceedings of the National Academy of Sciences of the United States of America, 2011. **108**(13): p. 5290-5295.
44. Croker, B.A., et al., *SOCS3 is a critical physiological negative regulator of G-CSF signaling and emergency granulopoiesis.* Immunity, 2004. **20**(2): p. 153-65.
45. Kreisel, D., et al., *Bcl3 prevents acute inflammatory lung injury in mice by restraining emergency granulopoiesis.* J Clin Invest, 2011. **121**(1): p. 265-76.
46. Ulich, T.R.d.C., J.; and Souza, L., *Kinetics and mechanisms of recombinant human granulocyte-colony stimulating factor-induced neutrophilia.* Am J Pathol, 1988. **133**: p. 630-638.
47. Auffray, C., M.H. Sieweke, and F. Geissmann, *Blood Monocytes: Development, Heterogeneity, and Relationship with Dendritic Cells.* Annual Review of Immunology, 2009. **27**: p. 669-692.
48. Mantovani, A. and A. Sica, *Macrophages, innate immunity and cancer: balance, tolerance, and diversity.* Curr Opin Immunol, 2010. **22**(2): p. 231-7.
49. Sica, A., et al., *Autocrine production of IL-10 mediates defective IL-12 production and NF-kappa B activation in tumor-associated macrophages.* J Immunol, 2000. **164**(2): p. 762-7.

50. Torroella-Kouri, M., et al., *Identification of a Subpopulation of Macrophages in Mammary Tumor-Bearing Mice That Are Neither M1 nor M2 and Are Less Differentiated.* Cancer Research, 2009. **69**(11): p. 4800-4809.
51. Porta, C., et al., *Tolerance and M2 (alternative) macrophage polarization are related processes orchestrated by p50 nuclear factor kappaB.* Proc Natl Acad Sci U S A, 2009. **106**(35): p. 14978-83.
52. Harrington, L.E., et al., *Interleukin 17-producing CD4(+) effector T cells develop via a lineage distinct from the T helper type 1 and 2 lineages.* Nature Immunology, 2005. **6**(11): p. 1123-1132.
53. Ries, C.H., et al., *Targeting tumor-associated macrophages with anti-CSF-1R antibody reveals a strategy for cancer therapy.* Cancer Cell, 2014. **25**(6): p. 846-59.
54. Wu, W.C., et al., *Circulating hematopoietic stem and progenitor cells are myeloid-biased in cancer patients.* Proc Natl Acad Sci U S A, 2014. **111**(11): p. 4221-6.
55. Coffelt, S.B., et al., *IL-17-producing gammadelta T cells and neutrophils conspire to promote breast cancer metastasis.* Nature, 2015. **522**(7556): p. 345-8.
56. Gerbal-Chaloin, S., et al., *Nuclear receptors in the cross-talk of drug metabolism and inflammation.* Drug Metab Rev, 2013. **45**(1): p. 122-44.
57. Wittke, A., et al., *Vitamin D receptor-deficient mice fail to develop experimental allergic asthma.* J Immunol, 2004. **173**(5): p. 3432-6.

Supplemental Data

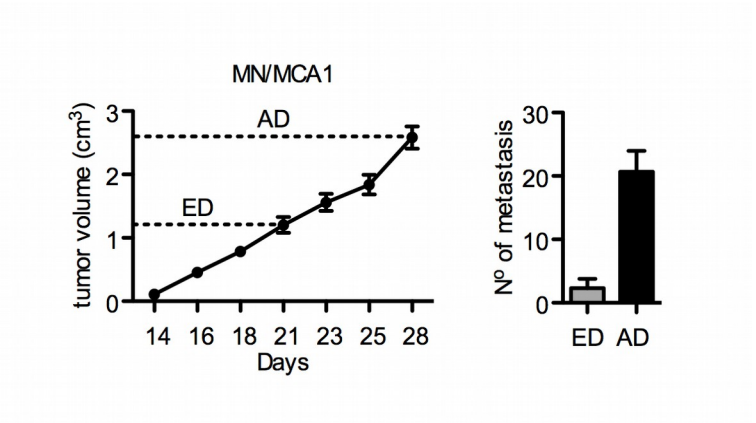

Fig. S1. (Related to Fig 1): Classification of MN/MCA1 bearing mice into early- (ED) and late-stage (AD) tumor bearers. Data are mean ± SEM in 30 mice. (Left) After tumor cell injection (day 0), tumor volume (cm^3) was measured starting from day 14 until day 28. (Right) Mean counts ± SEM of macroscopic lung metastases in 30 mice are shown.

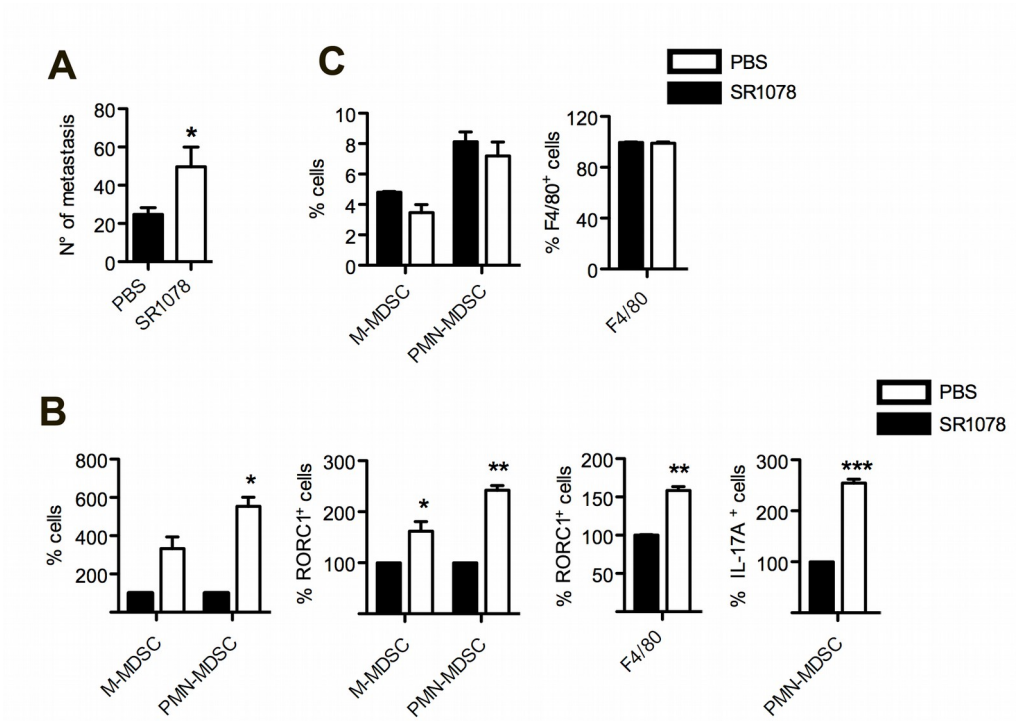

Fig. S2. (Related to Fig. 3): The RORC1 agonist SR1078 promotes metastasis formation and expansion of tumor promoting myeloid populations in tumor bearing mice. (A) Mean counts ± SEM of macroscopic lung metastases in untreated (PBS receivers) and SR1078 treated mice. (B) Data are mean percentages ± SEM of M-MDSC, PMN-MDSC; $RORC1^{+}$M-MDSC, $RORC1^{+}$PMN-MDSC, $RORC1^{+}CD11b^{+}F4/80^{+}$; $IL\text{-}17A^{+}$PMN-MDSC in spleen from MN/MCA1 bearing mice receiving PBS or SR1078. (C) Mean percentages ± SEM of M-MDSC, PMN-MDSC and $CD11b^{+}F4/80^{+}$ in spleen from tumor free mice receiving PBS or SR1078. The mean prevalence of myeloid subsets measured in mice treated with SR1078 is represented as relative value of the mean obtained in PBS-treated control mice, defined as 100%. 6 animals/group are shown. Statistical analysis: *$p < 0.05$, **$p < 0.01$, ***$p < 0.001$ (Student's t test).

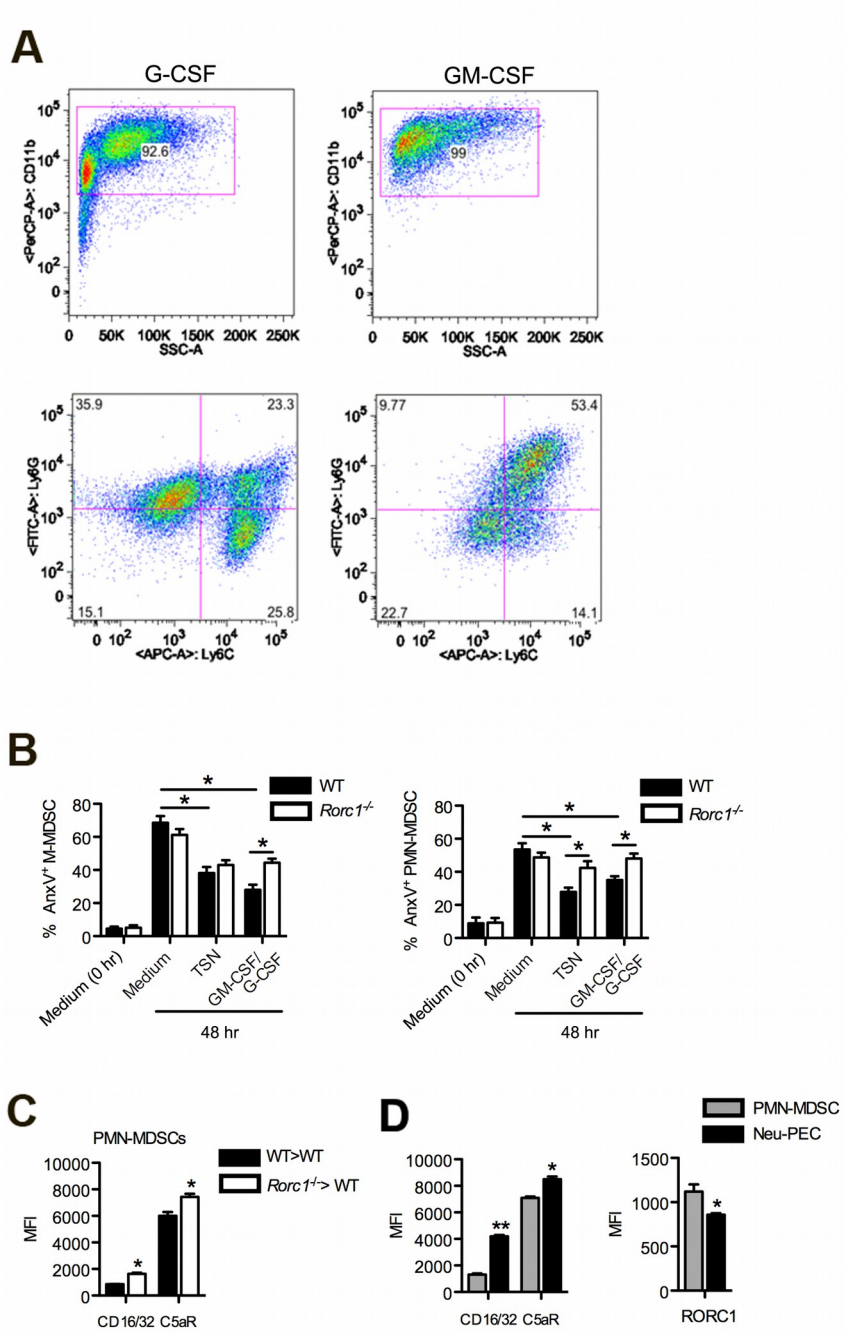

Fig. S3. (Related to Fig. 4): Role of RORC1 in M- and PMN-MDSC survival. (A) Different ratio of induction of the Gr1 $^{+}$Ly6C^{-} vs Gr1^{+}Ly6C^{+} myeloid populations, from the progenitors in response to G-CSF and GM-CFS. (B) FACS analysis of AnnexinV-binding (AnxV) to *in vitro* generated BM-derived M-MDSC and PMN-MDSC, from WT and *Rorc1*$^{-/-}$ mice, as indicated. AnxV binding was determined in response to 48 hr of culture with media, TSN (MN/MCA1) or

combination of recombinant GM-CSF (40 ng/ml) and G-CSF (40 ng/ml). Mean ± SD of 3 independent experiments is shown. (C and D) Effect of RORC1 on neutrophil maturation. (C) The histogram bars show the mean percentages ± SEM of CD16/CD32^{+} and C5aR^{+} PMN-MDSCs separated from the spleen of MN/MCA1 bearing WT>WT and *Rorc1* $^{-/-}$>WT chimeras. (D) The histogram bars show the mean ± SEM of the relative mean fluorescence (MFI) for CD16/CD32, C5aR and RORC1 in PMN-MDSC harvested from the spleen of MN/MCA1 bearers and in thioglycollate elicited peritoneal neutrophils (Neu-PEC) from tumor free mice. Data from 6 independent experiments are shown. Statistical analysis: *p < 0.05, **p < 0.01, ***p < 0.001 (Student's t test).

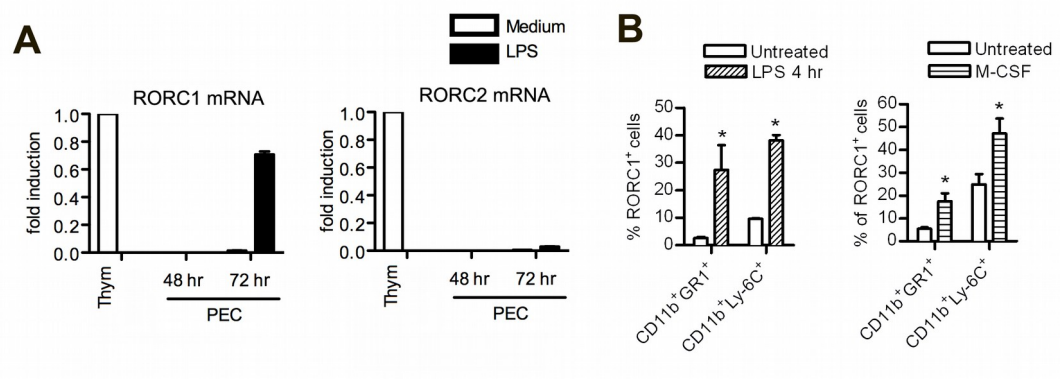

Fig. S4. (Related to Fig. 5): RORC1 expression by myeloid cells. (A) RORC1 mRNA expression in peritoneal macrophages (PEC). mRNA expression levels for *Rorc1* (left) and *Rorc2* (right) in LPS stimulated (48 or 72 hr) PEC were compared to constitutive levels expressed by unstimulated thymocytes. Mean ± SEM from 3 independent experiments is shown. (B) RORC1 is expressed during "emergency" granulo-monocytopoiesis. RORC1 expression in bone marrow CD11b $^{+}$GR1^{+} granulocytic and CD11b $^{+}$Ly6C^{+} monocytes from both LPS- and M-CSF-treated mice was analysed by FACS. Data shown are mean ± SEM of 6 mice. Statistical analysis: *p < 0.05, **p < 0.01, ***p < 0.001 (Student's t test).

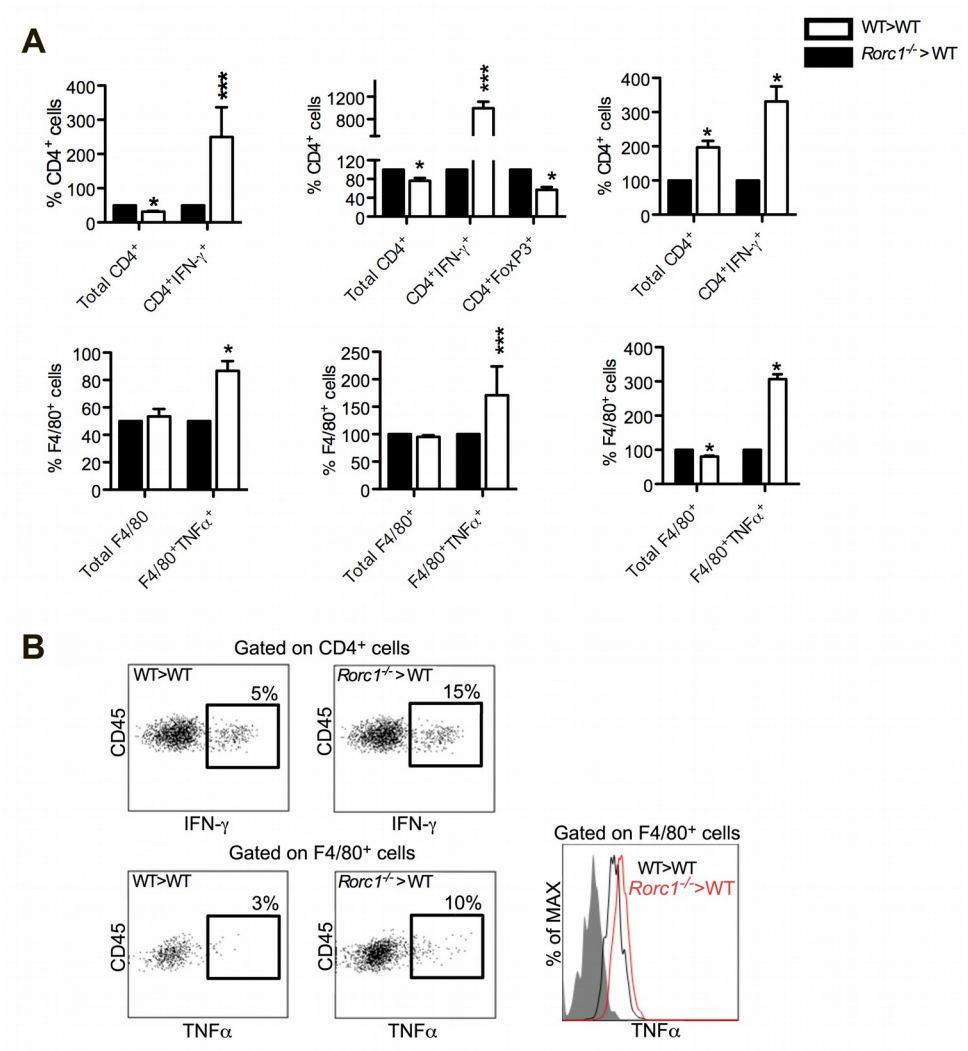

Fig. S5. (Related to Fig. 7): Influence of RORC1 on type I innate and adaptive effector responses. (A) Total CD4 $^{+}$ and CD4^{+}IFN-γ^{+} within the CD45^{+} gate (upper histograms) and total F4/80^{+} and F4/80 $^{+}$TNFα^{+} subsets within the CD11b $^{+}$CD45^{+} gate (lower histograms), in spleen from tumor free (Left), spleen from tumor bearers (Center) and from MN/MCA1 tumors (Right), in chimeric mice as indicated. The mean prevalence of CD4 and F4/80 subsets measured in *Rorc1*$^{-/-}$>WT chimeras is represented as relative value of the mean obtained in WT>WT chimeras (defined as 100%). Mean ± SEM of a representative experiment, of 6 independent experiments, with 6 mice/group is shown. (B) FACS-DOT PLOTs for CD4 $^{+}$IFN-γ^{+} and F4/80^{+}TNFα^{+} subsets in MN/MCA1 of one representative WT>WT and *Rorc1* $^{-/-}$>WT chimera with AD are shown. HISTO PLOTS of the relative mean fluorescence (MFI) of TNFa expression by F4/80 $^{+}$ MN/MCA1 infiltrating macrophages of one representative WT>WT and *Rorc1*$^{-/-}$>WT chimera with AD are shown. Statistical analysis: *p < 0.05, **p < 0.01, ***p < 0.001 (Student's t test).

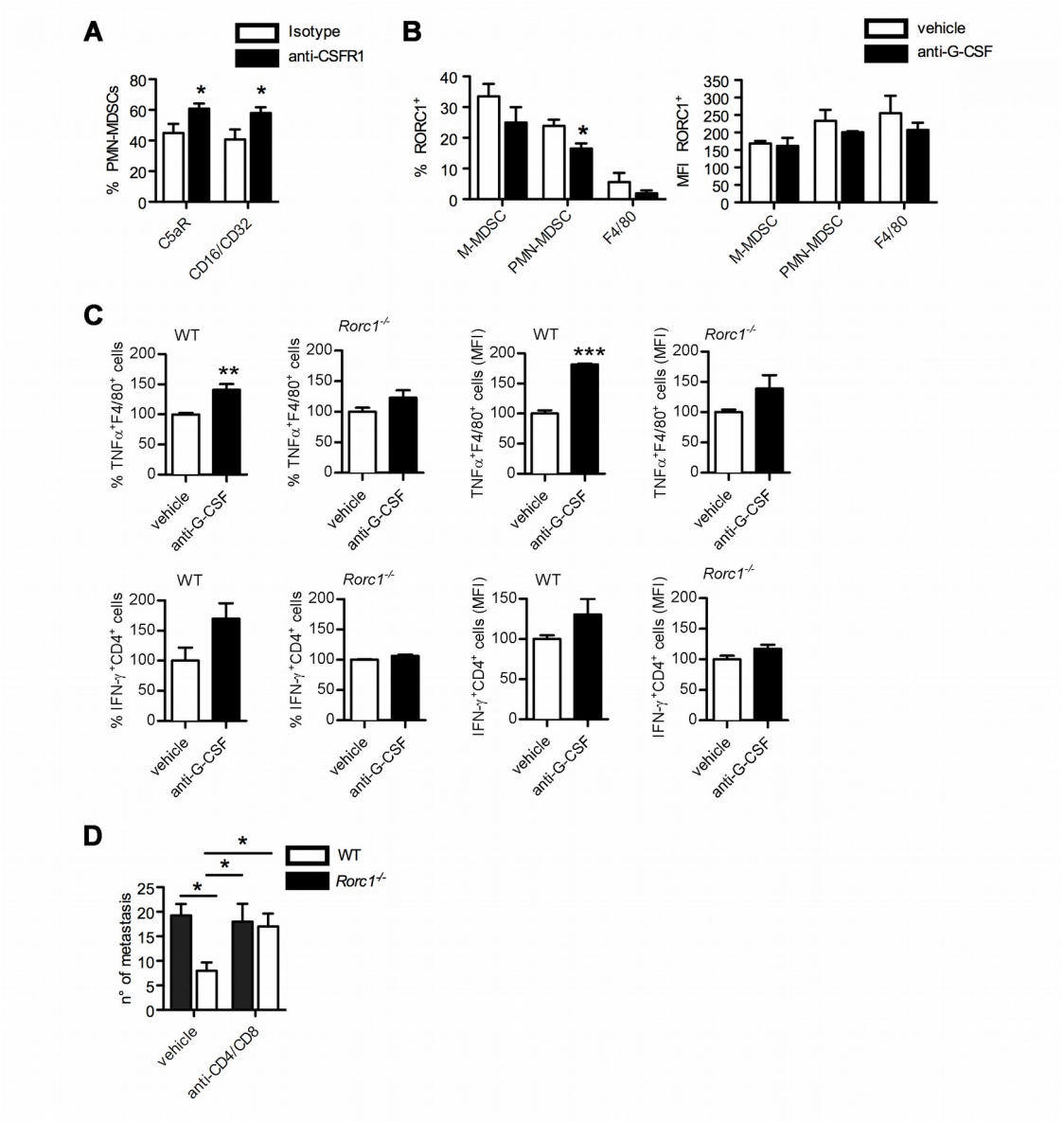

Fig. S6. (Related to Fig. 8): (A) Modulation of mature splenic neutrophils in anti-CSFR1 treated tumor bearing mice. Data are mean percentage ± SD for CD16/CD32 and C5aR expression in PMN-MDSC in MN/MCA1 from WT mice, treated with isotype IgG or ant-CSFR1 antibody, is shown. (B) Flow cytometry analysis of RORC1 expression in tumor infiltrating (MN/MCA1) M-MDSC, PMN-MDSC and F4/80 macrophages, in anti-G- CSF treated tumor bearing WT mice. Mean ± SD is shown. (C) Flow cytometry analysis of tumor infiltrating TNF $\alpha^{+}F4/80^{+}$ macrophages and IFN- $\gamma^{+}CD4^{+}$ T lymphocytes in anti-G-CSF treated tumor bearing WT and *Rorc1* $^{-/-}$ mice. Mean ± SD is shown. (D) Number of lung metastasis in WT and *Rorc1*$^{-/-}$ tumor bearing mice treated with anti-$CD4^{+}$ and anti-$CD8^{+}$ T cell depleting antibodies. Mean ± SEM of 7 animals/group are shown. Statistical analysis in panels A-D: *p < 0.05, **p < 0.01, ***p < 0.001 n=6 (Student's t test)

Supplemental Experimental Procedures

Ethics Statement. The study was designed in compliance with principles set out in the following laws, regulations and policies governing the care and use of laboratory animals: Italian Governing Law (Legislative Decree 116 of Jan. 27, 1992); EU directives and guidelines (EEC Council Directive 86/609, OJ L 358, 12/12/1986); Legislative Decree September 19, 1994, n. 626 (89/391/CEE, 89/654/CEE, 89/655/CEE, 89/656/CEE, 90/269/CEE, 90/270/CEE, 90/394/CEE, 90/679/CEE); the NIH Guide for the Care and Use of Laboratory Animals (1996 edition); Authorization n. 11/2006-A issued January 23, 2006 by Ministry of Health. The study was approved by the scientific board of Humanitas Clinical and Research Center. Humanitas Clinical and Research Center Institutional Regulations and Policies providing internal authorization for persons conducting animal experiments.

Animals. C57BL/6 mice were purchased from Charles River (Calco, Italy). Homozygous RORC1 mutant mice (B6.129P2(Cg)-*Rorctm*1Litt/J) [1] were donated by Prof. Dr. Dan Littman (New York University). Male MMTV-PyMT mice [2], were donated by Prof. Guido Forni (University of Turin, Orbassano, Italy) and mated with C57BL/6 females to obtain the F1 C57BL/6-MMTV-PyMT strain. IL-17A-deficient mice were donated by Prof. Dr. Burkhard Becher (University of Zuerich, CH).

Bone marrow Transplantation (BMT). 8 weeks old mice were lethally irradiated with two dose of 475 cGy before bone marrow transplantation (BMT). 5*106 CD45.2 RORC1 deficient (*Rorc1*$^{-/-}$), IL-17A$^{-/-}$, or WT bone marrow (BM) cells were injected intravenously into CD45.1 C57BL/6 WT male or C57BL/6-MMTV-PyMT female mice. 8 weeks later, BM engraftment was checked by staining blood cells with PerCP-conjugated CD45.1 antibody and

PE-conjugated CD45.2 antibody (BD Biosciences) and subsequent FACS analysis. Then, 10^5 murine fibrosarcoma (MN/MCA1) cells were injected intramuscularly in the left hind limb. Tumor growth was monitored 3 times a week with a caliper, starting from day 14. To chemically induce fibrosarcoma, 8 weeks after BMT mice received a single subcutaneous injection of 200 μg methylcholanthrene in corn oil. 12 weeks later tumor growth was monitored 3 times a week. 6-8 weeks after BMT, C57BL/6-MMTV-PyMT mice were monitored 3 times a week for breast carcinoma development.

Cell Culture and Reagents. TAMs and thioglycollate-elicited peritoneal exudate cells (PEC) were isolated from healthy or tumor bearing mice as previously described [3]. PEC and TAMs were incubated in RPMI 1640 containing 10% FCS, 2 mmol/L glutamine and 100 units/mL penicillin-streptomycin. BM-MDSCs were generated from bone marrow (BM) cells isolated from naïve WT or *Rorc1* $^{-/-}$ mice as previously described [4]. BM cells were cultured for 4 days in RPMI containing 10% FBS, supplemented with 40ng/ml of murine recombinant IL-6, GM-CSF and G-CSF (Peprotech). Spleen-derived MDSCs were isolated by MACS cell separation according to the manufacturer's instructions (Miltenyi Biotech). In details, MDSCs were first enriched by consequent serial negative selections with CD19 and CD11c microbeads (130-052-201 and 130-052-001 respectively), followed by positive selection with LY6G microbeads kit (130-092-332) (PMN-MDSCs). Finally, remaining cells were positively selected with CD11b$^+$ microbeads (130-049-601), which all stained positive for Ly6C marker (M-MDSC). The purity of both BM-MDSCs and spleen-derived M-MDSCs (CD11b$^+$Ly6C$^+$Ly6G^{low}), PMN-MDSC (CD11b$^+$Ly6G$^+$Ly6C^{low}) populations was >90%, as determined by flow cytometry, and the viability as determined by AnxV-binding (Immunostep) was >95% for WT>WT MDSCs subsets, whereas in contrast MDSCs isolated form *Rorc1* $^{-/-}$>WT animals showed a decreased viability (as stated in the text).

BM-MDSCs were cultured in RPMI 1640 containing 5% FCS, 2 mmol/L glutamine, 100 units/mL penicillin-streptomycin, 10 mM Hepes and 20 mM beta-mercaptoethanol and M-MDSCs and PMN-MDSCs subsets were cultured in DMEM containing 5% FCS, 2 mmol/L glutamine, 100 units/mL penicillin-streptomycin, 10 mM Hepes and 20 μM beta-mercaptoethanol. The concentration for the different in vitro, treatments were as follows: 100 ng/mL LPS from Salmonella Abortus, Equi S-form (Alexis), 200 U/mL IFN-γ, 40 ng/mL GM-CSF, 40 ng/mL G-CSF, 40 ng/mL IL-β (all from Peprotech) or MN/MCA1 tumor supernatant (TSN) diluted 1:1 in culture media.

Lineage cell separation from BM. Isolation of lineage-negative cells (depleted from mature hematopoietic cells such as T cells, B cells, monocytes/macrophages, granulocytes and erythrocytes) from BM harvested from naïve WT or *Rorc* $^{-/-}$ mice was performed by using the murine lineage cell separation kit from Miltenyi (130-090-858) as indicated by the manufacturers protocol. Separated lineage–negative progenitor cells were cultured in the presence of recombinant murine GM-CSF (40 ng/mL), G-CSF (40 ng/mL) (all from Peprotech) or culture media alone for up to 7-10 days. Then, to evaluate ckit^{+} macrophage/monocyte and granulocyte progenitors, cells were stained with anti-CD117 (ckit), CD11b, Ly6C, Ly6G, Gr1, and F4/80 antibodies (all from eBioscience) and analyzed by flow cytometry.

In vivo treatments. When the tumor became palpable (day 14) WT>WT and *Rorc1*$^{-/-}$>WT mice were treated with the following drugs: RORα/γ Agonist (SR1078, Calbiochem) was administered at the dose of 10mg/kg intra peritoneally (i.p.) four times a week for 2 weeks, control mice received PBS injections; CSFR1 antagonist (kindly donated by Dr. Carola Ries, Roche Diagnostic Gmbh, Penzberg, Germany) were administered as an initial dose of 60mg/kg followed by two doses of 30 mg/kg two times a week for a total of 2

weeks; anti-GCSF MAB 414 (R&D Systems), anti- GM-CSF 415NA (R&D Systems) were administered 1 mg/mouse i.p. daily for a total of 2 weeks; control mice were injected with isotype antibody 0,3 mg of both the anti-CD4 (Rat Anti-Mouse CD4 Monoclonal Antibody, Unconjugated, Clone GK1.5, BioXcell) and the anti-CD8 (Rat Anti-Mouse CD8a Monoclonal Antibody, Unconjugated, Clone 2.43, BioXcell) antibodies were injected IP once a week.

Patients. 10 patients with T2 or T3 CRC were enrolled in the study after signing Cancer Research Center Humanitas IRB-approved consent. Patients did not receive radiation or chemotherapy before sample collection. Peripheral blood was collected at the time of surgery from all patients. All blood samples were analyzed within 3 hr after collection by FACS-analysis (see section Flow Cytometry).

MLR. M-MDSCs ($CD11b^{+}Ly6C^{+}Ly6G^{low}$) populations were isolated from MN/MCA1 bearing WT>WT or *Rorc1*$^{-}$>WT chimeric mice by Milteny bead separation as described above. Serial dilutions of M-MDSC starting from $2*10^{5}$ cells were plated in 96 well plates in 100µL of RPMI medium ($2*10^{5}$, $1*10^{5}$, $5*10^{4}$, $2.5*10^{4}$ or $12.5*10^{4}$). Cells were then stimulated with IFN-γ (200 U/mL) or kept in culture media alone for 72 hr. Then, TSNs were harvested and tested for nitrite production (as control) and $2*10^{5}$ splenocytes from OT1 mice were added. Cells were incubated in DMEM containing 5% FCS, 2 mmol/L glutamine, 100 units/mL penicillin-streptomycin, 10 mM Hepes and 20 µM beta-mercaptoethanol and pulsed with ovalbumin peptide (OVA257–264) (250 µg/mL) for additional 72 hr. H3 thymidine was added for the last 16 hr of culture and its incorporation was analyzed by MicroBeta plate counter (Perkin Elmer). As controls OT-1 splenocytes alone were pulsed with OVA peptide (250 µg/mL), ConA (5 µg/mL) or kept in culture media. All conditions were evaluated in triplicates.

Flow cytometry. $5*10^5$ cells were re-suspended in HBSS (Hank's balanced salt solution, Lonza) supplemented with 0.5% BSA (Sigma). Staining was performed at 4°C for 20 minutes, with the following antibodies: anti-mouse CD45-PerCP, CD11b-PE, FITC or –APC, Gr1-PE or -APC, F4/80-PE or -APC, CD115 (CSFR1)-PE C5aR-PE and IFN-γ-PE (all from BD Biosciences; San Diego, CA); Ly6G-FITC and Ly6C-FITC or –PE (from Miltenyi Biotech; Teterow, Germany); FCII/IIIR –PE or –APC (CD16/CD32) (from Bio Legend; San Diego, SA); lineage markers (PE-CD3, -CD4, -CD8, –Mac-1, –Gr-1, -Ter119, and -B220), hematopoietic progenitor markers (Sca-1, c-Kit (CD117), IL7Rα, CD34,) IL-17A-APC, TNF α-Alexa647 and anti-mouse/human RORC1-APC (from eBioscience; San Diego, CA); anti-human CD14-PE, HLADR-Pacific Blue, CD15-FITC (BD Bioscience; San Diego, CA) and IL-17A-PE (BioLegend San Diego, CA). Further we used unconjugated CEBP/β (Millipore; Billerica, Massachusetts) and unconjugated IRF8 antibody (Cell Signaling) followed by incubation with secondary goat anti rabbit Alexa Fluor® 488 conjugated antibody (Invitrogen, Molecular Probes, Carlsbad, CA). For the gating of viable cells we used viability staining solution (7-ADD eBiosciences). For intra-cellular staining Cytofix/Cytoperm and Permwash staining kit (BD Pharmigen) were used according to the manufacturer's instruction. Cells were detected using the BD FACS Canto cytofluorimeter and analyzed with BD FACS Diva Software.

Gating strategy for the identification of human MDSCs, neutrophils and monocytes. Cells were stained with a cocktail of mABs to HLA-DR (clone L243), CD14 (clone M5E2), CD16 (Anti-human CD16 (PE-Cy7), Clone: CB16, eBioscience San Diego, CA), CD15 (clone HI98) (BD biosciences, San Diego, CA) and CD33 (clone WM53, BioLegend San Diego, CA). Identification of monocytes and neutrophils was carried out in whole blood from healthy or CR patients, by an immunophenotypic analysis through multiparameter flow

cytometry. The analysis was performed according to WHO criteria on antigens that are expressed by human monocytes and neutrophils. Neutrophils were identified as HLA-DR$^-$CD14$^-$CD15$^+$CD16$^+$CD33$^+$ cells, whereas monocytes were HLA-DR$^+$CD14$^+$CD15$^{low/-}$ CD16$^-$CD33^{++}. Analysis of MDSCs populations was performed on PBMC from healthy or CR patients. MDSCs were identified within the gate of HLA-DR $^-$ cells as CD33 ^{high} cells. Next within the CD33 ^{high} gate, the two subsets were resolved according to their expression of CD14 (M-MDSCs) or CD15 (G-MDSCs). Interestingly, differently from CD14$^+$ mature monocytes that retain HLA-DR expression, a condition that allow distinguishing them from M-MDSCs, granulocytes and G-MDSCs were both negative for HLA-DR expression. Therefore, in the whole blood, to further distinguish granulocytes from G-MDSCs we evaluated the level of expression of CD33 that were higher in G-MDSCs and almost negative in granulocytes. Notably according to other literature data we found that CD33 mAb that certainly marks M-MDSCs also stain circulating CD14$^+$ monocytes, a population that is also increased in advance colorectal cancer patients. In summary in PBMC from colorectal cancer patients we defined M-MDSCs as HLA-DR$^-$CD14$^+$CD33^{high} whereas G-MDSC were HLA-DR$^-$CD15$^+$CD33^{high}.

Histopathology and Immunohistochemistry. Histopathological analysis was performed on BM and spleens from WT, *Rorc1* $^{-/-}$ and chimeric mice on sections routinely stained with Haematoxylin and Eosin. Single- and double-marker immunohistochemistry on mouse and human tissue specimens were performed as previously described [5]. Briefly, four-micrometers thick sections were cut from formalin-fixed and paraffin-embedded tissue specimens and put onto slides; sections were deparaffinized through alcohol gradients and rehydrated to water. Antigenic retrieval was performed using TRIS- EDTA pH9 buffer in thermostatic bath at 98°C for 30 minutes. Mouse spleen sections were incubated with anti-mouse IL4R (Biolegend) and anti-mouse IL17A (Abcam) primary

antibodies and the binding was revealed using specific secondary antibodies and the streptavidin-biotin-peroxidase complex method. Sections from BM biopsies of patients with early-stage Hodgkin's lymphoma and uninvolved marrow (n=8) were incubated with anti-human IL-17A (LifeSpan, Biosciences, Inc.) or anti-human RORγ (LifeSpan, Biosciences, Inc.) and the binding was revealed by the means of specific secondary antibody and the alkaline-phosphatase anti-alkaline-phosphatase method (APAAP, Dako). Double-marker immunohistochemistry for IL-17A and CD3 was performed on sections from the same specimens by two sequential rounds of single-marker immunohistochemistry using the two different revelation systems mentioned above. Stained sections were analyzed by an expert pathologist (CT) using a Leica DM2000 optical microscope and microphotographs were collected with a Leica DFC320 digital camera using the Leica IM50 imaging software.

Real-Time PCR. Total RNA was extracted with TRIzol (Invitrogen) according to the manufacturer's instructions. 1 μg of total RNA was reverse-transcribed by the High Capacity cDNA Reverse Transcription kit (Applied Biosystems), amplified using Fast Syber Green Master Mix (Applied Biosystems), and detected by the 7900HT Fast Real-Time System (Applied Biosystems). The sequences of gene-specific primers are available upon request. Data were processed using SDS2.2.2 software (Applied Biosystems). Results were normalized to the expression of the housekeeping gene β-actin and then expressed as fold up-regulation with respect to the control cell population.

ELISA. MN/MCA1 supernatants were tested in sandwich ELISA (R&D Systems). Tumor cell-free supernatants were tested for the indicated cytokines/growth factors: Murine TNF α, GM-CSF, G-CSF, M-CSF, IL-1 β, IL-17A and VEGFA (Duoset Elisa kit, R&D).

Confocal Microscopy analysis. Cells were seeded on Poly-L-Lysine (Sigma-Aldrich) coated sterile rounded glasses at $2x10^5$ cells/ml in medium and fixed with 4% PFA for 10 minutes at room temperature. Cell permeabilization was obtained after 1 hr incubation with PBS 0.1% Triton-X100 (Sigma-Aldrich) plus 5% normal goat serum (Dako Cytomation, Carpinteria, CA USA) and 2% BSA, (Amersham Biosciences, Piscataway Township, NJ USA). Cells were then incubated with anti-mouse/human RORC1-APC (Clone: AFKJS-9, eBioscience; San Diego, CA) or rat IgG2a K isotype APC as control. Nuclei were counterstained with DAPI (Invitrogen, Molecular Probes). Samples were mounted with FluorPreserve Reagent (Calbiochem San Diego, CA USA) and analyzed with an Olympus Fluoview FV1000 laser scanning confocal microscope operating with lasers with 405 and 647 nm excitations. The resulting fluorescence emission was collected using a 460-to-490 nm (for DAPI) and 620-750 nm (for APC) band-pass filters. Samples were imaged with an oil immersion objective (40×1.30 NA Plan-Apochromat; Olympus).

Statistics. Statistical significance was determined by a two-tailed Student's t test (*$p < 0.05$, ** $p < 0.01$, *** $p < 0.001$).

References

1. Sun, Z.M., et al., *Requirement for ROR gamma in thymocyte survival and lymphoid organ development.* Science, 2000. **288**(5475): p. 2369-2373.
2. Guy, C.T.C., R.D.; and Muller, W.J., *Induction of mammary tumors by expression of polyomavirus middle T oncogene: a transgenic mouse model for metastatic disease.* Mol Biol Cell, 1992. **12**: p. 954-961.
3. Porta, C., et al., *Tolerance and M2 (alternative) macrophage polarization are related processes orchestrated by p50 nuclear factor kappaB.* Proc Natl Acad Sci U S A, 2009. **106**(35): p. 14978-83.
4. Marigo, I., et al., *Tumor-induced tolerance and immune suppression depend on the C/EBPbeta transcription factor.* Immunity, 2010. **32**(6): p. 790-802.
5. Tripodo, C., et al., *Stromal SPARC contributes to the detrimental fibrotic changes associated with myeloproliferation whereas its deficiency favors myeloid cell expansion.* Blood, 2012. **120**(17): p. 3541-3554.

Chapter 5

5. Discussion

Both recruitment and activation of tumor associated myeloid cells may be considered putative targets for therapeutic intervention; accordingly, because of their unique role in linking innate and adaptive immunity, macrophage-based immunotherapy is widely considered in clinical trials of cancer patients. Chemoattractants involved in monocyte recruitment include chemokines (e.g. CCL2, CCL5, CXCL4) [1-3], colony-stimulating factor-1 (CSF-1) [4, 5], and members of the VEGF family [6]. Recently, genetic evidence in the mouse suggested that complement components play an important role in the accumulation and functional polarization of TAMs [7, 8]. We identified p50 NF-κB also as an important regulator of macrophage migration. In particular we demonstrated that lack of p50 NF-κB impairs macrophage chemotactic responsiveness. Accordingly, nuclear accumulation of p50 NF-κB not only drives phenotypic traits of TAMs and LPS-tolerant macrophages, including the expression of anti-inflammatory M2 polarized genes [9], but also promotes their chemotactic response to complement anaphylatoxins C5a and C3a. Distinct $F4/80^{+}$ macrophage subsets characterized by different expression levels of F4/80 and the C5aR (CD88), respectively defined as $F4/80^{high}CD88^{high}$ and $F4/80^{low}CD88^{low}$, differentially accumulate into the inflammatory sites, in *in vivo* model of LPS-tolerance. Of relevance, p50-dependent induction of systemic tolerance [9] is a necessary event driving systemic accumulation of $F4/80^{high}CD88^{high}$ mono/macrophages, both in mouse and human. This result, along with the differential expansion of the $F4/80^{low}CD88^{low}$ and $F4/80^{high}CD88^{high}$ populations, observed also in the preclinical MN/MCA1 fibrosarcoma and B16 melanoma model, indicates that expansion of $F4/80^{high}CD88^{high}$ macrophages is promoted through emergency hematopoiesis. Moreover, in line with the LPS-tolerance model, ablation of p50 NF-κB resulted in significant impairment of F4/80 $^{high}CD88^{high}$ TAMs accumulation in primary

tumors, which correlated with inhibition of tumor growth [10] and vascularization.

Consistent with other reports where lack of complement factors (C3 or C5aR) in tumor bearers resulted in impaired MDSCs accumulation, as well as in resistance to tumor development and metastasis formation [11-15], we observed that reduced fibrosarcoma growth and lung metastasis formation in C3 $^{-/-}$ mice, as compared to wt mice, was paralleled by significant impairment recruitment of F4/80^{high} TAMs, in both primary tumor and lung metastasis. This result was mimicked by treatment with an anti-CSFR1 antibody, indicating that blocking accumulation of F4/80 ^{high} macrophages in the tumor microenvironment impairs tumor growth and tumor angiogenesis.

Strikingly, adoptive transfer of F4/80^{low} TAMs in wt tumor bearing mice resulted in inhibition of tumor growth and in reduced formation of lung metastasis, while, conversely, transfer of wt F4/80^{high} TAMs in p50$^{-/-}$ tumor bearing mice caused restoration of tumor growth and increased metastasis formation. Accordingly, transfer of F4/80 ^{high} TAMs also increased tumor vessels density and length, indicating that the ratio between the F4/80 ^{high} and F4/80 ^{low} TAMs critically controls the angiogenic switch in growing tumors [16]. A distinct role of F4/80^{high} and F4/80^{low} TAMs in tumor development was also confirmed by analysis of their transcriptomes, showing that distinct gene profiles characterize the transcriptional programs of these populations.

Thus, we show that distinct macrophage subsets with different functions arise during infection- and cancer-driven inflammation, in a p50 NF-κB-dependent manner and that complement-mediated pathways selectively drive their infiltration of inflammatory sites, including solid tumors.

In addition, we demonstrate that the retinoic-acid-related orphan receptor (RORC1/RORγ) fuels cancer-promoting inflammation by enhancing survival and expansion of CD16/32^{low}/ C5aR^{low} immature MDSCs, with reduced

expression of M1 cytokines (IL-1β and TNF-α) and increased suppressive activity, and promoting terminal macrophage differentiation. Our study indicates that RORC1 impinges on cancer-driven myelopoiesis by suppressing negative (Socs3 and Bcl3) [17, 18] and promoting positive (C/EBPβ) [19] transcriptional regulators of ‘‘emergency’’ granulopoiesis, while instating the expression of macrophage-specific tran- scription factors IRF8 and PU.1 [20]. Depletion of RORC1^{+}F4/80^{+}CD115^{+} TAMs with anti-CSFR1 antibody enhanced the recruitment of mature (CD16/CD32^{high}) RORC1 inflammatory neutrophils, with diminished expansion of immature RORC1^{+}(CD16^{low}/CD32^{low}) PMN-MDSCs. This result, along with the observed competition between the commitment of myeloid precursors for the monocytic versus granulocytic lineage, observed with the anti-G-CSF and anti-CSFR1 treatments, respectively, may indicate that blocking M-CSF-dependent myelopoiesis unleashes expansion and maturation of granulocytic cells, which would favor the increase of tumor-infiltrating neutrophils. These events deflect the inflammatory microenvironment to adverse the tumor, increasing infiltration of CD4^{+} IFN-γ^{+} T cells and F4/80^{+}TNF-α^{+} M1 polarized macrophages. Our results indicate that high RORC1 expression acts as pro- resolving mediator of myeloid inflammation and that antagonists to RORC1 might hold the potential to prevent tumor-promoting myeloid differentiation. We also report that IL-17 expression is disjointed from RORC1 in the monocyte/macrophage lineage (M-MDSCs and CD11b^{+}F4/80^{+} TAMs). Wu *et al.* have recently described that tumor-infiltrating inflammatory dendritic cells activate IL-17-producing RORγt^{+} γδT17 cells to secrete IL-8, TNF-α, and GM-CSF cells and sustain the subsequent intratumor accumulation of immunosuppressive PMN-MDSCs in colorectal cancer [21]. Further, an inflammatory cascade encompassing the IL-1β-mediated production by IL-17 in γδT cells resulted in systemic G-CSF-dependent expansion of suppressive neutrophils and formation of breast cancer metastasis [22]. Our observation that IL-17 is selectively expressed, but not

secreted by immature granulocyte/neutrophil subsets, does not support a direct role of myeloid-cell-derived IL-17 in the expansion of MDSCs during cancer development, but rather indicates that IL-17A is a hallmark of immature myeloid responses in cancer bearers. This notion is further supported by the observation that expression of IL-17 and RORC1 localizes within the immature myeloid cells precursor-rich areas lining the bone trabeculae of BM biopsies from patients under diagnosis of Hodgkin's lymphoma. Moreover, in contrast to *Rorc1*$^{-/-}$ BM transplantation, chimeric mice receiving the I*l17a*$^{-/-}$ BM had no defect in developing tumor-associated myeloid cells, in both the BM and spleen (data not shown). It remains to be established whether IL-17A expression by circulating MDSCs is dependent on the disease stage, as we did not observe its expression in blood from T2/T3 CRC patients.
Along with other reports, our observation highlights the relevance of members of the nuclear receptor superfamily in regulation of inflammation [23, 24] and suggests RORC1 as central regulator of cancer associated myelopoiesis and key driver of the protumor differentiation of MDSCs and TAMs.

Nowadays anticancer therapies are not only directed against cancer cells, but different approaches have been investigated to harness the potency of the immune system to target cancer. These have been essentially focused on enhancing the immunogenicity of the tumor or on the induction and expansion of immune effector cells to potentially target and eradicate the tumor. However, immune-modulating activities of chemotherapeutic agents are often very complex to understand, due to the fact that same molecules may play opposite roles depending on tumor type, immune contexts and/or precise therapeutic strategy. Accordingly, the tight balance between immune activating and immune suppressive events plays a crucial role in defining the clinical outcome of cancer patients. These complexities highlight the need for an ever more profound comprehension of the dynamic changes in the tumor microenvironment and in systemic immune response, as tumors evolve,

progress and respond to therapy. An improved knowledge of these aspects will facilitate the rational design of highly efficient, synergistic regimens that combine anticancer agents and immunotherapies [25].

In this scenario, our studies are intended to shed light on novel key pathways driving lineage commitment of myeloid precursors during cancer-related "emergency" myelopoiesis, their recruitment and functional transcription in cancer bearers, in order to estimate whether they may represent novel prognostic indicators and targetable elements in anticancer immunotherapy. Collectively our data identify RORC1 as key orchestrator of pathological differentiation of myeloid suppressor cells in cancer bearers and describe a novel role of p50 NF-κB in guiding expansion, recruitment and the tumor promoting functions of the M2-like F4/80^{high} TAMs subset. Hence, RORC1 and p50 provide a new axis of cancer associated myelopoiesis that drive the protumor differentiation of MDSCs and TAMs.

Bibliography

1. Movahedi, K. and J.A. Van Ginderachter, *The Ontogeny and Microenvironmental Regulation of Tumor-Associated Macrophages.* Antioxid Redox Signal, 2016.
2. Qian, B.Z., et al., *CCL2 recruits inflammatory monocytes to facilitate breast-tumour metastasis.* Nature, 2011. **475**(7355): p. 222-5.
3. Weitzenfeld, P. and A. Ben-Baruch, *The chemokine system, and its CCR5 and CXCR4 receptors, as potential targets for personalized therapy in cancer.* Cancer Letters, 2014. **352**(1): p. 36-53.
4. Chitu, V. and E.R. Stanley, *Colony-stimulating factor-1 in immunity and inflammation.* Curr Opin Immunol, 2006. **18**(1): p. 39-48.
5. Hume, D.A. and K.P.A. MacDonald, *Therapeutic applications of macrophage colony-stimulating factor-1 (CSF-1) and antagonists of CSF-1 receptor (CSF-1R) signaling.* Blood, 2012. **119**(8): p. 1810-1820.
6. Linde, N., et al., *Vascular endothelial growth factor-induced skin carcinogenesis depends on recruitment and alternative activation of macrophages.* J Pathol, 2012. **227**(1): p. 17-28.
7. Bonavita, E., et al., *Phagocytes as Corrupted Policemen in Cancer-Related Inflammation.* Adv Cancer Res, 2015. **128**: p. 141-71.
8. Cho, M.S., et al., *Autocrine Effects of Tumor-Derived Complement.* Cell Reports, 2014. **6**(6): p. 1085-1095.
9. Porta, C., et al., *Tolerance and M2 (alternative) macrophage polarization are related processes orchestrated by p50 nuclear factor kappaB.* Proc Natl Acad Sci U S A, 2009. **106**(35): p. 14978-83.
10. Saccani, A., et al., *p50 nuclear factor-kappaB overexpression in tumor-associated macrophages inhibits M1 inflammatory responses and antitumor resistance.* Cancer Res, 2006. **66**(23): p. 11432-40.
11. Vadrevu, S.K., et al., *Complement C5a Receptor Facilitates Cancer Metastasis by Altering T-Cell Responses in the Metastatic Niche.* Cancer Research, 2014. **74**(13): p. 3454-3465.
12. Markiewski, M.M., et al., *Modulation of the antitumor immune response by complement.* Nature Immunology, 2008. **9**(11): p. 1225-1235.
13. Corrales, L., et al., *Anaphylatoxin C5a Creates a Favorable Microenvironment for Lung Cancer Progression.* Journal of Immunology, 2012. **189**(9): p. 4674-4683.
14. Gunn, L., et al., *Opposing Roles for Complement Component C5a in Tumor Progression and the Tumor Microenvironment.* Journal of Immunology, 2012. **189**(6): p. 2985-2994.
15. Wang, Y., et al., *Autocrine Complement Inhibits IL10-Dependent T-cell-Mediated Antitumor Immunity to Promote Tumor Progression.* Cancer Discovery, 2016. **6**(9): p. 1022-1035.

16. Lin, E.Y. and J.W. Pollard, *Tumor-associated macrophages press the angiogenic switch in breast cancer.* Cancer Res, 2007. **67**(11): p. 5064-6.
17. Croker, B.A., et al., *SOCS3 is a critical physiological negative regulator of G-CSF signaling and emergency granulopoiesis.* Immunity, 2004. **20**(2): p. 153-65.
18. Kreisel, D., et al., *Bcl3 prevents acute inflammatory lung injury in mice by restraining emergency granulopoiesis.* J Clin Invest, 2011. **121**(1): p. 265-76.
19. Hirai, H., et al., *C/EBP beta is required for 'emergency' granulopoiesis.* Nature Immunology, 2006. **7**(7): p. 732-739.
20. Friedman, A.D., *Transcriptional control of granulocyte and monocyte development.* Oncogene, 2007. **26**(47): p. 6816-28.
21. Wu, W.C., et al., *Circulating hematopoietic stem and progenitor cells are myeloid-biased in cancer patients.* Proc Natl Acad Sci U S A, 2014. **111**(11): p. 4221-6.
22. Coffelt, S.B., et al., *IL-17-producing gammadelta T cells and neutrophils conspire to promote breast cancer metastasis.* Nature, 2015. **522**(7556): p. 345-8.
23. Gerbal-Chaloin, S., et al., *Nuclear receptors in the cross-talk of drug metabolism and inflammation.* Drug Metab Rev, 2013. **45**(1): p. 122-44.
24. Wittke, A., et al., *Vitamin D receptor-deficient mice fail to develop experimental allergic asthma.* J Immunol, 2004. **173**(5): p. 3432-6.
25. Vacchelli, E., et al., *Trial Watch: Immunostimulatory cytokines.* Oncoimmunology, 2012. **1**(4): p. 493-506.

Chapter 6

6. List of publications

“RORC1 regulates tumor-promoting "emergency" granulo-monocytopoiesis.”
Strauss L, Sangaletti S, Consonni FM, Szebeni G, Morlacchi S, Totaro MG, Porta C, Anselmo A, Tartari S, Doni A, Zitelli F, Tripodo C, Colombo MP, Sica A.
Cancer Cell. 2015 Aug 10;28(2):253-69.

"VEGF blockade enhances the antitumor effect of BRAF^{V600E} inhibition"
Comunanza V, Cora D, Orso F, Consonni FM, Middonti E, Di Nicolantonio F, Sica A, Medico E, Sangiolo D, Taverna D, Bussolino F.
EMBO Molecular Medicine. 2016 Dec 14; doi: 10.15252/emmm.201505774.